AD-A107 198 AIR FORCE INST OF TECH WRIGHT-PATTERSON AFB OH F/G 9/5
AUTOMATIC MICROWAVE NETWORK ANALYZER CALIBRATION BY REFERENCE T--ETC(U)
OCT 81 J P DIBENEDITTO
UNCLASSIFIED AFIT-CI-81-120 NL

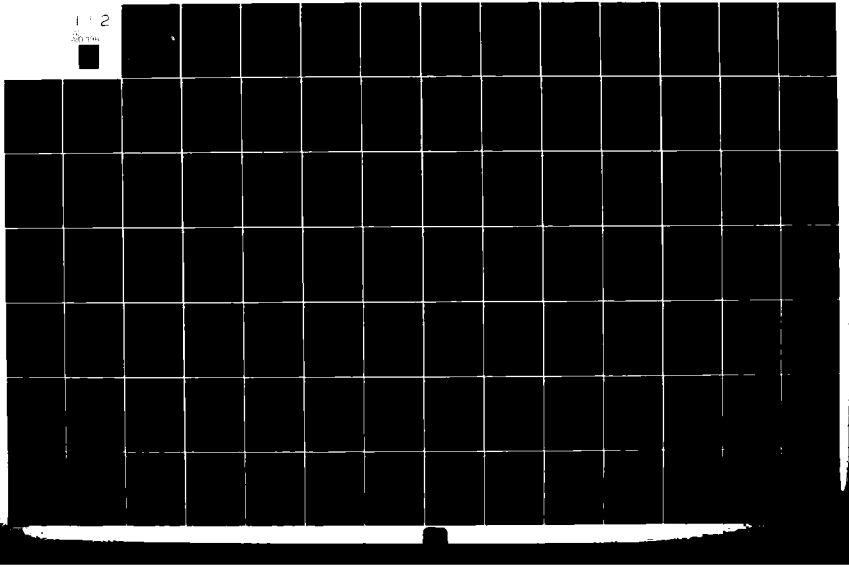

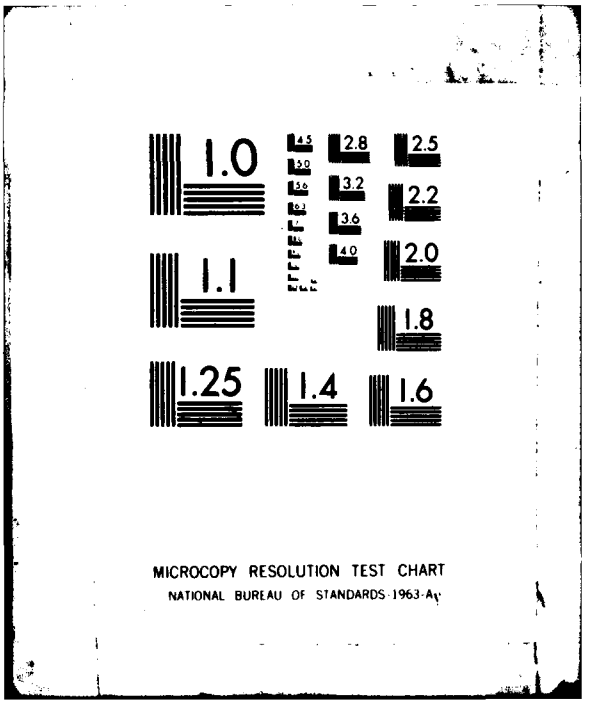
1.0
1.1
1.25
1.4
1.6
1.8
2.0
2.2
2.5
2.8
3.2
3.6
4.0
MICROCOPY RESOLUTION TEST CHART
NATIONAL BUREAU OF STANDARDS-1963-A

UNCLASS

SECURITY CLASSIFICATION OF THIS PAGE (When Data Entered)

REPORT DOCUMENTATION PAGE

READ INSTRUCTIONS BEFORE COMPLETING FORM

1. REPORT NUMBER: 81-12D (6)
2. GOVT ACCESSION NO.: AD-A107 198
3. RECIPIENT'S CATALOG NUMBER:
4. TITLE (and Subtitle): Automatic Microwave Network Analyzer Calibration by Reference to a Transmission-Line Standard with Applications to Characterization of Adapters, Devices, and Coaxial Lines with SMA Connectors
5. TYPE OF REPORT & PERIOD COVERED: THESIS/DISSERTATION
6. PERFORMING ORG. REPORT NUMBER:
7. AUTHOR(s): Capt Joseph Peter DiBeneditto (10) (1)
8. CONTRACT OR GRANT NUMBER(s):
9. PERFORMING ORGANIZATION NAME AND ADDRESS: AFIT STUDENT AT: Tuft Univ (9) Doctoral thesis,
10. PROGRAM ELEMENT, PROJECT, TASK AREA & WORK UNIT NUMBERS:
11. CONTROLLING OFFICE NAME AND ADDRESS: AFIT/NR, WPAFB OH 45433
12. REPORT DATE: October 1981 (11)
13. NUMBER OF PAGES: 188 (12)
14. MONITORING AGENCY NAME & ADDRESS (if different from Controlling Office): LEVEL II
15. SECURITY CLASS. (of this report): UNCLASS
15a. DECLASSIFICATION/DOWNGRADING SCHEDULE:
16. DISTRIBUTION STATEMENT (of this Report): APPROVED FOR PUBLIC RELEASE; DISTRIBUTION UNLIMITED (14) AFIT-CI-81-12D
17. DISTRIBUTION STATEMENT (of the abstract entered in Block 20, if different from Report)
18. SUPPLEMENTARY NOTES: APPROVED FOR PUBLIC RELEASE: IAW AFR 190-17

20 OCT 1981

Fredric C. Lynch

FREDRIC C. LYNCH, Major, USAF
Director of Public Affairs
Air Force Institute of Technology (ATC)
Wright-Patterson AFB, OH 45433

Air Force Institute of Technology (ATC)
Wright-Patterson AFB, OH 45433

19. KEY WORDS (Continue on reverse side if necessary and identify by block number)

20. ABSTRACT (Continue on reverse side if necessary and identify by block number): ATTACHED

DD FORM 1 JAN 73 1473 EDITION OF 1 NOV 65 IS OBSOLETE

UNCLASS

SECURITY CLASSIFICATION OF THIS PAGE (When Data Entered)

AD A107198

DTIC FILE COPY

DTIC ELECTE NOV 6 1981 D H

81 10 2 150

012205

ABSTRACT

This dissertation describes the development of new techniques for calibrating a microwave automatic network analyzer (hereafter ANA) for complex reflection measurements. These techniques promise significant advantages for miniature connector systems. They include the use of an experimentally-derived characterization of an APC-7 open-circuit termination as a high-reflection calibration standard, adapter correction based on low dissipative losses, and a length of transmission line instead of a sliding load or fixed termination as a low-reflection standard.

Gains afforded by these new techniques are reduced operator intervention during calibration, less wear of the measurement port connectors, lower equipment and maintenance costs, and calibrations referenced to standards truly relevant to the interconnecting transmission medium. Computer memory requirements are increased, but the cost of the increase is insignificant compared to the cost of microwave instrumentation. Slightly longer calibration times are offset by reduced demands upon operator skill.

Methods of extending these calibration techniques to full two-port measurements will be discussed.

81-12D

AFIT RESEARCH ASSESSMENT

The purpose of this questionnaire is to ascertain the value and/or contribution of research accomplished by students or faculty of the Air Force Institute of Technology (ATC). It would be greatly appreciated if you would complete the following questionnaire and return it to:

AFIT/NR
Wright-Patterson AFB OH 45433

RESEARCH TITLE: Automatic Microwave Network Analyzer Calibration by Reference to a Transmission-Line Standard, with Applications to Characterization of Adapters, Devices, and Coaxial Lines with SMA Connectors/

AUTHOR: Capt Joseph Peter DiBenedetto

RESEARCH ASSESSMENT QUESTIONS:

1. Did this research contribute to a current Air Force project?

( ) a. YES ( ) b. NO

2. Do you believe this research topic is significant enough that it would have been researched (or contracted) by your organization or another agency if AFIT had not?

( ) a. YES ( ) b. NO

3. The benefits of AFIT research can often be expressed by the equivalent value that your agency achieved/received by virtue of AFIT performing the research. Can you estimate what this research would have cost if it had been accomplished under contract or if it had been done in-house in terms of manpower and/or dollars?

( ) a. MAN-YEARS _____ ( ) b. $_____

4. Often it is not possible to attach equivalent dollar values to research, although the results of the research may, in fact, be important. Whether or not you were able to establish an equivalent value for this research (3. above), what is your estimate of its significance?

( ) a. HIGHLY SIGNIFICANT ( ) b. SIGNIFICANT ( ) c. SLIGHTLY SIGNIFICANT ( ) d. OF NO SIGNIFICANCE

5. AFIT welcomes any further comments you may have on the above questions, or any additional details concerning the current application, future potential, or other value of this research. Please use the bottom part of this questionnaire for your statement(s).

NAME GRADE POSITION

ORGANIZATION LOCATION

STATEMENT(s):

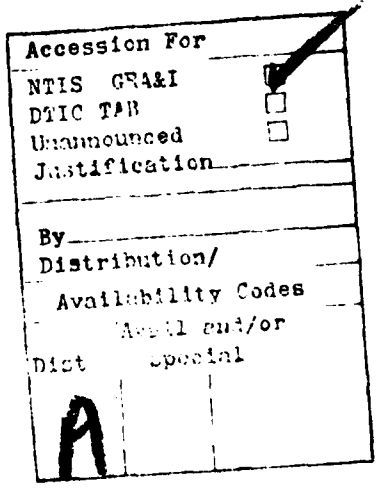

81-12D

Automatic Microwave Network Analyzer Calibration by Reference to a Transmission-Line Standard, with Applications to Characterization of Adapters, Devices, and Coaxial Lines with SMA Connectors

A Dissertation

submitted by

Capt. Joseph Peter DiBeneditto, USAF

In partial fulfillment of the requirements
for the degree of

Doctor of Philosophy

TUFTS UNIVERSITY
October 1981

ABSTRACT

This dissertation describes the development of new techniques for calibrating a microwave automatic network analyzer (hereafter ANA) for complex reflection measurements. These techniques promise significant advantages for miniature connector systems. They include the use of an experimentally-derived characterization of an APC-7 open-circuit termination as a high-reflection calibration standard, adapter correction based on low dissipative losses, and a length of transmission line instead of a sliding load or fixed termination as a low-reflection standard.

Gains afforded by these new techniques are reduced operator intervention during calibration, less wear of the measurement port connectors, lower equipment and maintenance costs, and calibrations referenced to standards truly relevant to the interconnecting transmission medium. Computer memory requirements are increased, but the cost of the increase is insignificant compared to the cost of microwave instrumentation. Slightly longer calibration times are offset by reduced demands upon operator skill.

Methods of extending these calibration techniques to full two-port measurements will be discussed.

ACKNOWLEDGMENTS

I would like to express my sincere thanks and appreciation to M.I.T. Lincoln Laboratory, particularly Richard Dolbec and Walker Merritt, for their immeasurable support and encouragement during my research and for their contribution of countless hours of HP 8542B ANA time without which this dissertation would have been seriously handicapped.

I would also like to especially thank my advisor, Dr. Arthur Uhlir, Jr., for his guidance and assistance during this entire project.

TABLE OF CONTENTS

LIST OF ILLUSTRATIONS

LIST OF TABLES

Automatic Microwave Network Analyzer Calibration by Reference to a Transmission-Line Standard, with Applications to Characterization of Adapters, Devices, and Coaxial Lines with SMA Connectors

INTRODUCTION

The HP 8542B ANA has been the laboratory standard of one-and two-port microwave measurement systems for frequencies up to 18 GHz since its introduction to the electronics marketplace in 1969. Its function is to make highly-repeatable frequency-domain measurements of precise standard terminations, to compute a set of error correction coefficients from these data, to apply these corrections to measurement data of unknown devices, and to output the results in one or more of the many tabular or graphic formats available. In spite of the ANA's twelve-year availability, its calibration procedures have remained essentially unchanged.

The purpose of this dissertation is to present innovative calibration techniques developed during the research for this project. These techniques offer significant benefits compared to the previous calibration procedures.

For one, an experimentally-derived characterization of an APC-7 open circuit's frequency dependence, which very closely corroborates a theoretical characterization (Ref. 1), permits the elimination of offset short circuits as high-reflection calibration standards. Open circuits offer at least two major advantages over offset shorts. First, a single open circuit can be used in a wide-band

calibration (i.e., 2-18 GHz), obviating the need for connection of several offset shorts (one for each band, 2-4, 4-8, 8-12.4, 12.4-18 GHz). As a result, wear of the connectors at the measurement port can be reduced significantly. Connector wear is the fundamental limit on the usefulness of the "stored calibration" principle.

Second, the length of each offset short represents the $\lambda/4$ plane only at the center frequency of each band. Thus, the use of offset shorts can lead to band-edge loss of accuracy.

Further, the adoption and implementation of an adapter correction procedure theorized by A. Uhlir, Jr. (Ref. 2), provided a means by which an APC-7 calibration can be extended for use in any other transmission format without the need for a complete calibration kit in that format. Calibration kits are very expensive and, in the case of SMA (Figs. 90 and 91 show sectioned views of typical SMA connectors and line), the components are extremely delicate, sensitive to wear, and easily damaged even when handled with care. Their use also shortens the useful life of the adapter as a tool for precise measurements.

Furthermore, the employment of a fixed load and a fixed length of transmission line in the exact measurement medium, as a replacement for the air sliding load as a zero-reflection standard, eliminates the discontinuity

errors or ambiguity inherent in attempting to define zero-reflection in a dielectric filled medium (i.e., SMA) with an air-dielectric standard. In addition, the incorporation of a double running average technique to cancel the effect of reflection residuals of the load and line eliminates the errors (or, more rarely, divergences) in the circle-fitting routines incorporated in the standard software for the system.

The combined effect of these developments is to lessen operator interaction, to decrease wear of the measurement port connectors, to reduce the number of required calibration standards, and to diminish certain systematic errors. Thus, the changes presented here improve the functioning of automatic microwave network analyzers and extend their applicability to a wider variety of transmission media.

GENERAL BACKGROUND

The Hewlett-Packard HP 8542B automatic microwave network analyzer (ANA) is the basis for this research although the techniques developed here can readily be adapted for use with other microwave measurement systems. This ANA is a versatile transfer-function measurement system which can make rapid, highly accurate, repeatable measurements of scattering parameters from 110 MHz to 18 GHz in all coaxial and waveguide formats for which standard impedances are available for calibration purposes. This research broadens the domain of suitable standards.

All the research for this document was conducted using the HP 8542A ANA at M.I.T.-Linclon Laboratory which has been updated and modified to be essentially equivalent to an HP 8542B. The most important feature of this updating is crystal-controlled frequency synthesis.

In addition, this system contains several options which make it as powerful and convenient as any more recently developed systems. Three options which proved invaluable throughout this project are the 8500A System Console (Maxi System), the TODS-II Test Oriented Disc System, and the Versatec Matrix 200 plotter.

The 8500A System Console consists of a keyboard, control panel, interface unit, display generator, large-screen CRT display, track ball, and alpha-numeric printer. The TODS-II Disc System provides storage of and ready access to source and data files. A core resident monitor program performs directory search, program loading, and control of the operator terminal. A hard copy of both alphanumeric and graphic data can be obtained from the Versatec Matrix 200 Plotter. A block diagram of the total system is displayed in Figure 1.

All the controlling computer programs were written in Hewlett-Packard combined ATS and ANA BASIC which offered full measurement, computational and output flexibility, required no compilation, and enabled instantaneous line-by-line editing from the operator console. The programs assume that the TODS-II Disc System is available and require at least 8K of usable core memory. They perform all the necessary manipulations for storing data, controlling RF measurements, computing correction coefficients, applying the corrections to Device Under Test (DUT) data, and outputing the results in an appropriate format for meaningful interpretation.

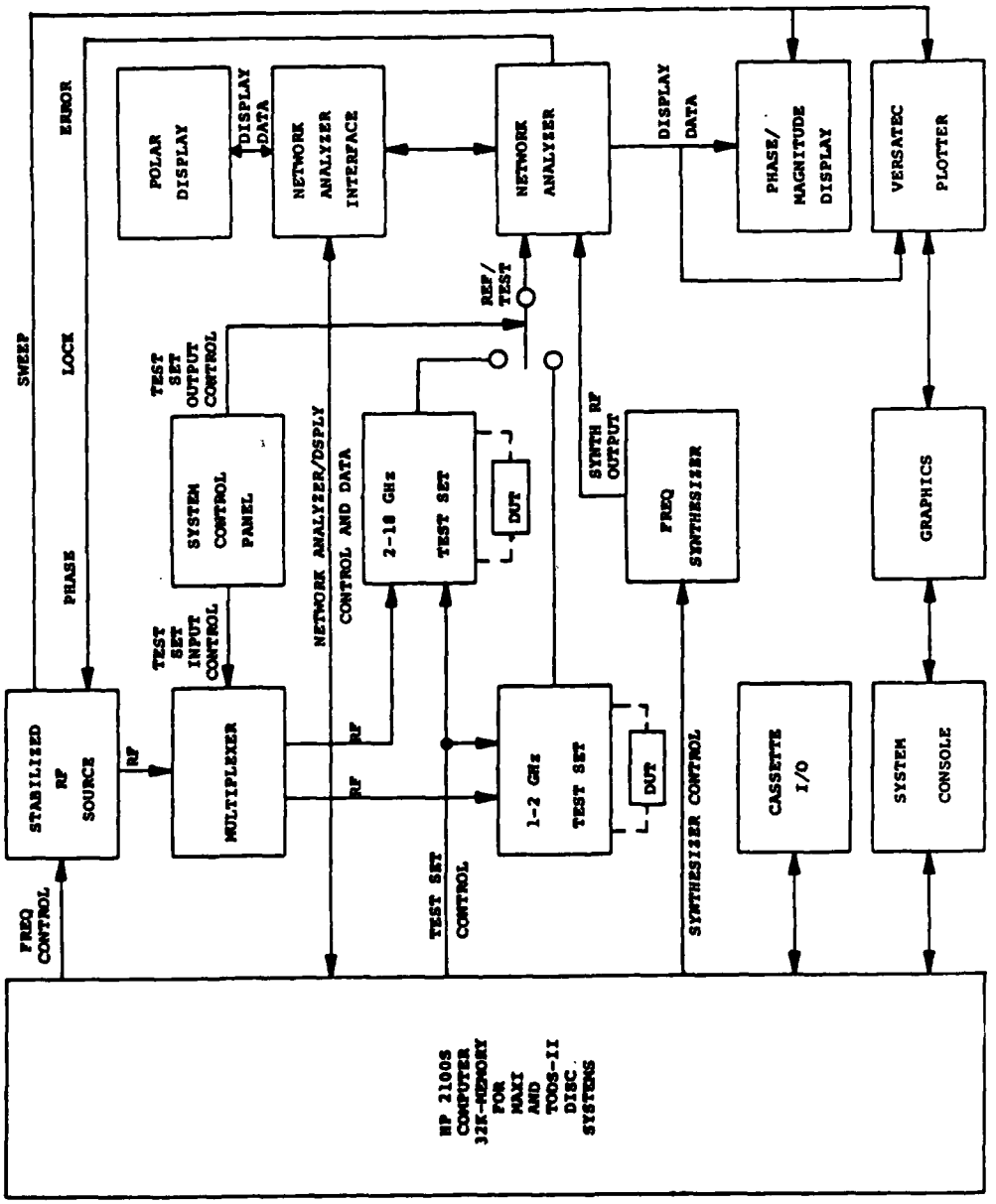

Fig. 1. Block diagram of HP 8542B ANA. (Refs. 4, 5)

The use of BASIC will permit the programs to be adapted to newer ANA models which are exclusively programmed in variants of BASIC. (The HP 8542B would operate faster and have more available memory if the programs were written in FORTRAN.)

FREQUENCY CHARACTERIZATION OF APC-7 OPEN-CIRCUIT REFLECTION

Open-circuit coaxial standards have been generally used only at relatively low frequencies (below 2 GHz) where frequency dependence of phase can be approximated as linear. It appeared that an open circuit would be an excellent reflection standard at all the usable frequencies of the ANA (up to 18 GHz) if a highly accurate, reproducible phase characterization could be experimentally obtained. Recently, a theoretical analysis of the open-circuit capacitance and its frequency dependence has been reported (*Ref.* 1). *Measurements* in 7-mm precision coaxial line, included in that report, were consistent with the theory, but not quite accurate enough conclusively to discriminate against previously reported values.

The HP 8542A ANA used to make the experimental measurements for Ref. 1 did not have the capability of generating synthesized frequencies referenced to a quartz crystal and accurate to 1 part in 10^7 as did the HP 8542B analyzer used for this research. As a result, a more exact experimental corroboration of the theoretical values will be presented. It will also be noted that the relative frequency variation of the "effective position" is smaller than that of the "effective capacitance".

Open circuits are especially convenient high reflection standards when used along with short circuits in the wide band (i.e., 2-18 GHz) calibration of ANA's since the attachment of several different offset shorts (one for each frequency band, 2-4, 4-8, 8-12.4, 12.4-18 GHz) becomes unnecessary: the result being a significant reduction in wear of the measurement port connectors. Additionally, since the length of each offset short represents the $\lambda/4$ plane only at the center frequency of each band, their use can and does lead to noticeable band-edge inaccuracies. These inaccuracies are illustrated in Figs. 2-4, which represent the reflection measurement of an APC-7 open circuit using a standard carefully performed GPM1 calibration of the ANA. Since it is reasonable to expect the reflection of an open circuit to be smooth with respect to frequency, any discontinuities would have to result from the calibration. As can be seen, when the marker was placed on each of these discontinuities, the frequencies returned by the analyzer were indeed 4, 8, and 12.4 GHz. Use of the open circuit instead of offset short circuits should eliminate these anomalies.

Since the profits to be gained by obtaining an accurate reflection characterization of the open circuit seemed so substantial, research was conducted in the

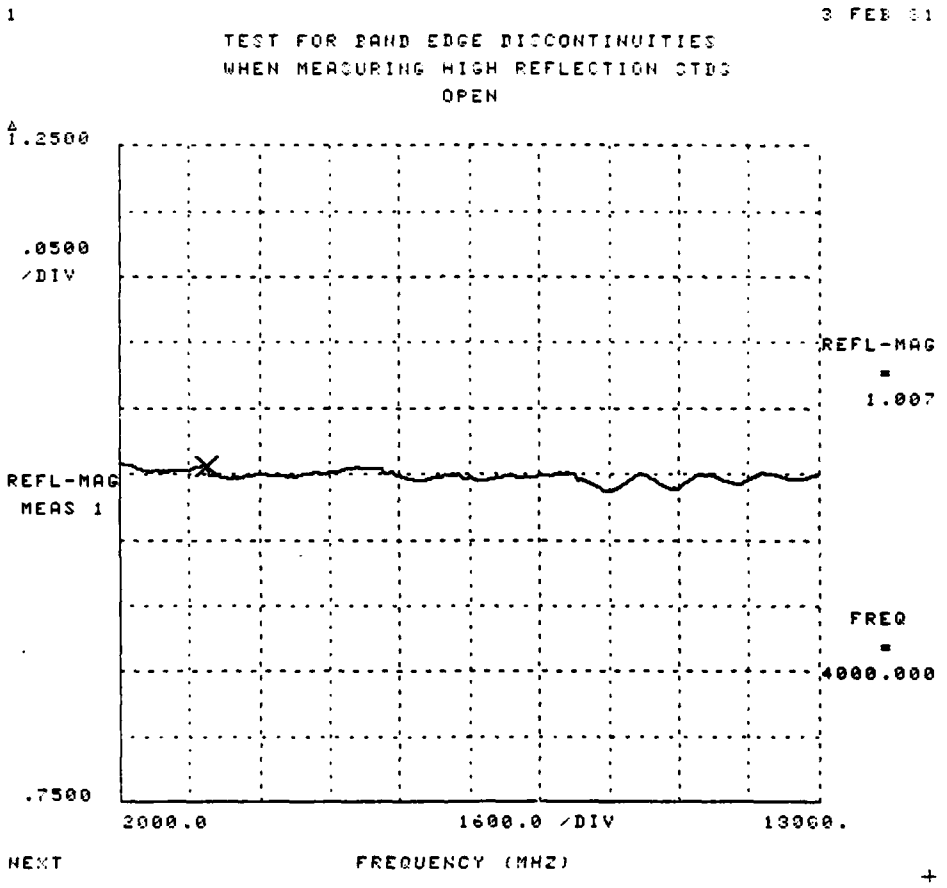

Fig. 2. Illustration of 4 GHz band-edge discontinuity.

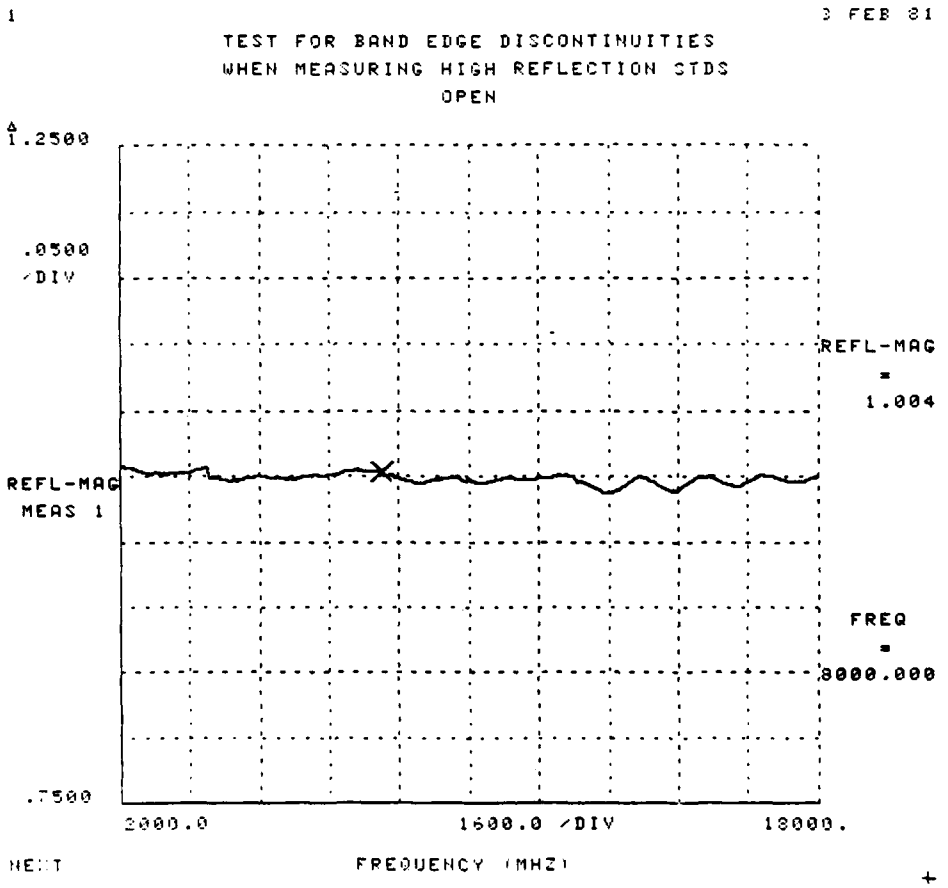

Fig. 3. Illustration of 8 GHz band-edge discontinuity.

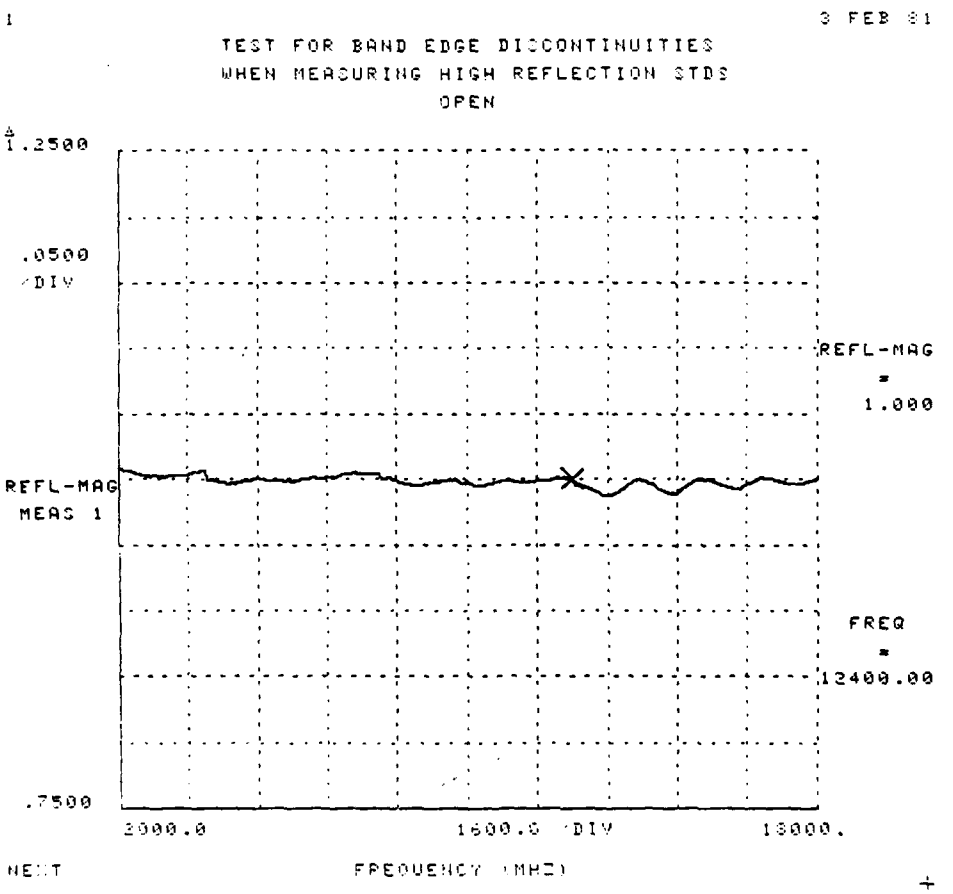

Fig. 4. Illustration of 12.4 GHz band-edge discontinuity.

following manner. The HP 8743A Reflection Test Set (which had been selected for extended frequency use to 18 GHz) was employed throughout.

The trombone delay line of the 8743A was adjusted so that the time delay of the reference path was substantially equal to that of the signal path. This was accomplished by manually sweeping the 8-12.4 GHz frequency band, and adjusting the delay line until the display of the reflection for a zero-plane short circuit on the HP 8414 Polar display approximated a dot. This precaution minimizes the effect of frequency jitter, if any.

A standard HP 7-mm calibration kit and air sliding load provided the necessary reflection standards for the calibration of the ANA. Previous measurements made with this calibration kit laid suspicion that the actual constructed lengths of the offset shorts differed from those specified (Ref. 3). Therefore, the offset shorts were measured using a Starrett Model 653P Dial Comparator. Several measurements were performed around the center conductor of each offset short to establish that the shorting plane was indeed perpendicular to the line (no exceptions were noted). However, Table 1 shows that the nominal lengths differed from the measured lengths by as much as .12-mm. As a result, the measured lengths were used in all calculations.

Offset Number	Nominal Length (mm)	Measured Length (mm)	Difference (mm)
4	63.44	63.32	.12
5	31.70	31.65	.05
6	18.66	18.58	.08
7	13.36	13.29	.07

Table 1 - Nominal and measured lengths of HP APC-7 offset shorts.

To obviate the possibility of interaction between zero-length short circuit and the APC-7 bead, offset shorts were used for both the reference plane and the offset reflection plane. Special software was developed using the HP error-correction algorithms but which allowed specification of the offset lengths for both planes. Corrected reflection measurements were then made of the open circuit.

Special attention was given to frequencies where the difference between the two offset lengths was nearly $\lambda/4$, where calibration accuracy is expected to be optimum. For each of these frequencies, four sliding load measurements were taken, each with the load displaced by $\lambda/8$. A complex average of these measurements was then used to establish the residual reflection. This technique differed from HP's which uses a circle fitting routine to find the residual. In some cases, where the load approaches ideal and noise is present in the measurements, HP's circle-fitting routine could diverge and thus give a defective calibration. The complex average, however, can never yield a result worse than the largest single measurement in the average, and clearly cannot suffer from inaccuracies due to divergences. Principal weight was given to each of the favored frequencies mentioned and to the fact that the phase of the open circuit must be zero at zero frequency in the curve fitting. However, a-

greement at other frequencies was found to be so good that these precautions may not have been necessary.

Using standard linear regression techniques to reduce the data, the following frequency characterization was obtained, where $\Delta\phi$ is the excess (capacitive) phase of the open circuit, in radians, and f is frequency in megahertz:

$$\Delta\phi = (5.02 \times 10^{-5})f + (1.126 \times 10^{-14})f^3 \qquad (1)$$

This result implies that the "effective position" of the open circuit lies beyond the physical end of the center conductor by a distance d(f) in millimeters given by:

$$d(f) = 1.198 + 2.69 \times 10^{-10} f^2 \qquad (2)$$

For comparison with other work, the effective capacitance is calculated from

$$C_e = \frac{1}{2\pi (fx10^6) Z_o} \tan \frac{\Delta\phi}{2} \qquad (3)$$

where Z_o is characteristic impedance of the transmission line being used.

The empirical results for the effective position and effective capacitance are tabulated in Table 2 along with the theoretical results given in Ref. 1, where the interpolation formula

$$C_e = 79.70 \sqrt{1 - (f/34450)^2} \qquad (4)$$

is suggested.

Table 2 shows that representation by effective position (beyond the physical end of the center conductor) is less frequency-dependent than the effective capacitance representation. Thus, the effective position varies by 7 percent, while the effective capacitance varies 18 percent, from 0-18 GHz.

From similitude, the effective position (or capacitance) for 14-mm line (at half the frequency) should be twice that for 7-mm line. The 14 mm GR900-WO open circuit has a closed end, however, while the 7 mm open circuits in general use have open ends. By applying similitude to measurements on closed-end 7-mm open circuits, we find that no measurable difference in effective position could be attributed to this constructional difference. Thus, the effective position for 14-mm line would range from 2.40 mm at 1 GHz to 2.57 mm at 9 GHz. This range falls within the specifications for the GR900-WO (2.40 - 2.80 mm)

Frequency (MHz)	Effective Position Empirical (mm), Eq. 2	Equivalent Capacitance Empirical (fF), Eq. 1, 3	Theory, Ref. 1
1000	1.198	79.9	79.7
2000	1.199	80.0	79.8
5000	1.205	80.0	80.5
8000	1.215	82.2	81.9
11000	1.231	84.3	84.1
14000	1.251	97.4	87.2
16000	1.267	90.0	90.0
18000	1.285	93.1	93.5

Table 2 - Comparison of empirical results to theory for APC-7 open circuit phase.

and leads to a much tighter definition of the 14-mm open circuit than one could hope to establish with a precision slotted line.

The empirical characterization of the open circuit presented here was undertaken prior to the publication of the theoretical frequency dependence. Initial close agreement between the two characterizations was so impressive, when the nominal lengths of the offset shorts were used, that we were inspired to measure the offset shorts. The substitution of these measured lengths for the nominal lengths reduced the difference from 3 percent to less than 0.5 percent between the two characterizations.

Also, ANA calibrations ordinarily include a flat short circuit placed directly at the connection plane of the conductor. The characterization of the open circuit was repeated using this more conventional standard along with the measured offset short circuits. Over the 2-18 GHz range, the deviation in reflection phase between this characterization and the previous one was nowhere greater than 0.5 degrees (See Table 3). This observation indicates that interaction between the zero-plane short and the measuring port bead is negligible.

Based on these results, it is apparent that frequency-corrected open circuits can replace offset

Frequency (MHz)	Measurement of open circuit phase based on zero-plane short circuit calibration (degrees)	$-\Delta\phi$, Eq. 1 (degrees)
2000	-5.9	-5.8
3000	-8.4	-8.7
4000	-11.0	-11.5
6000	-17.2	-17.4
8000	-23.3	-23.3
10200	-29.7	-30.0
12000	-35.8	-35.6
12400	-36.7	-36.9
14000	-41.6	-42.0
14600	-43.7	-44.0
16000	-48.5	-48.7
18000	-55.3	-55.5

Table 3 - APC-7 open circuit phase measurements based on zero-plane short circuit calibration compared to empirically derived $\Delta\phi$.

shorts as high reflection standards with no loss of phase accuracy, compared to the specified accuracy of the HP 8542B (reflection phase, from 1^{o} at 2 GHz to 1.5^{o} at 18 GHz).

ADAPTER CORRECTION

Since the HP 8542B is equipped with APC-7 precision connectors, the discussion of the previous section shows how a wide-band calibration can be accomplished without the need for multiple connections of offset short circuits in this primary connector system. However, there are so many different kinds of transmission-lines, waveguides, and connector types in general use today that it would be entirely impractical to construct a measurement system based on each type available. Therefore, the only reasonable solution to this measurement dilemma is to perform these measurements through passive, reciprocal adapters which form a transition between the primary connector system and that of the DUT (secondary connector system). The present method for carrying out measurements in the secondary connector system requires that a complete calibration be made (including offset shorts) in this connecting system. As a result, this technique requires that a complete calibration kit be maintained in every connector and transmission format used in measurements.

The cost of obtaining and maintaining an extensive inventory of these calibration kits is astounding and can be prohibitive when appreciable engineering is required to design and prove them. For example, all the arguments

presented in the previous section against the need for connection of several offset shorts in APC-7 applies even more dramatically to SMA lines which are more delicate and easily damaged. Wear of these connectors is an important factor and, ideally, the adapters and standards would have to be replaced at frequent intervals. The cost of this proposition makes it impractical and unrealistic for most applications. Aside from this cost factor, any procedure requiring many interconnections for each calibration may be unreliable when wear is of primary concern.

Of course, all measurements depend upon the quality of the contacts made to the actual DUT. The probability of acquiring an accurate calibration would definitely be increased, however, if fewer contacts are made during calibration. The technique put forward in the previous section of using an open circuit characterization to replace the offset shorts, is equally impractical, because a different characterization would not only have to be made for each connector type, but also for each sex of type. Pin lengths of no inherent significance to the connection would enter into some of the open-circuit characterizations and would, therefore, have to be controlled.

Further complicating the problem would be the questionable propriety of mating an air open-circuit

standard to a dielectric-filled connection system. A theoretical characterization would, at least, be more difficult than the case already solved.

For these reasons, an alternative approach of accounting for the adapter calibration was adopted. It employs the approximation of treating the adapter as dissipationless (Ref. 2). This approximation is not at all unreasonable since all precision adapters are constructed from good dielectrics and good conducting surfaces. Under the dissipationless assumption, one needs only a zero-reflection standard to adjust for chart center and a zero-plane short circuit to define phase at the secondary port connector.

As prescribed by this adapter correction technique, the ANA is calibrated for reflection measurements at the primary connector port according to the methods described in the previous section. Then the adapter is attached and connected with what is assumed to be an ideal termination. This ideal termination can be simulated by a precision fixed load, an air sliding load or by an improved technique where a line and fixed load are computer averaged as discussed in a later section under Double Running Average.

For each frequency, a measurement is made of the thus-terminated adapter, corrected with respect to the primary connector calibration and stored as M_L. Then the adapter is terminated with a zero-plane short circuit, the same type of correction measurement is accomplished and stored as M_S. Lastly, reflection measurements are made on the adapter and DUT, likewise corrected with respect to the primary connector port and stored as M_D. Then the computer performs the necessary manipulations to correct M_D for reference with respect to the secondary connector and represented by the reflection Γ_D.

By letting S represent the scattering matrix of the adapter where port 1 is the primary connector and port 2 the secondary, then

$$M_D = S_{11} + \frac{S_{21}^2 \Gamma_D}{1 - S_{22} \Gamma_D} \tag{5}$$

After applying the principles of reciprocity and conservation of power the following formula for adapter correction is derived (Ref. 2).

$$\Gamma_D = \frac{M_D - M_L}{1 - M_L^* M_D} e^{-j2\theta} \tag{6}$$

where M_L^* is the complex conjugate of M_L and the phase factor, $e^{-j2\theta}$, is now to be determined.

With the short circuit as a phase reference, Γ_D must be equal to -1. Therefore, substituting M_S for M_D and -1 for Γ_D one obtains:

$$-1 = \frac{M_S - M_L}{1 - M_S M_L^*} e^{-j2\theta} \tag{7}$$

or

$$e^{-j2\theta} = \frac{1 - M_S M_L^*}{M_L - M_S} \tag{8}$$

where M_L, M_S, M_L, M_L^* are all known, allowing calculation of phase factor $e^{-j2\theta}$.

If E1 represents the computer calculation of

$$\frac{1 - M_S M_L^*}{M_L - M_S} \tag{9}$$

then the complete complex solution for the adapter correction becomes

$$\Gamma_D = \frac{M_D - M_L}{1 - M_D M_L^*} \quad [E1] \tag{10}$$

Since $|e^{-j2\theta}|$ must always equal 1, and, because limitations on significance in computer calculations may not yield a result where $|E1| = 1$, E1 is normalized by dividing E1 by its magnitude $|E1|$ before applying it to the final adapter correction.

The analysis has been presented for a single frequency. The computer can easily perform these manipulations for many frequencies in little time.

Since a great proportion of analyzer measurements are being accomplished through adapters to other connection formats, such as SMA, this technique drastically simplifies calibration procedures for secondary connector types. In addition, it reduces the chances of error in calibrations of connector types, such as SMA, which are extremely susceptible to lossy connections, by requiring connection of fewer standards in that format. The accuracy of all measurements are limited by the quality of the DUT connections, but calibration errors due to possible poor connection of multiple standards is minimized. Furthermore, a recalibration is not necessary when the adapter type is changed. Only the measurement of the new adapter terminated by, first, its matched load, and, second, its zero-plane short circuit need be reaccomplished in order to modify the adapter corrections for the new connector type. This feature offers the advantage of a great

time savings when measurements are to be made in more than one connector or transmission format at the same time.

Considerable interchanging of adapters is necessary for the measurement of non-insertable two-ports (e.g., devices with two connectors of the same sex). The application of the adapter correction technique to this case will be discussed under Extension of Adapter Correction to Two-Port Device De-Embedding.

CHARACTERIZATION OF PERFECTLY MATCHED TERMINATION

In the absence of a perfectly matched termination in the real world, beadless air-dielectric sliding loads have been the standard of choice for calibrating the HP 8542B ANA. Three or more measurements must be made on the sliding load at each frequency. Then a circle fitting algorithm (CENT) must be applied to find the center of the complex circle circumscribed by these points (the center representing the reflection of an ideal load)(Ref. 6). There are at least four major drawbacks to this method of characterization.

First, in using a sliding load for measurements over wide frequency bands, three positions will not suffice for accuracy. Four or five measurements at each frequency are required and choosing the length of each slide so that the measurements form a relatively well defined circle at all frequencies is no trivial matter. Second, the CENT program used for the circle fitting can diverge and introduce large errors, when used to fit data collected on a load which approaches perfect at some frequencies and which may be displaced by noise in the measurements. The above problems have been studied (Ref. 7). That is, the optimum pattern of slides to minimize the errors introduced by the CENT program has been sought for

broad-band calibration. In addition, of course, one must expect errors in the measurement process.

Third, this established method of calibration makes no use of information at other frequencies to assist in the calibration at any particular frequency. Fourth, some connection systems (e.g., the popular SMA system) are based on the concept of complete filling with a solid dielectric ($\varepsilon \approx 2.08$) throughout the connectors and transmission line. The use of an air-dielectric sliding load as a standard in a solid-dielectric transmission format can be expected to lead to measurable error at relatively high frequencies within the operating range of this connection format. Ideally, the reflection coefficient of a standard should be specified with respect to the transmission system used to interconnect the components or DUT.

The last problem could be addressed by applying a correction when an air-dielectric standard is used. The diameter changes implied by a dielectric constant can be expected to lead to a discontinuity capacitance at the transition from dielectric to air. This discontinuity capacitance can be theoretically estimated and applied as a small correction, its importance increasing with frequency. Our experimental investigations of this matter

quickly showed that practical connectors introduced much larger discrepancies (with more complicated frequency dependence) than the estimated discontinuity capacitance. As a result, it was considered all the more important to be able to use practical terminations as low reflection standards, when evaluating devices intended for use with such interconnecting systems.

The policy of using a physical transmission line and a fixed load as a standard of zero reflection has long been advocated for swept-frequency measurement of reflection magnitude (Refs. 8, 9, 10). These methods only had the capability of dealing with reflection magnitudes and were not capable of extracting phase information from the measurements. On the contrary, implementation of a similar policy on the ANA is not only convenient, but is also capable of performing and recording phase measurements.

A time-domain reflectometer has been synthesized in software (TIMED) by Fourier transformation of reflection data obtained in the frequency domain with an ANA (Ref. 11). In the time domain, the reflection from an imperfect termination of a finite length of transmission line can easily be identified. One could replace this time-domain reflection by an extrapolation equivalent to a

perfect termination. The inverse Fourier transform would then provide, at all frequencies, the equivalent of calibration measurements on a perfect load.

The discussion of TIMED indicates that wide-band measurements of a fixed length of imperfectly terminated transmission line should contain the information necessary to characterize a perfectly matched termination. However, the present research has established the validity of a simpler method, using only frequencies in the general vicinity of the particular frequency of interest (frequency window).

Recently, the development of 3.5 mm air-dielectric line (WSMA) was purported to relieve "nagging SMA measurement problems" (Ref. 12). However, this approach still does not avoid the compromise of defining a zero reflection standard for a dielectric environment using air lines as standards. The method to be presented here provides a practical solution to all of the four problems mentioned above.

The errors in the reflection measurement are assumed to be linear, as in the present calibration procedures for the HP 8542B. The ultimate goal is to determine the uncorrected reading that would be given by the system if a perfect load was obtainable: "perfect" here meaning a match to the intended connecting system. Since no

"perfect load" is physically available, this is accomplished by making a corrected measurement of reflection for a practical load. This reading will be referred to as the reflection residual of the load or, simply, residua (Γ_R). After these measurements are acquired for each frequency, they can be applied as corrections to measurements on DUT's thereby synthesizing a "perfect load" reference.

The method of characterizing a perfect load (without resorting to Fourier analysis) is based on the assumption that the system errors vary relatively slowly with frequency. Relatively slowly means that the round-trip reflection delay time T for the transmission line being used as a standard is such that the variation in the system error may be neglected over a frequency interval 1/T. Also assumed is that the imperfect termination has a reflection coefficient whose magnitude also varies relatively slowly with frequency in the same sense. The reflection coefficient of the load is considered to include that of the connector used to attach it to the end of the transmission line. Even with this inclusion, the frequency dependence of the physical load would be expected, on the grounds of small size and nonresonant design, to be less of a problem than the system errors.

The input reflection coefficient of such a terminated line of electrical length ℓ would be

$$\Gamma = e^{-2\alpha\ell}\, e^{-2j\beta\ell}\, \Gamma_L \qquad (11)$$

where α is the attenuation constant, β is the propagation constant ($R * f$ where $R = 2.0965 \times 10^{-4}$ radians/MHz/cm in air and f is frequency in MHz), and Γ_L is the reflection coefficient of the imperfect load. Substituting $R * f$ for β and rearranging Eq. (11) yields

$$\Gamma = e^{-2\alpha\ell}\, e^{-2jR\ell f}\, \Gamma_L \qquad (12)$$

If the frequency dependence of α, R, and Γ_L can be neglected, the input reflection will describe a circle as frequency is varied. The average of this complex reflection over a frequency interval 1/T (frequency window), being the center of this circle, will vanish.

However, because the reflectometer used for measurement is not perfect, the input reflection will still trace a circle, but the center of the circle will be offset from zero due to system errors. The input reflection can be represented as

$$\Gamma = \Gamma_R + A\, e^{-2jR\ell f}\, \Gamma_L \qquad (13)$$

where $A = e^{-2\alpha\ell}$ and $\Gamma_L = |\Gamma_L| e^{j\theta_L}$. If the frequency dependence of Γ_L is neglected over one cycle, θ_L is a constant, and Γ_R is the center of the circle representing the system error and is usually accepted as being an approximation to the uncorrected measurement of a perfect load.

The real and imaginary components of Γ become

$$\text{Re}\,[\Gamma] = \text{Re}\,[\Gamma_R] + A|\Gamma_L| \cos\,(2R\ell f - \theta_L) \qquad (14)$$

and

$$\text{Imag}\,[\Gamma] = \text{Imag}\,[\Gamma_R] - A|\Gamma_L| \sin\,(2R\ell f - \theta_L) \qquad (15)$$

which are clearly the sum of a constant (reflection residual or system error) and a sinusoidal component (ripple factor) caused by the imperfect load.

Since the network analyzer is capable of making complex reflection measurements, a rather simple algo-

rithm can be used to average out the sinusoidal components. This running average is, therefore, equivalent to applying a low-pass* filter yielding an adjusted $\Gamma_a = \Gamma_R$ which can now be used to correct for the reflection residuals (system error).

Two variations of this running average technique were investigated for this project and each will be described in detail shortly. A Single Running Average Technique was effective, but required a minimum of 23 points per cycle for the average. However, a Double Running Average became the filter of choice for the new HP 8542B calibration technique, because it offered the same effectiveness as the Single Running Average while only requiring 10 points to compute the average.

The initial attempts to apply the above procedures (calculating the Single Running Averages of the real and imaginary parts of the uncorrected reflection coefficient) did not work well at all. The system errors, particularly in K_u band, did not satisfy the condition of being slowly varying over the 168 MHz frequency interval required by the reference line of 89.4 cm. electrical length used. The prospect of using a longer line and closer spaced frequencies was unattractive.

---

*low-pass in the time domain

Fortunately, it was conjectured subsequently that these variations must be caused by echos within the long lines inside the analyzer and were, therefore, a part of every uncorrected or raw measurement. Consequently, complex division of any raw measurement by the raw reflection measurement of a short circuit should eliminate these variations greatly reducing the frequency dependence of the errors. In fact, this relatively simple partial correction of normalizing by division did suppress the apparent echoes and revealed the sinusoidal periodicity well enough to conduct a plausible running average. One can remultiply the averaged quotient by the raw measurement of the short circuit to establish the "raw measurement" one would have obtained if the reference transmission line was terminated perfectly. Of course, any high-reflection standard could be used for the normalizing. This concept afforded the possibility of calibrating the ANA without the need for a sliding load.

Figure 5 shows the real part of a normalized reflection coefficient measurement of a terminated SMA line with an electrical length of 89.4 cm. superimposed by the single running average. Normalization was accomplished by dividing the uncorrected measurements by the uncorrected measurements of a short circuit placed at the SMA end of the adapter. The Single Running Average is based

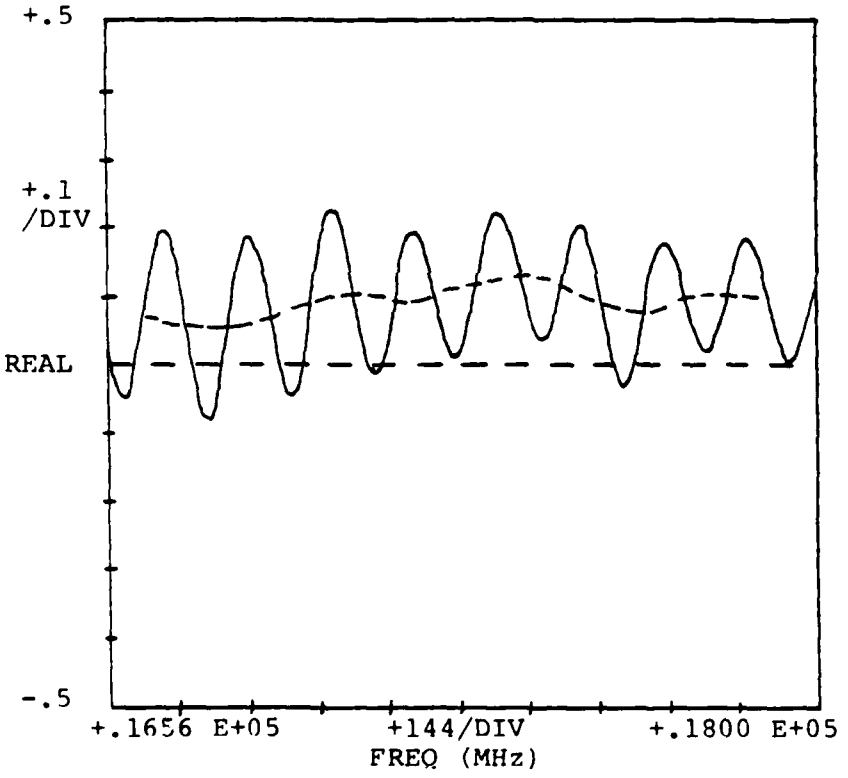

Fig. 5. Results of Single Running Average using 23 points per cycle.

on 23 points equally spaced in frequency. Thus, the imperfections of the load are manifested in the variations having a period of 168 MHz in the frequency domain.

It was initially hoped that this technique of employing a running average could be adopted as a general replacement for sliding loads, but subsequent experimentation revealed that for APC-7 lines with their excellent impedance characteristics, precision connectors, and air environment, the established method of employing a sliding load for characterization could not be improved upon. Therefore, the sliding load technique was retained for APC-7 calibrations. However, for connection systems such as SMA, where the dielectric filling and the extreme fragility of sliding loads makes the whole concept of referencing against transmission lines more relevant, the results were remarkably satisfying. As a result, the averaging technique was adopted to characterize a perfect load for the adapter correction sequence.

Hence, the following calibration procedures for the HP 8542B were developed. The system is first calibrated in APC-7 using the short, open, and sliding load as standards at all measurement frequencies for APC-7 or at all frequencies necessary to perform a running average for adapter corrected measurements. If adapter correction is

called for, then measurements are made on the adapter and short and then on the adapter and transmission line reference. These measurements are then corrected against the APC-7 calibration. Since this step corrects the transmission line measurements for system errors, it became unnecessary to perform the normalization described earlier while still attaining the same results. The Double Running Average is then computed and stored.

Measurements are then carried out on the adapter and DUT at the ultimate frequencies of interest, corrected against the APC-7 calibration, and then adapter corrected. The results are output in any of a variety of formats. Repeat measurements can be readily performed on the same adapter without recalibration.

Another important factor is that when employing a computer with sufficiently large storage capacity, a change of adapter can be achieved by simply redoing the adapter correction sequence. Present procedures for HP 8542B require a complete calibration in the new transmission format, an extremely tedious operation with ever present hazards of normal wear, or of abnormal wear on adapter or standards from misconnection or improper tightening.

The new calibration procedures described here offer the following advantages. The number of standards in the APC-7 cal kit are reduced, calibration kits in other transmission formats become unnecessary, sliding loads other than APC-7 are eliminated, and operator interaction is reduced. The benefits far outweigh the relatively minor drawbacks of slightly longer computation time and the increased computer memory (a very inexpensive commodity today).

SINGLE RUNNING AVERAGE

The Single Running Average was the first filtering technique investigated for this study. Even though it was eventually abandoned in favor of the Double Running Average (to be discussed later), valuable information was gained during the experimentation which was directly beneficial to the application of the Double Running Average. It is of significance to note here that the Single Running Average was not replaced because it did not function well, but because it required a minimum sample size of 23 points per cycle in order to work adequately.

Figure 5 shows the corrected real component of a reflection measurement of a terminated 89.4 cm SMA line superimposed with its Single Running Average. Twenty-three samples per cycle were used, and, as can be seen, the ripple factors are diminished to an extent that they are rendered invisible. In Fig. 6, the real component for the same line is presented superimposed by a Single Running Average with a sample size of 21 points per cycle. The ripple factor has clearly become visible in this plot. After thorough investigation, the conclusion was reached that a minimum of 23 samples per cycle were required for the single running average.

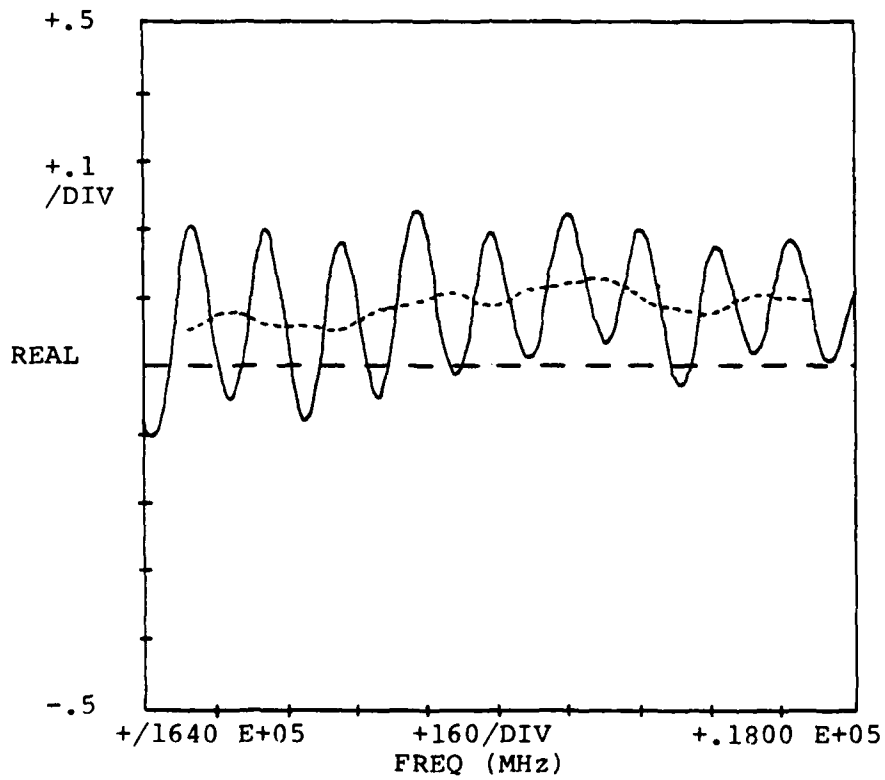

Fig. 6. Results of Single Running Average using 21 points per cycle.

The Single Running Average was set up and computed in the following manner. A frequency window, ΔF, was chosen such that $2R\ell\ \Delta F = 2\pi$ and then the input reflection Γ is measured at n equispaced points, $f_1,\ldots,f_n$, separated by a frequency interval, Δf, where $n \geq 23$ and odd such that $(n-1)\Delta f = \Delta F$. The real and imaginary components of Γ are then averaged over ΔF weighting the redundant end points (Fig. 7a). These end points were weighted by 1/2, and their combined total treated as one point to obviate the chance of biasing caused by the redundancy. The sinusoidal ripple factors vanish leaving an adjusted $\Gamma = \Gamma_R$ for $f_{\frac{n-1}{2}}$ the center frequency of ΔF (Fig. 7b).

Two separate and distinct methods of employing the Single Running Average were developed, each having its own advantages under different circumstances. The first method, called discrete running average, was set up by simply measuring Γ at $\frac{n-1}{2}\Delta f$ frequency intervals each side of the frequencies of interest (FI's) and applying the algorithm exactly as described above. This method was particularly suited for wide band measurements where the FI's are far apart (where difference between adjacent FI's > ΔF). Indeed, the discrete running average was adaptable to most any interval of FI's, but suffered from the following disadvantages. First, a minimum of 23 dis-

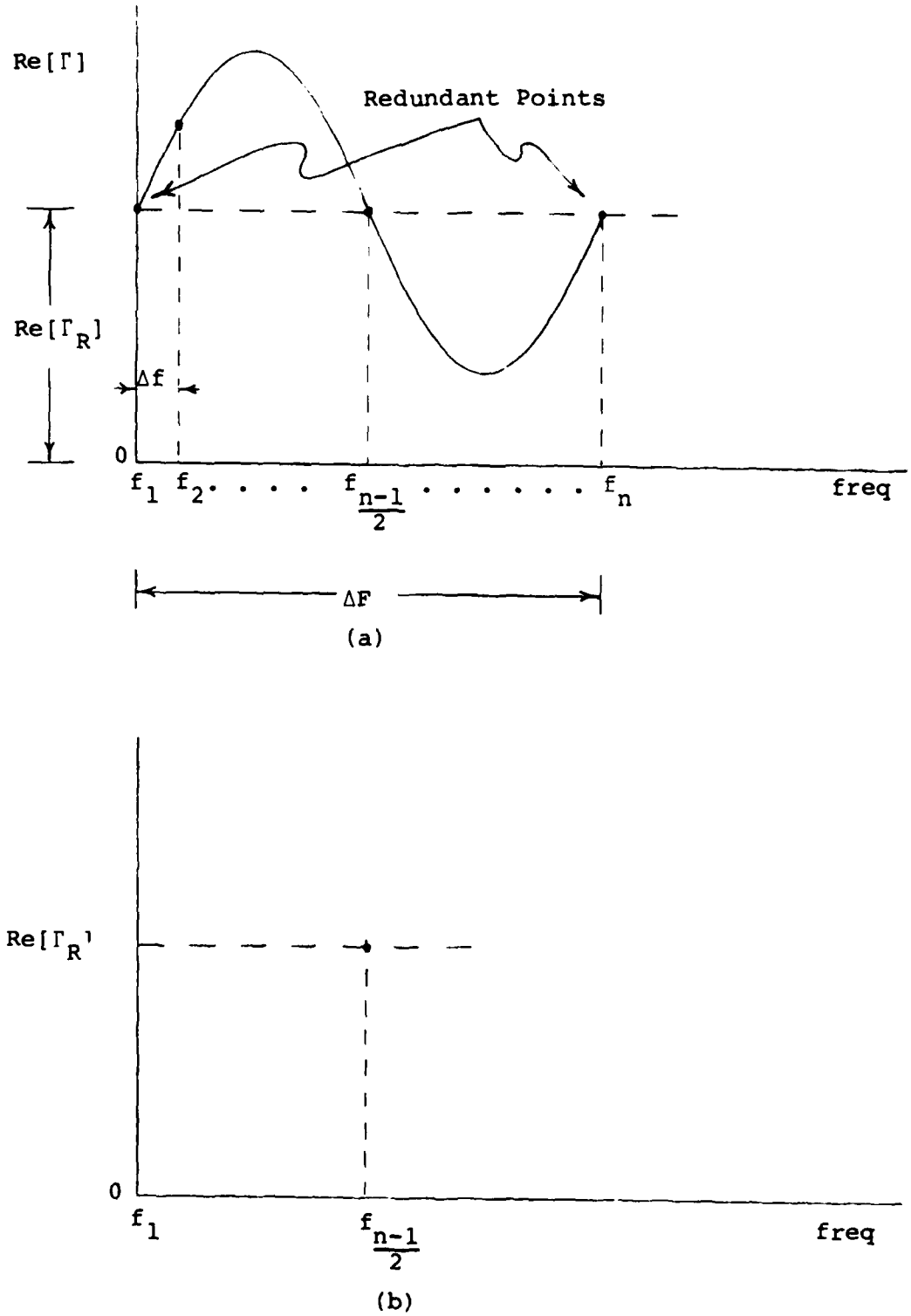

Fig. 7. Plot of Re[Γ] (a) before and (b) after averaging.

tinct measurements were required for each FI resulting in the need for large amounts of computer storage for computation. Also, since the complete algoithm had to be computed for each frequency of interest, the algorithm was rather slow.

A second method, called a sliding running average, was conceived which could handle the special case where the difference between adjacent FI's = Δf. This algorithm was particularly suitable for relatively narrow-band measurements and offered the advantages of reduced storage requirements and remarkably faster speed.

For the first FI (FI_1), the discrete method was used to compute the running average. However, since the difference between adjacent FI's equals Δf, the calculation of the algorithm for $FI_2, \ldots, FI_m$ was much simpler. Since

$$\Gamma_{FI_1} = \frac{\Gamma_{f_1}/2 + \Gamma_{f_2} + \Gamma_{f_3} + \ldots + \Gamma_{f_{n-1}} + \Gamma_{f_n}/2}{n - 1} \qquad (16)$$

and

$$\Gamma_{FI_2} = \frac{\Gamma_{f_2}/2 + \Gamma_{f_3} + \Gamma_{f_4} + \ldots \Gamma_{f_n} + \Gamma_{f_{n+1}}/2}{n - 1} \qquad (17)$$

Then Γ_{FI_2} could be quickly calculated by subtracting $\frac{\Gamma_{f_1}}{2(n-1)}$ and $\frac{\Gamma_{f_2}}{2(n-1)}$ and by adding $\frac{\Gamma_{f_n}}{2(n-1)}$ and $\frac{\Gamma_{f_{n+1}}}{2(n-1)}$ to Γ_{FI_1}. For $FI_3,\ldots, FI_m$, the process is repeated in the same manner. This process eliminated the need for storing measurements at overlapping frequencies and greatly reduced the number of calculations required for second and succeeding Γ_{FI}'s.

The disadvantages of this method were that it was only adaptable to the special cases where measurements are being made over a relatively narrow band and that the frequency spacing was limited to Δf.

Since the Single Running Average required such a large sample size to compute, investigations into another running average technique ensued. Several aspects of the discrete and sliding average proved to be useful in the development of the Double Running Average Technique, to be discussed next.

DOUBLE RUNNING AVERAGE

Because the number of points per cycle necessary to compute the Single Running Average was so large, it was hoped that another digital low-pass filter could be found which was much more efficient (i.e. required fewer points per cycle).

A computationally-simple candidate was the Double Running Average. First, the Single Running Average is applied to the corrected real and imaginary measurements on the load. Then the resulting data is Single Running Averaged again to obtain the final result at the frequency of interest. Thus, the corrected real and imaginary measurements are subject to a Double Running Average. This process is equivalent to a single weighted average with a triangular set of weights, but avoids multiplications.

This procedure also had the gratifying effect of reducing the number of measurement points required per cycle of ripple from 23 to 5 for an equally satisfactory suppression of the ripple. However, as a factor of safety, 7 measurements per cycle were adopted for the technique.

Mathematically, the Double Running Average is computed in the following manner. Treatment of the real component will be described. The imaginary component is found in exactly the same way.

A frequency window of $2\Delta F$ must be used where $2R\ell\ \Delta F = 2\pi$ (frequency window must be two cycles wide). The system-corrected measurements of the reflection A(I) are obtained at 4M + 1 equispaced points, $f_1, \ldots,$ $f_{2M+1}, \ldots, f_{4M+1}$, separated by a frequency interval, Δf, where $M \geq 3$ such that $2M\Delta f = \Delta F$, and where f_{2M+1} is the FI. Let B(I) = Re[A(I)] at each frequency, then for J = M + 1 to 3M + 1 let

$$D(J) = \frac{B(J-M)}{2} + \sum_{K=J-M+1}^{J+M-1} B(K) + \frac{B(J+M)}{2} \qquad (18)$$

As in the case for the Single Running Average the redundant end points are weighted by 1/2 and their combined weight is treated as one point in the average.

The second average is now computed yielding

$$R(N) = \frac{\frac{D(N-M)}{2} + \sum_{P=N-M+1}^{N+M-1} D(P) + \frac{D(N+M)}{2}}{36} \qquad (19)$$

where N = 2M + 1 or f_N is the FI. As can be seen, the redundant end points are weighted and treated in the same manner as above. Figure 8 shows a pictorial view of the progression of the averages.

As in the case of the Single Running Average, there are two different methods of employing the Double Running Average, discrete and sliding. Of particular significance, however, is that in both the discrete and sliding Double Running Average, the first application of the Single Running Average lends itself well to the use of the Sliding Running Average. A considerable reduction in memory fetches and computation time are realized by taking advantage of this simplification.

In the case where measurements are being made in such a way that ultimate FI's in the Double Running Average are equispaced Δf apart, the sliding average principal can be applied to both the first and second Single Running Averages resulting in an even greater savings of computation time and an extra benefit of reduced computer memory requirements compared to the discrete Double Running Average technique. This technique, however, is subject to the same limitations discussed under the sliding Single Running average of being only useful over relatively narrow bands and of having a frequency spacing limited to Δf.

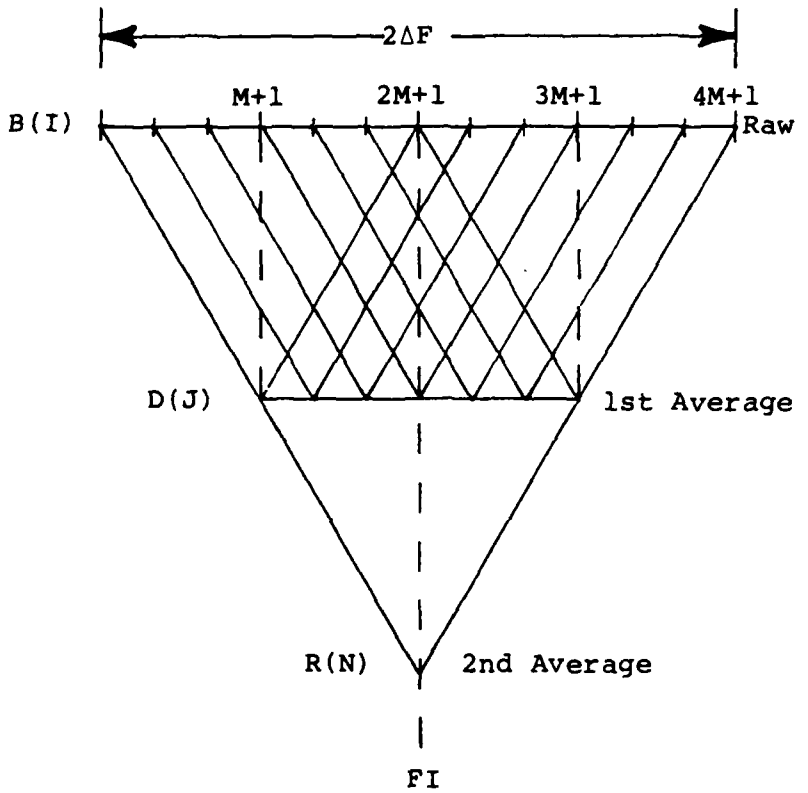

Fig. 8. Diagram showing progression of averages in Double Running Average.

Adoption of the Double Running Average over the Single Running Average resulted in a 70% reduction in the required number of points per cycle while only increasing the number of computations by approximately 23%. On a computer with only 8K of memory, the decrease in storage requirements was a much more important factor than computation time. In fact, investigations showed that the computation time was fast enough that the increase was hardly noticeable.

The minimum number of samples per cycle required for the Double Running Average was experimentally found to be five (Fig. 9). This number is only slightly larger than the theoretical limit of three imposed by the Sampling Theorem for a periodic waveform. In most practical applications of this theorem, the limit is usually accepted to be twice the theoretical limit as a factor of safety. Therefore, the seven samples per cycle used for the Double Running Average appeared to be the smallest odd number of samples which could reasonably be expected to perform successfully in a practical sense.

Since the Double Running Average did an equally good job of removing the ripple factor as the Single Running Average did (see Figs. 9 and 10) and since further reduction in the number of sample points per cycle seemed unpromising on the basis of the above reasoning, it became the digital filter of choice for this project.

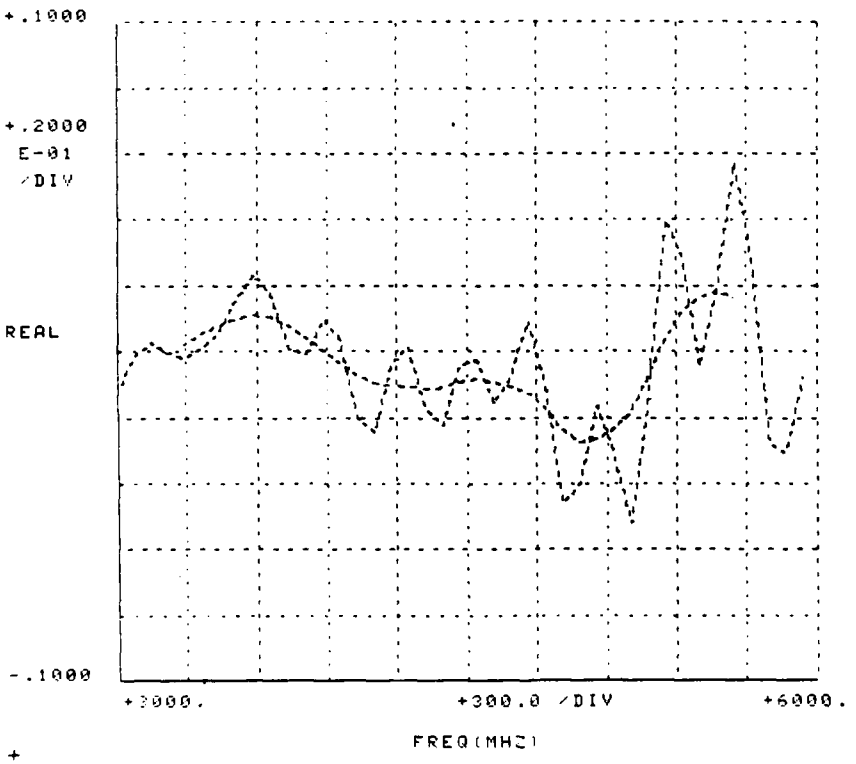

Fig. 9. Results of Double Running Average using 5 points per cycle.

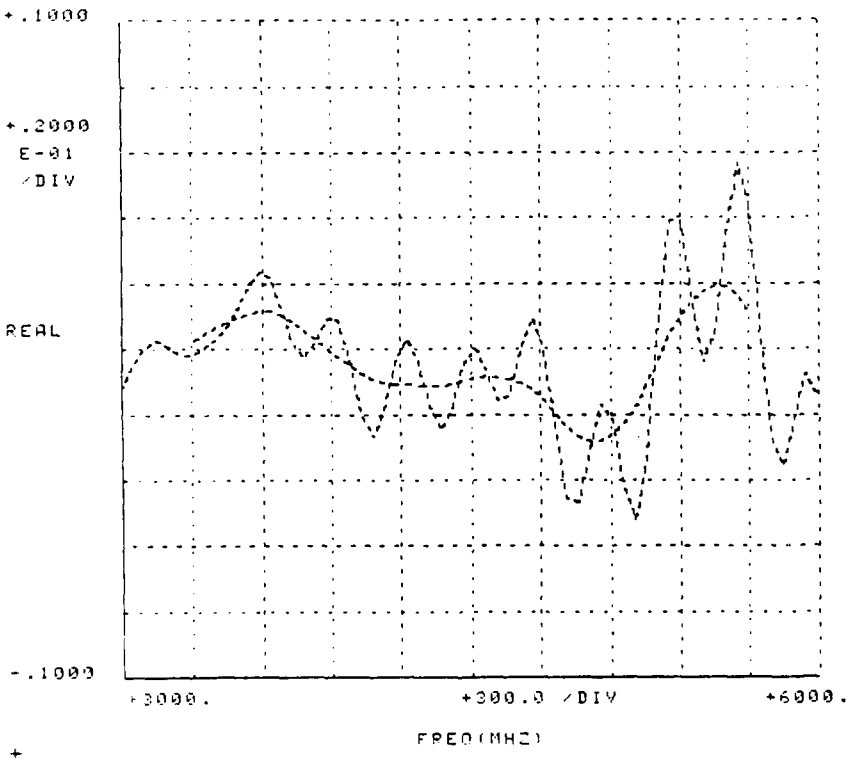

Fig. 10. Results of Double Running Average using 7 points per cycle.

DERIVATION OF CALIBRATION

For all the reflection calibrations, the standard HP linear error correction model (Ref. 13) was used which is diagrammed below:

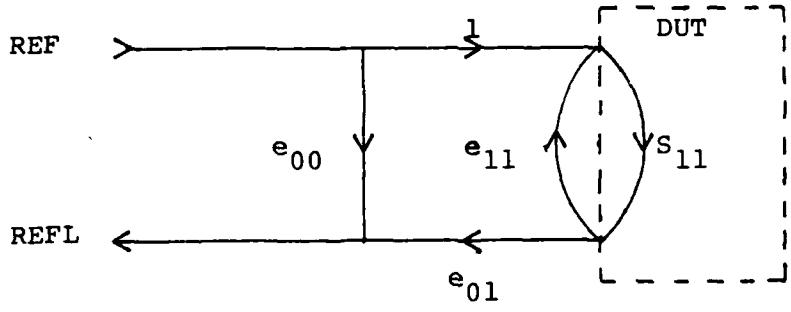

Fig. 11. HP error correction model for reflection measurements.

and which assumes that $S_{12} \cdot S_{21} = 0$. Using this flowgraph to solve for $\frac{REFL}{REF} = \Gamma$ the following relation is extracted

$$\Gamma_{MEAS} = e_{00} + \frac{e_{01} S_{11}}{1-e_{11} S_{11}} \qquad (20)$$

where Γ_{MEAS} represents the measured reflection coefficient of DUT and S_{11}, the actual reflection coefficient of DUT.

e_{00} is the crosstalk error due to imperfect directivity of the coupler, e_{01} is the error due to the imperfect gain tracking between test and reference channels, and e_{11} is the mismatch error due to imperfect Port 1 match.

It is clear that three reflection standards could be used to solve for the three error correction coefficients e_{00}, e_{01}, and e_{11}. The three standards chosen for this project were the short, open, and characterization of a perfectly matched load. If Γ_L is the measured reflection coefficient of the load, Γ_S of the short, and Γ_0 of the open circuit, then $S_{11}(L) = 0$, $S_{11}(S) = -1$, and $S_{11}(0) = \Gamma$ where $\Gamma = 1e^{-j\phi(f)}$. It has been shown that for the 7-mm precision 50 ohm open-circuit $\phi(f) = 5.02 \times 10^{-5} f + 1.126 \times 10^{-14} f^3$ radians where f is frequency in MHz. Substituting the stated values of S_{11} into Eq. (20) for each standard, one obtains the following equations:

$$\Gamma_L = e_{00} \tag{21}$$

$$\Gamma_S = e_{00} - \frac{e_{01}}{1 + e_{11}} \tag{22}$$

$$\Gamma_O = e_{00} + \frac{e_{01}\,\Gamma}{1 - e_{11}\,\Gamma} \tag{23}$$

Substituting Γ_L for e_{00} in (22) and (23) and rearranging terms gives

$$\Gamma_S - \Gamma_L = \frac{-\,e_{01}}{1 + e_{11}} \tag{24}$$

$$\Gamma_O - \Gamma_L = \frac{e_{01}\,\Gamma}{1 - e_{11}\,\Gamma} \tag{25}$$

Dividing Eq. 24 by 25 and multiplying both sides by Γ, one finds

$$\Gamma\,\frac{\Gamma_S - \Gamma_L}{\Gamma_O - \Gamma_L} = \frac{e_{11}\,\Gamma - 1}{e_{11} + 1} \tag{26}$$

Let

$$Q = \Gamma\,\frac{\Gamma_S - \Gamma_L}{\Gamma_O - \Gamma_L} \tag{27}$$

which is now calculable and Eq. 26 becomes

$$Q = \frac{e_{11}\,\Gamma - 1}{e_{11} + 1} \tag{28}$$

Therefore,

$$e_{11} = \frac{Q + 1}{\Gamma - Q} \tag{29}$$

From Eq. 22

$$e_{01} = (\Gamma_L - \Gamma_S)(1 + e_{11}) \tag{30}$$

The system now has enough information to make fully corrected reflection measurements (is "calibrated"). Equation 20 can now be reversed to find S_{11} in terms of Γ_{MEAS} which is the ultimate aim and it becomes

$$S_{11}\ (DUT) = \frac{1}{\frac{e_{01}}{\Gamma_{MEAS} - e_{00}} + e_{11}} \tag{31}$$

Therefore, fully corrected reflection measurements can be made after first calibrating the system using the three reflection standards with known S_{11}'s.

CALIBRATION AND MEASUREMENT PROGRAMS

The calibration and measurement programs will now be presented in detail. The programs are written in HP combined ANA, ATS, and TODS-II BASIC languages, and run on an HP-2100S computer which is equipped with 8K usable memory, and convenient graphics output devices.

Due to core memory limitations, the complete sequence (including adapter correction) is controlled by six programs which are maintained in disc files and automatically chained into memory. The APC-7 sliding load, short, and open are used for the initial calibration. The adapted zero-plane short and running averaged load are employed in the adapter correction. The discrete Double Running Average is incorporated for maximum flexibility.

Figure 12 shows the flowgraph for program 1 which is tasked with making all measurements necessary for the APC-7 calibration. Figures 13-14 show the listing of program 1. It first requests the electrical length of the reference line which will be used for the load characterization in the adapter correction. From this, it computes $F = \Delta F$ and displays the minimum and maximum frequencies available within equipment limits, and asks for the start, stop, and step frequencies in order to compute the FI's. It then computes $F9 = \Delta f$ and N(the number of FI's), F3

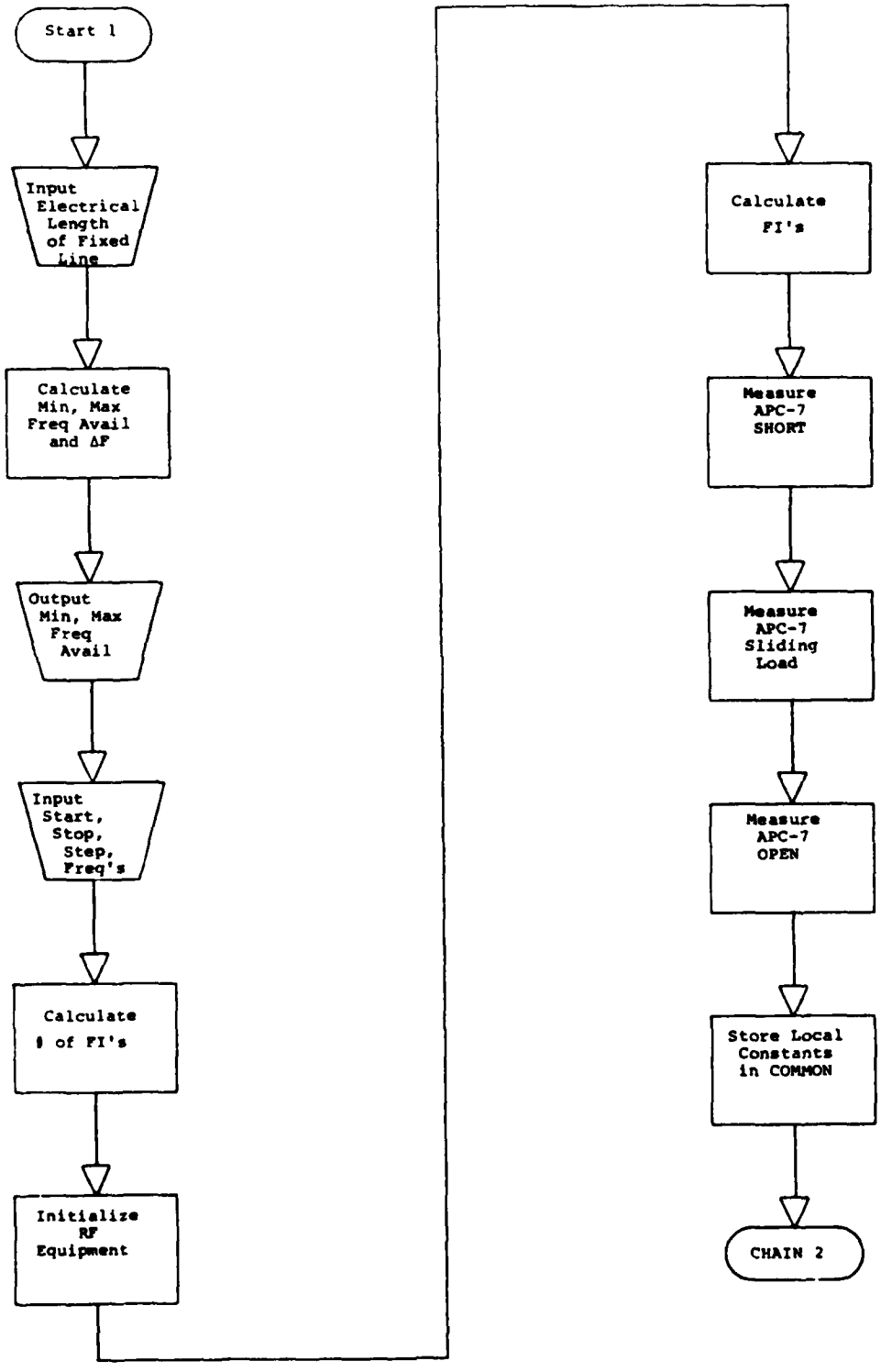

Fig. 12. Flowchart for Program 1.

```
                                                                PAGE  1

1  REM THIS PROGRAM, DEVELOPED ON 11/5/80, IS DESIGNED
2  REM TO MAKE AN APC-7 CALIBRATION IN PREPARATION FOR
3  REM THE DOUBLE RUNNING AVERAGE IN THE ADAPTER CORRECTION
4  REM    REV 11/24/80       REM 12/22/80       1:ANU72.S
20   COM C[13,51],L[13,51],O[13,51]
40   COM F[51],N[10]
100   DISPLAY "WHAT IS LENGTH(CM) OF LINE";
120   BELL
140   INPUT L
150   REM CALC 1/PERIOD FOR LENGTH OF LINE AND UPPER AND
151   REM LOWER FREQ LIMITS FOR RUN AVG
160   LET F=29980/(2*L)
180   LET F1=INT(101*F)
200   LET F2=INT(18000-F)
220   DISPLAY "FREQ(MHZ) AVAILABLE  ~  MIN=";F1,"MAX=";F2
240   DISPLAY "FREQ(MHZ) - START,STOP,STEP";
260   BELL
280   INPUT F1,F2,S
290   REM CALC NUMBER OF FREQ STEPS ASKED FOR IN THE OUTPUT
300   LET N=INT(1+(F2-F1)/S)
310   REM INITIALIZE THE MEASUREMENT EQUIPMENT
320   LET F9=F/6
340   LET F3=F1-6*F9
360   FCALF(F3)
380   BCNT1(F3)
400   SDEL1(11)
420   WAIT (50)
430   REM CALC AND STORE THE OUTPUT FREQS
440   FOR K=1 TO N
460   LET F[K]=F1+(K-1)*S
480   NEXT K
500   DISPLAY "CONNECT APC-7 SHORT"
520   PAUSE
530   REM MAKE MEASUREMENTS AT ALL FREQS ON APC-7 SHORT
540   FOR K=1 TO N
560   LET F3=F[K]-6*F9
580   FOR J=1 TO 13
600   FREQ2(F3)
620   MEAS1(150,X,Y)
640   CPAK(X,Y,C[J,K])
660   LET F3=F3+F9
680   NEXT J
700   NEXT K
720   DISPLAY "CONNECT APC-7 SLIDING LOAD"
740   PAUSE
750   REM MAKE MEASUREMENTS AT ALL FREQS ON APC-7 SLIDING LOAD
760   FOR K=1 TO N
780   LET F3=F[K]-6*F9
800   FOR J=1 TO 13
820   FREQ2(F3)
840   MEAS1(150,X,Y)
860   CPAK(X,Y,L[J,K])
880   LET F3=F3+F9
900   NEXT J
920   NEXT K
940   DISPLAY "CONNECT APC-7 OPEN"
960   PAUSE
970   REM MAKE MEASUREMENTS AT ALL FREQS ON APC-7 OPEN
```

Fig. 13. Page 1 of listing for Program 1.

```
980   FOR K=1 TO N
1000   LET F3=F[K]-6*F9
1020   FOR J=1 TO 13
1040   FREQ2(F3)
1060   MEAS1(150,X,Y)
1080   CPAK(X,Y,O[J,K])
1090   LET F3=F3+F9
1100   NEXT J
1120   NEXT K
1130   REM STORE ALL NECESSARY LOCAL VARIABLES IN COMMON
1140   LET N[1]=F1
1160   LET N[2]=F2
1180   LET N[3]=F9
1200   LET N[6]=S
1220   LET N[7]=N
9980   REM BRING IN NEXT PROGRAM AUTOMATICALLY
9990   CHAIN("1:ANU73.S")
```

Fig. 14. Page 2 of listing for Program 1.

(the first measurement frequency), and initializes the RF measurement equipment. The FI's are then calculated and stored. Lines 500 to 700 perform measurements on the APC-7 short at all satelite frequencies (frequency measurements around each FI necessary to compute discrete Double Running Average for the FI's). Lines 720 to 920 and 940-1120 perform the same measurements on the APC-7 sliding load and the APC-7 open, respectively. The local variables are then stored in COMMON to be passed to subsequent programs, and the program ends by chaining program 2 into memory.

The flowgraph of program 2 appears in Fig. 15 and the listing in Fig. 16. This program is tasked with characterizing the open circuit and computing the error correction coefficients. It begins by recalling the local variables from COMMON (assigning more descriptive names) and by defining the complex constants 1 + j0 and -1 + j0. Then for each frequency, open circuit-phase adjustments are calculated and applied to the ideal reflection coefficient of the open circuit to obtain Γ in Eq. 23. The error correction coefficients are then calculated. Lines 340-400 are the code to compute Q in Eq. 27, lines 420-460 to compute e_{11} in Eq. 29, and lines 480-520 to compute e_{01} in Eq. 30. These coefficients then replace the

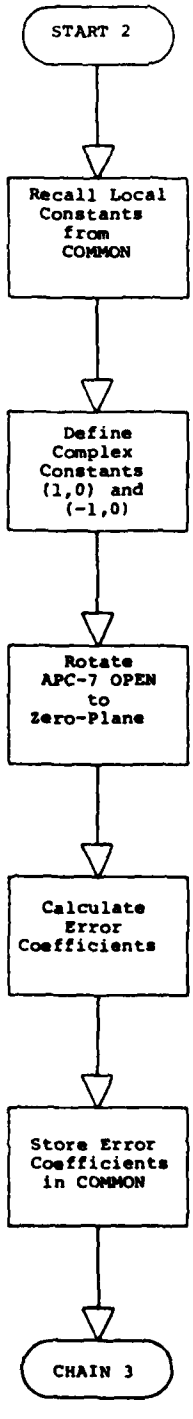

Fig. 15. Flowchart for Program 2.

```
1   REM THIS PROGRAM, DEVELOPED ON 11/5/80, IS DESIGNED
2   REM TO CALCULATE THE ERROR CORRECTION COEFFICIENTS
3   REM FOR THE APC-7 CALIBRATION
4   REM     REV 11/7/80      REM 3/13/81        1:ANU73.S
20   COM S[13,51],L[13,51],O[13,51]
40   COM F[51],N[10]
90   REM RECALL LOCAL VARIABLES FROM COMMON
100   LET F9=N[3]
120   LET S=N[6]
140   LET N=N[7]
150   REM DEFINE COMPLEX CONSTANTS (1,0) AND (-1,0)
160   CPAK(1,0,D2)
180   CPAK(-1,0,D3)
190   REM GENERATE ERROR CORRECTION COEFFICIENTS FOR ALL FREQS
200   FOR K=1 TO N
220   LET F3=F[K]-6*F9
240   FOR J=1 TO 13
250   REM CORRECT APC-7 OPEN CIRCUIT PHASE
260   LET C9=5.02E-05+1.126E-14*F3↑2
280   LET C9=-C9
300   PSFT(0,F3,C9,D2,P1)
310   REM COMPUTE ERROR COEFFICIENTS
311   REM E0=E00,E1=E11,E2=E21
320   LET E0=L[J,K]
340   CSUB(S[J,K],E0,N1)
360   CSUB(O[J,K],E0,D1)
380   CDIV(N1,D1,N1)
400   CMPY(P1,N1,Q5)
420   CADD(Q5,D2,N1)
440   CSUB(P1,Q5,D1)
460   CDIV(N1,D1,E2)
480   CSUB(E0,S[J,K],N1)
500   CADD(D2,E2,D1)
520   CMPY(N1,D1,E1)
531   REM SAVE ERROR CORRECTION COEFICIENTS IN COMMON
540   LET S[J,K]=E0
560   LET L[J,K]=E1
580   LET O[J,K]=E2
590   LET F3=F3+F9
600   NEXT J
620   NEXT K
9980   REM LOAD NEXT PROGRAM AUTOMATICALLY
9990   CHAIN("1:ANU74.S")
```

Fig. 16. Listing for Program 2.

APC-7 measurements in COMMON since they are no longer needed, and program 3 is chained into memory.

Figures 17 and 18-19 display the flowgraph and listing for program 3 which makes system-corrected measurements on adapter, reference line, and load and computes the Double Running Average for each FI. It starts with virtually the same variable recalling and initialization as program 2. The adapter, load, and line are then measured and corrected for system errors (lines 520-580 represent Eq. 31). Lines 680-960 represent the code for computing the first running average sum. Note the application of the sliding running average in lines 900-960. The second running average sum is calculated in lines 980-1100 with the average being completed in lines 1140-1160. COMMON is then rearranged so that a transition to single subscripted arrays can be accomplished and so that a large block of memory can be freed in program 4 since only information at the FI's is required from this point on. Program 4 is now chained into memory.

The flowgraph and listing of program 4 are displayed in Figs. 20 and 21, respectively. This program initializes the equipment, measures the adapter and short, corrects the data for system error, and chains program 5 into memory. At this point all the information necessary

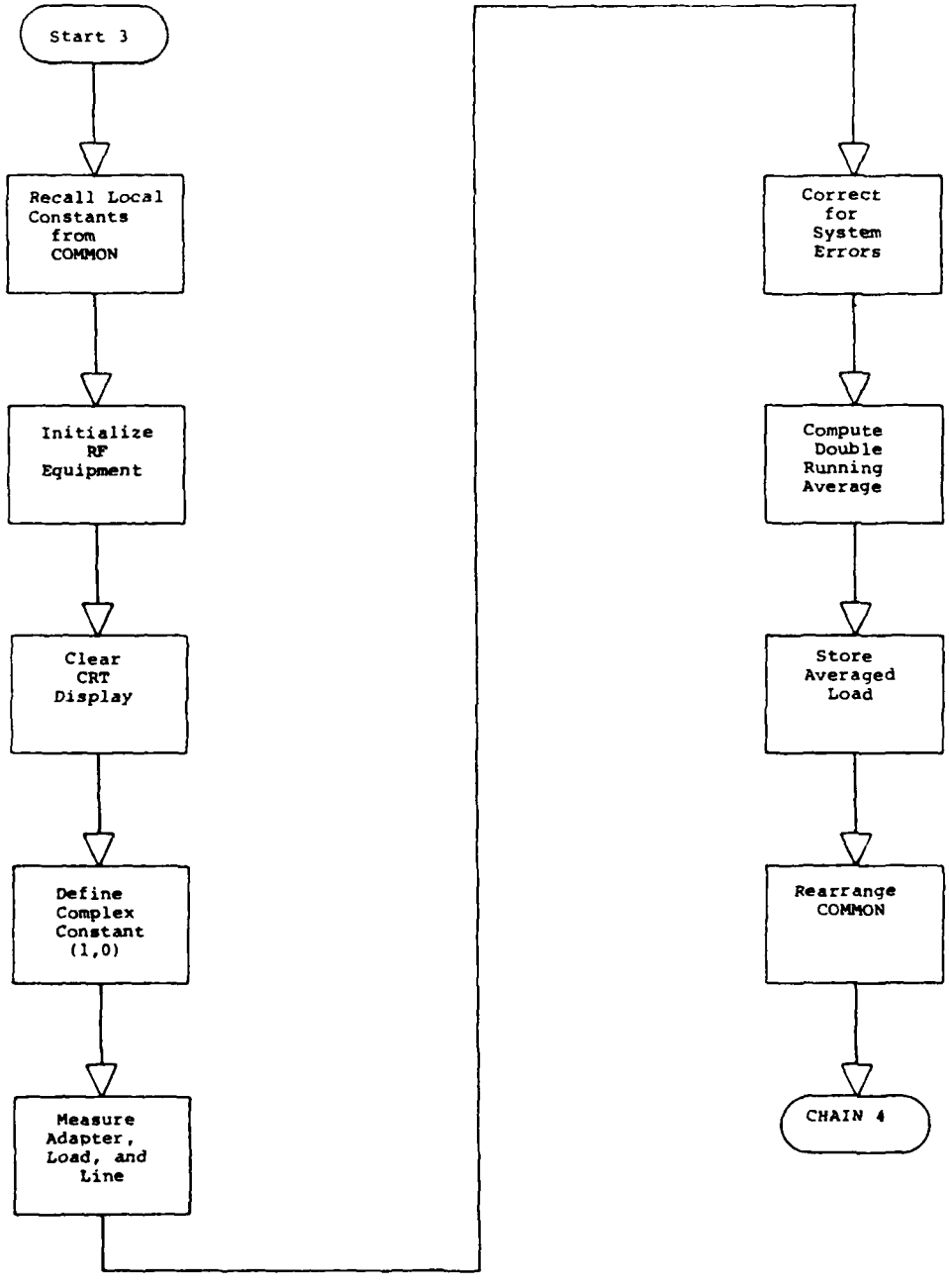

Fig. 17. Flowchart for Program 3.

```
1   REM THIS PROGRAM, DEVELOPED ON 11/5/80, IS DESIGNED
2   REM TO COMPUTE THE DOUBLE RUNNING AVERAGE FOR THE
3   REM ADAPTER CORRECTION
4   REM     REV 11/7/80        REM 3/13/81        1:ANU74.S
20   COM A[13],B[13],C[13],D[13],E[13]
40   COM S[13,51],L[13,51],O[13,51]
50   COM F[51],N[10]
90   REM RECALL LOCAL VARIABLES FROM COMMON
100   LET F1=N[1]
120   LET F2=N[2]
140   LET F9=N[3]
160   LET N=N[7]
170   REM INITIALIZE THE MEASUREMENT EQUIPMENT
180   FCALF(F[1]-6*F9)
200   BCNT1(F[1]-6*F9)
220   SSEL1(11)
240   WAIT (50)
250   REM CLEAR DISPLAY
260   CLEAR(0)
270   REM DEFINE COMPLEX CONSTANT (1,0)
280   CPAK(1,0,D2)
360   DSPLAY "CONNECT SMA LOAD AND LINE"
380   PAUSE
400   FOR K=1 TO N
420   LET F3=F[K]-6*F9
430   REM MAKE TWO CYCLE MEASUREMENTS FOR OUTPUT POINT K
431   REM ON ADAPTER, LINE, AND LOAD
440   FOR J=1 TO 13
460   FREQ2(F3)
480   MEAS1(150,X,Y)
500   CPAK(X,Y,Z)
510   REM PERFORM ERROR CORRECTION ON ADAPTER, LOAD, AND LINE
520   CSUB(Z,S[J,K],D1)
540   CDIV(L[J,K],D1,D1)
560   CADD(D1,O[J,K],D1)
580   CDIV(D2,D1,A[J])
600   LET B[J]=REA(A[J])
620   LET C[J]=IMG(A[J])
640   LET F3=F3+F9
660   NEXT J
670   REM SET UP DOUBLE RUNNING AVERAGE FOR POINT K
671   REM MAKE SEVEN MEASUREMENTS PER CYCLE
680   LET M=3
690   REM COMPUTE FIRST RUN AVG SUM FOR POINTS NEEDED TO COMPUTE
691   REM SECOND RUNNING AVERAGE FOR OUTPUT POINT K
700   LET I=M+1
720   LET D[I]=B[I-M]/2
740   LET E[I]=C[I-M]/2
750   FOR J=I-M+1 TO I+M-1
760   LET D[I]=D[I]+B[J]
800   LET E[I]=E[I]+C[J]
820   LET J1=J
840   NEXT J
860   LET D[I]=D[I]+B[J1+1]/2
880   LET E[I]=E[I]+C[J1+1]/2
890   REM COMPUTE SLIDING RUN AVG SUMS FOR REST OF POINTS NEEDED
891   REM TO COMPUTE SECOND RUN AVG FOR POINT K
900   FOR I=M+2 TO 13-M
```

Fig. 18. Page 1 of listing for Program 3.

```
920  LET D[I]=D[I-1]+(-B[I-M-1]-B[I-M]+B[I-M-1+J1]+B[I-M+J1])*.5
940  LET E[I]=E[I-1]+(-C[I-M-1]-C[I-M]+C[I-M-1+J1]+C[I-M+J1])*.5
960  NEXT I
961  REM COMPUTE SECOND RUN AVG SUM FOR POINT K
980  LET I=2*M+1
1000  LET U=D[I-M]/2
1020  LET T=E[I-M]/2
1040  FOR J=I-M+1 TO I+M-1
1060  LET U=U+D[J]
1080  LET T=T+E[J]
1100  LET J1=J
1120  NEXT J
1121  REM DIVIDE BY TOTAL WEIGHTED SUM TO GET SECOND RUN
1122  REM AVG FOR POINT K
1140  LET U=(U+D[J1+1])/21/36
1160  LET T=(T+E[J1+1])/21/36
1161  REM STORE RUN AVG LOAD AND REARRANGE COMMON IN PREPARATION
1162  REM FOR VARIABLE REASSIGNMENTS IN NEXT PROGRAM
1180  CPAK(U,T,O[12,K])
1200  LET O[8,K]=O[7,K]
1220  LET O[9,K]=L[7,K]
1240  LET O[10,K]=O[7,K]
1260  NEXT K
9980  REM LOAD NEXT PROGRAM AUTOMATICALLY
9990  CHAIN("1:ANU75.3")
```

Fig. 19. Page 2 of listing for Program 3.

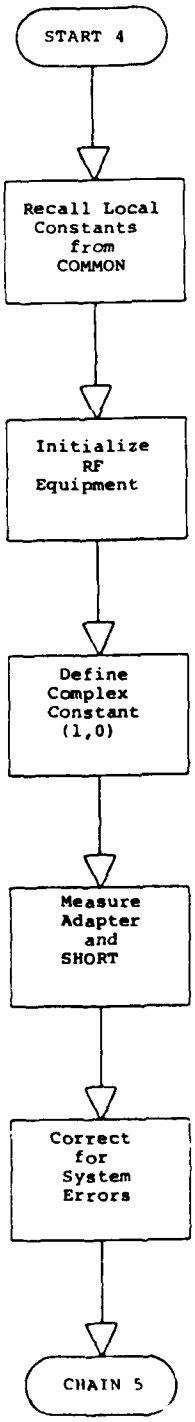

Fig. 20. Flowchart for Program 4.

```
1   REM THIS PROGRAM, DEVELOPED ON 11/5/80, IS DESIGNED
2   REM TO COMPUTE THE ADAPTER CORRECTION COEFFICIENTS
3   REM      REV 11/24/80     REM 3/13/81      1:ANU75.3
20   COM C[3,51],S[51],L[51],M[51]
40   COM F[51],N[10]
41   REM RECALL LOCAL VARIABLES FROM COMMON
100   LET N=N[7]
110   REM INITIALIZE MEASUREMENT EQUIPMENT
120   FCALF(F[1])
140   BCNT1(F[1])
160   SCEL1(11)
180   WAIT (50)
200   DISPLAY "CONNECT SMA SHORT"
220   PAUSE
230   REM DEFINE COMPLEX CONSTANT (1,0)
240   CPAK(1,0,D2)
250   REM MAKE CORRECTED MEASUREMENTS ON ADAPTER AND SHORT
260   FOR I=1 TO N
280   FREQ2(F[I])
300   MEAS1(150,X,Y)
320   CPAK(X,Y,Z)
340   CSUB(Z,C[1,I],D1)
360   CDIV(C[2,I],D1,D1)
380   CADD(D1,C[3,I],D1)
400   CDIV(D2,D1,S[I])
440   NEXT I
9980   REM LOAD NEXT PROGRAM AUTOMATICALLY
9990   CHAIN("1:ANU76.3")
```

Fig. 21. Listing for Program 4.

to make fully corrected measurements has been obtained, and the system is prepared to measure the complex reflection coefficient of DUT's.

Figures 22 and 23 show the flowgraph and listing for program 5 which has the job of measuring a DUT and fully correcting for system error and the adapter. After initializing it makes measurements on a DUT and corrects it for system error in the usual way. Lines 460-540 computes the value of E1 in Eq. 9. Lines 553-556 normalize E1 to make sure that it is indeed equal to $e^{-j2\theta}$. Lines 560-640 complete the calculations of Eq. 10 yielding the fully corrected reflection coefficient of the DUT. This result will now be output in program 6.

Program 6, whose flowchart and listing appears in Figs. 24 and 25-26, provide plots of Real (Γ) vs. freq., Imag (Γ) vs. frequency, Mag (Γ) vs. frequency, and Ang (Γ) vs. frequency. It will then provide, if desired, a complete printout of the above mentioned parameters. Program 5 is then chained into memory and the system is ready to measure another DUT of the same connector type.

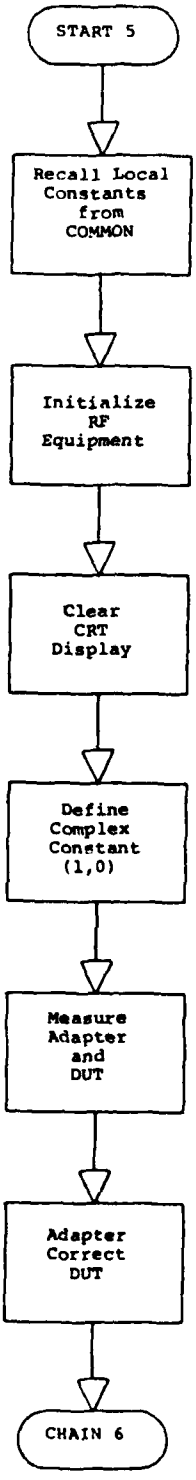

Fig. 22. Flowchart for Program 5.

```
1   REM THIS PROGRAM, DEVELOPED ON 11 5/80, IS DESIGNED
2   REM TO ADAPTER CORRECT THE MEASUREMENT OF THE UNKNOWN
3   REM     REV 12/22/80        REM 3/13/81          1:ANU76.S
20   COM C[3,51],S[51],L[51],M[51]
40   COM F[51],N[10]
50   REM RECALL LOCAL VARIABLES FROM COMMON
100   LET N=N[7]
110   REM INITIALIZE MEASUREMENT EQUIPMENT
120   FCALF(F[1])
140   BCNT1(F[1])
160   SSEL1(11)
180   WAIT (50)
185   REM CLEAR DISPLAY
190   CLEAR(0)
200   DISPLAY "CONNECT 3MA UNKNOWN"
220   PAUSE
230   REM DEFINE COMPLEX CONSTANT (1,0)
240   CPAK(1,0,D2)
250   REM MAKE ERROR CORRECTED MEASUREMENTS ON UNKNOWN
260   FOR I=1 TO N
280   FREQ2(F[I])
300   MEAS1(150,X,Y)
320   CPAK(X,Y,Z)
340   CSUB(Z,C[1,I],D1)
360   CDIV(C[2,I],D1,D1)
380   CADD(D1,C[3,I],D1)
400   CDIV(D2,D1,M[I])
420   NEXT I
430   REM MAKE ADAPTER CORRECTIONS FOR ALL OUTPUT POINTS
440   FOR I=1 TO N
460   CSUB(L[I],S[I],D1)
480   CPAK(REA(L[I]),-IMG(L[I]),N2)
500   CMPY(S[I],N2,N1)
520   CSUB(D2,N1,N1)
540   CDIV(N1,D1,N3)
553   CPAK(MAG(N3),0,N4)
556   CDIV(N3,N4,N3)
560   CSUB(M[I],L[I],N1)
580   CMPY(M[I],N2,D1)
600   CSUB(D2,D1,D1)
620   CDIV(N1,D1,N1)
640   CMPY(N1,N3,M[I])
660   NEXT I
9980   REM LOAD NEXT PROGRAM AUTOMATICALLY
9990   CHAIN("1:ANU77.S")
```

Fig. 23. Listing for Program 5.

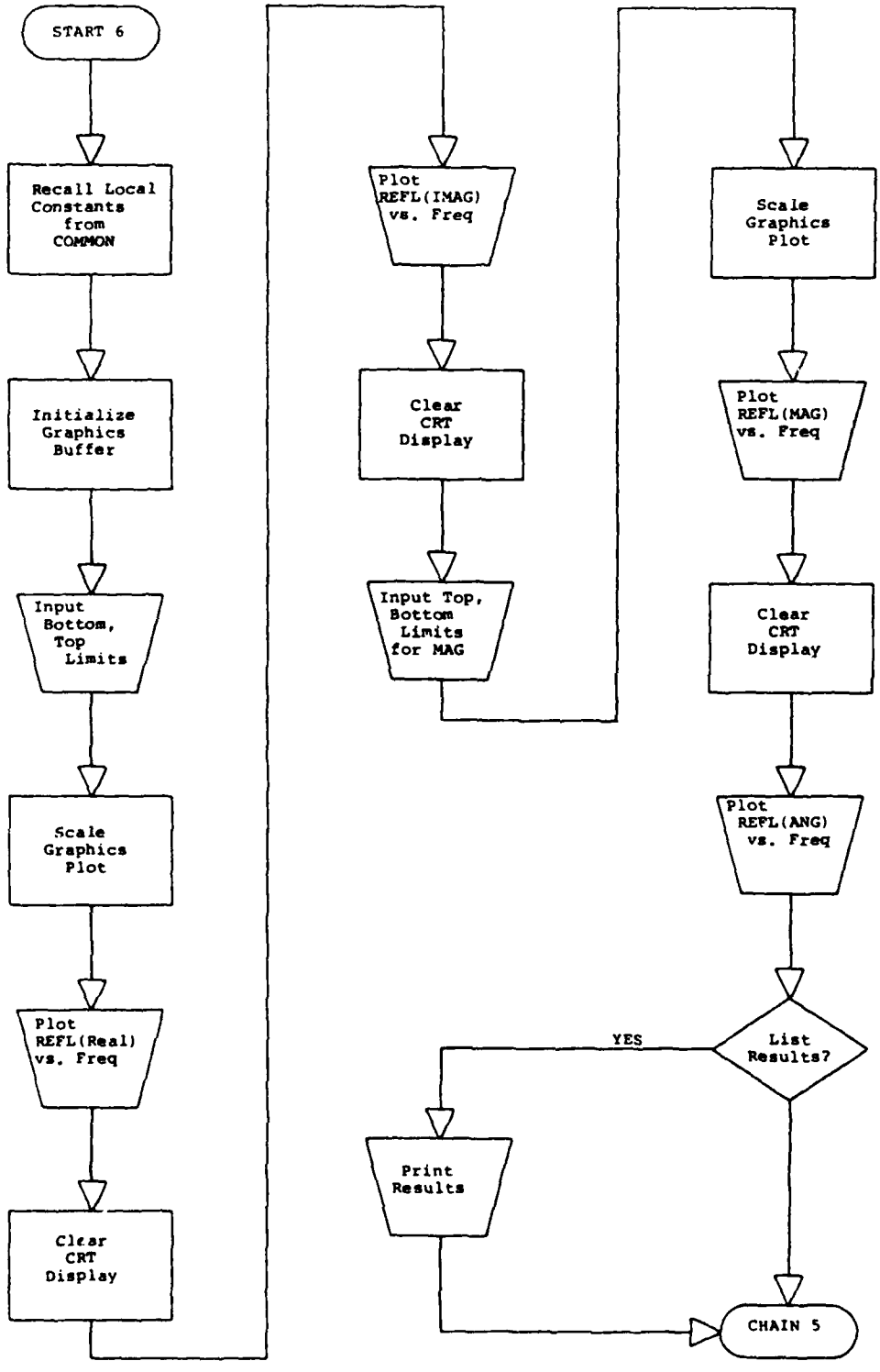

Fig. 24. Flowchart for Program 6.

PAGE 1

```
1   REM THIS PROGRAM, DEVELOPED ON 11/5/80, IS DESIGNED
2   REM TO OUTPUT THE CORRECTED MEASUREMENTS
3   REM    REV 11/7/80      REM 12/22/80          1:ANU77.S
20   COM C[3,51],S[51],L[51],M[51],F[51],N[10]
90   REM RECALL LOCAL VARIABLES FROM COMMON
100   LET F1=N[1]
120   LET F2=N[2]
140   LET S=N[6]
160   LET N=N[7]
170   REM INITIALIZE GRAPHICS DISPLAY AND BUFFER
180   BUF(100)
200   CLEAR(0)
220   DSPLAY "WHAT ARE BOTTOM AND TOP LIMITS";
240   BELL
260   INPUT B1,T1
280   LET S1=(T1-B1)/10
290   REM CLEAR DISPLAY, SCALE, AND PLOT REAL PART OF REFLECTION
300   CLEAR(0)
320   SCALE(F1,F2,B1,T1)
340   LET F3=(F2-F1)/10
360   SAXES(F3,S1)
380   DSPLAY VTAB(15),TAB(0),"REFL"
400   DSPLAY VTAB(31),TAB(28),"FREQ(MHZ)"
420   LABEL VTAB(16),TAB(0),"REAL"
440   BLOCK(B2)
460   FOR I=1 TO N
480   PLOT(F[I],REA(M[I]),2)
500   NEXT I
520   PAUSE
530   REM CLEAR REAL PLOT AND PLOT IMAGINARY
540   CLEAR(2)
560   SAXES(F3,S1)
580   LABEL VTAB(16),TAB(0),"IMAG"
600   BLOCK(B2)
620   FOR I=1 TO N
640   PLOT(F[I],IMG(M[I]),2)
660   NEXT I
680   PAUSE
700   CLEAR(0)
720   DSPLAY "WHAT ARE BOTTOM AND TOP LIMITS FOR MAG";
740   BELL
760   INPUT B2,T2
770   REM CLEAR DISPLAY AND PLOT REFLECTION MAGNITUDE
780   CLEAR(0)
800   LET S2=(T2-B2)/10
820   SCALE(F1,F2,B2,T2)
840   SAXES(F3,S2)
860   DSPLAY VTAB(15),TAB(0),"REFL"
880   DSPLAY VTAB(31),TAB(28),"FREQ(MHZ)"
900   LABEL VTAB(16),TAB(0),"MAG"
920   BLOCK(B3)
940   FOR I=1 TO N
960   PLOT(F[I],MAG(M[I]),2)
980   NEXT I
1000   PAUSE
1010   REM CLEAR MAGNITUDE PLOT AND PLOT REFLECTION ANGLE
1020   CLEAR(2)
1040   LET B3=-180
```

Fig. 25. Page 1 of listing for Program 6.

```
1060  LET T3=180
1080  LET S3=(T3-B3)/10
1100  SCALE(F1,F2,B3,T3)
1120  SAXES(F3,S3)
1140  LABEL VTAB(16),TAB(0),"ANG"
1160  BLOCK(B2)
1180  FOR I=1 TO N
1200  PLOT(F[I],ANG(M[I]),2)
1220  NEXT I
1230  REM CLEAR DISPLAY AND PRINT ALL RESULTS FOR ALL
1231  REM FREQS IF REQUESTED
1240  PAUSE
2000  CLEAR(0)
2020  DSPLAY "WANT TO PRINT RESULTS(1=YES,2=NO)";
2040  BELL
2060  INPUT H1
2080  IF H1=1 GOTO 9000
2090  REM INITIALIZE AUTOMATIC GRAPHICS BUFFER PAGE TURNER
2100  TRAP 0 GOSUB 3000
2120  CLEAR(0)
2140  BUF(800)
2180  DSPLAY "FREQ(MHZ)    REFL(REA)    REFL(IMG)    REFL(MAG)";
2200  DSPLAY "    REFL(ANG)"
2220  DSPLAY
2240  FOR I=1 TO N
2250  REM SET OUTPUT FORMAT IN BASIC NOTATION
2260  FDSP(F[I],7,0)
2280  DSPLAY "       ";
2300  FDSP(REA(M[I]),6,3)
2320  DSPLAY "       ";
2340  FDSP(IMG(M[I]),6,3)
2360  DSPLAY "       ";
2380  FDSP(MAG(M[I]),6,3)
2400  DSPLAY "       ";
2420  FDSP(ANG(M[I]),6,1)
2440  DSPLAY
2460  NEXT I
2470  COPY
2475  PAGE
2477  PAGE
2480  GOTO 9000
2990  REM SUBROUTINE FOR AUTOMATIC PAGE TURNING WHEN GRAPHICS
2991  REM BUFFER BECOMES FULL
3000  COPY
3010  PAGE
3015  PAGE
3020  CLEAR(0)
3040  RETURN
3990  REM LOAD MEASUREMENT PROGRAM AUTOMATICALLY
9000  CHAIN("1:ANU75.3")
```

Fig. 26. Page 2 of listing for Program 6.

CALIBRATION PROCEDURES

The calibration procedures are not difficult to accomplish. In fact, the computer gives rather explicit instructions for each step, and always signals with a bell when operator action is required.

Only the first program must be loaded into memory manually (the rest are sequenced automatically). It first asks for the electrical length of the reference line being used for the load characterization. It then returns the minimum and maximum frequency limits and asks for the start, stop, and step frequencies. This information is then used to calculate the FI's. The operator is next prompted to connect an APC-7 short, an APC-7 sliding load, and then an APC-7 open. After calculating the system error correction coefficients, the program asks that the adapter, reference line, and load be attached after which it computes the Double Running Averaged load characterization. Connection of the adapter and short is then requested, and the calibration is complete and the system is prepared to make fully corrected measurements on any DUT.

After attaching a DUT to the adapter, the system makes measurements, corrects these measurements, and then asks for the bottom and top limits of the Γ(Real) and

Γ(Imag) plots versus frequency. After displaying these plots, the program requests the bottom and top limits for the Γ(Mag) plot versus frequency. This is output and the Γ(Ang) plot versus frequency automatically follows.

The operator can now choose if a printed listing of the frequencies and above parameters are to be output. Whether or not the listings are requested, the computer automatically asks for another DUT to be attached to the adapter, and the sequence repeats until the operator interrupts the program by pressing the BREAK button on the console.

COMPARISON OF TRANSMISSION LINES

As was stated earlier, use of the Double Running Average for characterization of an ideal load, for the first time, permits direct comparison of transmission lines and connection systems. For instance, two or more lengths of transmission line can be directly compared against each other to obtain an exact impedance match at the frequency or band of interest.

However, this procedure cannot be conducted using the calibration and measurement programs as already described. They must be modified and these modifications will now be presented. Programs 1 and 2 remain completely unchanged and program 3 requires only a change in the CHAIN statement to the new program 4 (Program 4A).

Figures 27 and 28 show the flowgraph and listing for program 4A. This program recalls the local variables from COMMON, opens a disc file for data storage, and then asks for identification of the transmission line for which data is being stored (up to 4 lines can be compared at one time with this program). The line data is then stored on the disc along with the error correction coefficients. The program then halts. If another line is to be measured

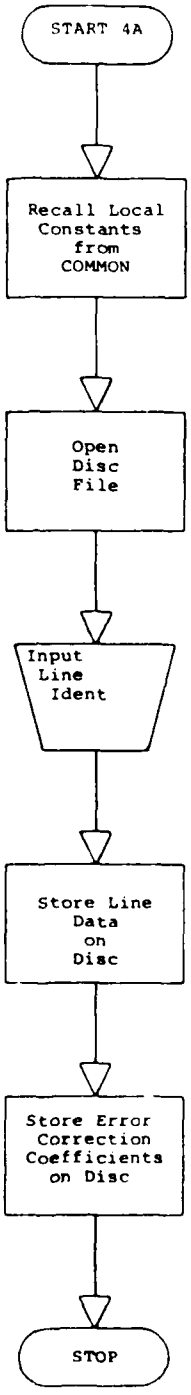

Fig. 27. Flowchart for Program 4A.

```
                                                                PAGE  1

1   REM THIS PROGRAM, DEVELOPED ON 11/5/80, IS DESIGNED TO
2   REM STORE THE AVERAGED LINE DATA ON DISC FOR COMPARISON
3   REM OF DIFFERENT LINES DIRECTLY
4   REM    REV 11 24/81     REM 3/13/81       1:ANU73.S
5   REM THIS PROGRAM MUST REPLACE 1:ANU75.S WHEN
6   REM GENERATING THE DATA FILE FOR COMPARISON OF
7   REM LOADS AND LINES
10   COM C[3,51],D[51],L[51],M[51]
40   COM F[51],N[10]
95   REM RECALL LOCAL VARIABLES FROM COMMON
100   LET N=N[7]
110   REM OPEN DISC FILE FOR DATA STORAGE
120   OPEN#1,0,"1:ANU75.D",E1
130   REM DATA FOR UP TO FOUR LINES CAN BE STORED
140   DISPLAY "WHICH LINE(1=OURS,2=SHORT,3=LONG,4=SPLINE)";
150   BELL
160   INPUT D
190   REM DEPOSIT DATA IN DISC FILE
200   DRITE(10, D-1)*51+1,L[1],51,E1
220   DRITE(10,205,C[1,1],153,E1
9999   END
```

Fig. 28. Listing for Program 4A.

AD-A107 198 AIR FORCE INST OF TECH WRIGHT-PATTERSON AFB OH F/G 9/5
AUTOMATIC MICROWAVE NETWORK ANALYZER CALIBRATION BY REFERENCE T--ETC(U)
OCT 81 J P DIBENEDITTO
UNCLASSIFIED AFIT-CI-81-120 NL

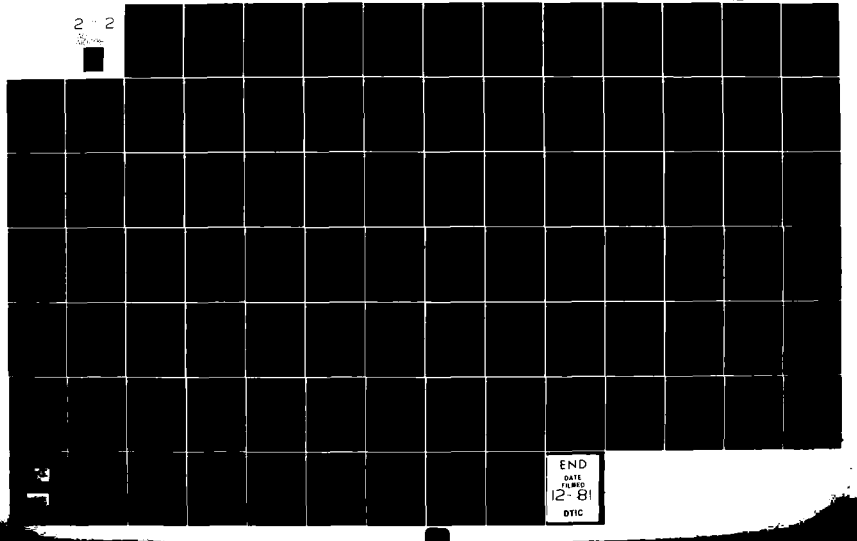

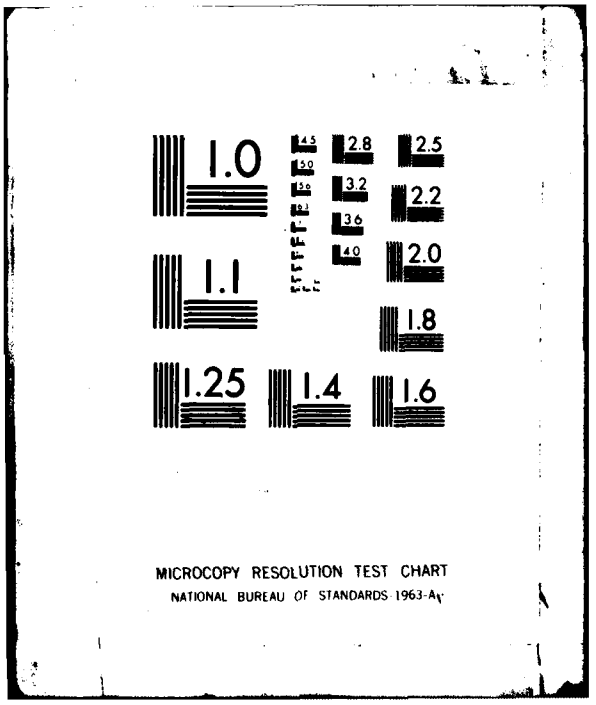
1.0
1.1
1.25
1.4
1.6
1.8
2.0
2.2
2.5
2.8
3.2
3.6
4.0
MICROCOPY RESOLUTION TEST CHART
NATIONAL BUREAU OF STANDARDS 1963-A

then program 1 must be reloaded into memory and the sequence repeated. After all lines have been measured, program 5A can be loaded and run.

The flowgraph and listing of this program are display in Figs. 29 and 30. This program must measure the adapter and short, correct it for system errors and store this data, the frequency list and COMMON variables on the disc. All the data necessary for comparing the lines has now been stored on disc.

Programs 4B, 5B and 6 are used to perform the actual line comparisons and to output the results. The sequence is started by loading and running program 4B. The program sequence progresses automatically from this stage. Program 4B [Figs. 31 and 32] begins by loading all the data (except line data) into COMMON. It then asks which line will be used as the reference line and loads the appropriate data into COMMON.

Program 5B (Figs. 33 and 34) is then automatically chained into memory. This program requests which line will be used as the DUT and loads that data into COMMON from the disc. It then performs the adapter correction, which, in this case, actually represents the line comparison.

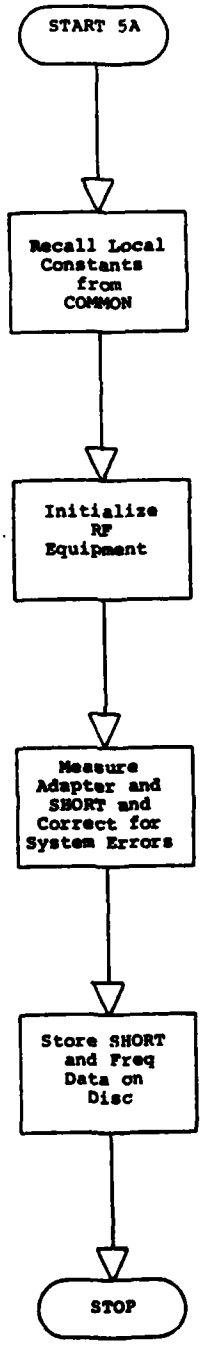

Fig. 29. Flowchart for Program 5A.

```
                                                                PAGE  1

1   REM THIS PROGRAM, DEVELOPED ON 11/5/80, IS DESIGNED
2   REM TO MEASURE AND STORE DATA FOR LINE COMPARISON
3   REM     REV 11/24/80       REM 3/13/81         1:ANU79.3
4   REM THIS PROGRAM MUST REPLACE 1:ANU75.S WHEN
5   REM STORING THE ADAPTED SHORT AND FREQ DATA FOR AVERAGED
6   REM LOAD AND LINE COMPARISON
20   COM C[3,51],S[51],L[51],M[51]
40   COM F[51],N[10]
90   REM RECALL LOCAL VARIABLES FROM COMMON
100   LET N=N[7]
110   REM INITIALIZE RF EQUIPMENT
120   FCALF(F[1])
140   BCNT1(F[1])
160   SSEL1(11)
180   WAIT (50)
190   REM MEASURE AND STORE ADAPTER AND SHORT
200   DSPLAY "CONNECT SMA SHORT"
220   PAUSE
230   REM DEFINE COMPLEX CONSTANT (1,0)
240   CPAK(1,0,D2)
260   FOR I=1 TO N
280   FREQ2(F[I])
300   MEAS1(150,X,Y)
320   CPAK(X,Y,Z)
330   REM CORRECT MEASUREMENTS FOR SYSTEM ERRORS
340   CSUB(Z,C[1,I],D1)
360   CDIV(C[2,I],D1,D1)
380   CADD(D1,C[3,I],D1)
400   CDIV(D2,D1,S[I])
420   NEXT I
430   REM OPEN DISC FILE
440   OPEN(10,"1:ANU75.D",E)
450   REM STORE SHORT, FREQUENCY,AND COMMON DATA ON DISC
460   DRITE(10,358,S[1],51,E)
480   DRITE(10,409,F[1],61,E)
9990   END
```

Fig. 30. Listing for Program 5A.

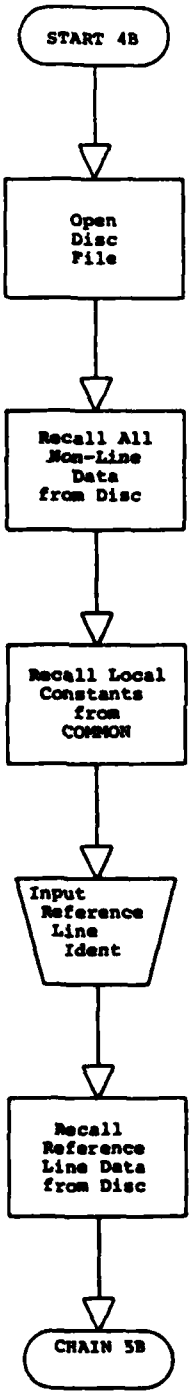

Fig. 31. Flowchart for Program 4B.

```
1   REM THIS PROGRAM, DEVELOPED ON 11/5/80, IS DESIGNED
2   REM TO SET UP REFERENCE LINE FOR LINE COMPARISON
3   REM       REV 5/8/81      REM 3/13/81       1:ANU80.S
4   REM THIS PROGRAM MUST REPLACE 1:ANU75.S WHEN COMPARING
5   REM ONE AVERAGED LOAD AND LINE TO ANOTHER AFTER THE
6   REM DATA FILES HAVE BEEN GENERATED
20   COM C[3,51],S[51],L[51],M[51]
40   COM F[51],N[10]
50   REM OPEN DISC FILE WHERE DATA IS STORED
60   OPEN(10,"1:ANU75.D",E)
70   REM RECALL SHORT DATA FROM DISC
80   DREAD(10,358,S[1],51,E)
85   REM RECALL FREQUENCY DATA AND COMMON VARIABLES FROM DISC
90   DREAD(10,409,F[1],61,E)
92   REM RECALL ERROR CORRECTION COEFFICIENTS FROM DISC
95   DREAD(10,205,C[1,1],153,E)
97   REM RECALL LOCAL VARIABLES FROM COMMON
100   LET N=N[7]
140   DSPLAY "WHICH LINE TO BE USED AS REFERENCE"
160   DSPLAY "(1=OURS,2=SHORT,3=LONG,4=SPLINE)";
180   BELL
200   INPUT Q
210   REM READ IN REFERENCE LINE DATA
220   DREAD(10,(Q-1)*51+1,L[1],51,E)
9000   REM AUTOMATICALLY LOAD NEXT PROGRAM
9990   CHAIN("1:ANU81.S")
```

Fig. 32. Listing for Program 4B.

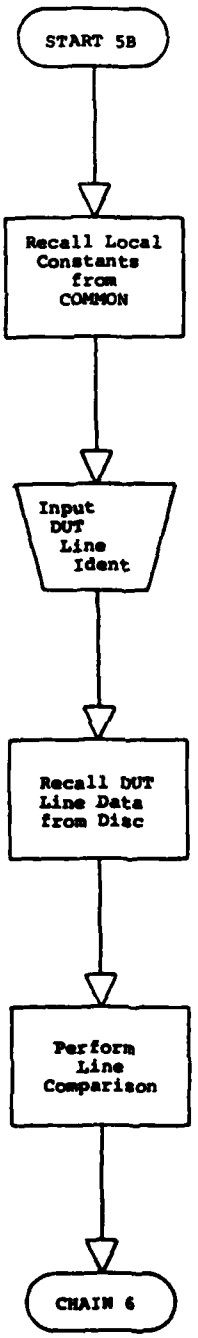

Fig. 33. Flowchart for Program 5B.

```
1   REM THIS PROGRAM, DEVELOPED ON 11/5/80, IS DESIGNED
2   REM TO COMPLETE LINE COMPARISON
3   REM      REV 5/8/81        REM 3/13/81        1:ANU81.S
4   REM THIS PROGRAM MUST REPLACE 1:ANU76.S WHEN COMPARING
5   REM ONE AVERAGED LOAD AND LINE TO ANOTHER AFTER DATA
6   REM FILE GENERATION
20   COM C[3,51],S[51],L[51],M[51]
40   COM F[51],N[10]
90   REM RECALL LOCAL VARIABLES FROM COMMON
100   LET N=N[7]
180   REM CLEAR DISPLAY
190   CLEAR(0)
195   REM OPEN DISC FILE WHERE LINE DATA IS STORED
200   OPEN(10,"1:ANU75.D",E)
220   DSPLAY "WHICH LINE TO BE USED AS UNKNOWN"
240   DSPLAY "(1=OURS,2=SHORT,3=LONG,4=SPLINE)";
260   BELL
280   INPUT Q
290   REM READ IN DATA FOR DUT LINE FROM DISC
300   DREAD(10,(Q-1)*51+1,M[1],51,E)
310   REM DEFINE COMPLEX CONSTANT (1,0)
320   CPAK(1,0,D2)
430   REM ADAPTER CORRECT DUT DATA
440   FOR I=1 TO N
460   CSUB(L[I],S[I],D1)
480   CPAK(REA(L[I]),-IMG(L[I]),N2)
500   CMPY(S[I],N2,N1)
520   CSUB(D2,N1,N1)
540   CDIV(N1,D1,N3)
553   CPAK(MAG(N3),0,N4)
556   CDIV(N3,N4,N3)
560   CSUB(M[I],L[I],N1)
580   CMPY(M[I],N2,D1)
600   CSUB(D2,D1,D1)
620   CDIV(N1,D1,N1)
640   CMPY(N1,N3,M[I])
660   NEXT I
9000   REM AUTOMATICALLY LOAD NEXT PROGRAM
9990   CHAIN("1:ANU82.S")
```

Fig. 34. Listing for Program 5B.

Program 6 (previously discussed) is then chained into memory, unchanged, and the results are output in graphic and/or tabular form.

Thus, lines can now be compared directly against one line that serves as a standard, without need for a perfect termination or sliding load in the transmission line adopted as a standard: a procedure not heretofore available.

RESULTS

Four different SMA lines were used to evaluate the techniques presented in this document.

1. A Narda Serial #W11 3015292G1, which was fitted with Narda 4401 Female connectors on both ends, had an electrical length of 89.4 cm, obtained from Tufts' stock. This cable will be titled "our" line.
2. and 3. Two lines were constructed at Lincoln Laboratory from Uniform Tubes SMA coaxial cable fitted with an OSM 210-1 male connector on one end and an OSM 207-9776SF female connector on the other. The "short" line had an electrical length of 113.9 cm while the "long" one was 228.1 cm in length.
4. The fourth cable, also constructed at Lincoln Laboratory, was unusual in the sense that it was constructed from a 173.6 cm electrical length of Precision Tubes 141 series air-articulated 3.5 mm line fitted with Solitron/Microwave 2902-6057 male connectors on both ends. This line was not dielectric filled and was called the "spline" line.

These four lines offered the chance of testing three conventional SMA lines, two of which were identical in construction and one which was a significant departure in design.

The first set of results to be displayed will be the adapter-corrected reflections of a zero-plane short, an HP offset 4 short, and an open circuit referenced to the running averaged load characterization of each line measured from 2-17 GHz. A female SMA adapter was used at the measurement port for all the measurements and a standard SMA fixed load was used to terminate each line for load characterization.

As can be seen in Figs. 35-38, the measurement of the zero-plane short circuit was virtually identical for all the lines, with a 0.03 maximum deviation from unity reflection coefficient magnitude. Some of this deviation may be attributed to the slight power dissipation in the adapter, which is assumed tc be dissipationless. The variations are probably caused by the frequency varying directivity of the directional coupler. It is speculated that a coupler which is smoother in directivity over the frequency band (or a broadband SWR bridge, such as a Wiltron 58A50) would be more satisfactory in this respect.

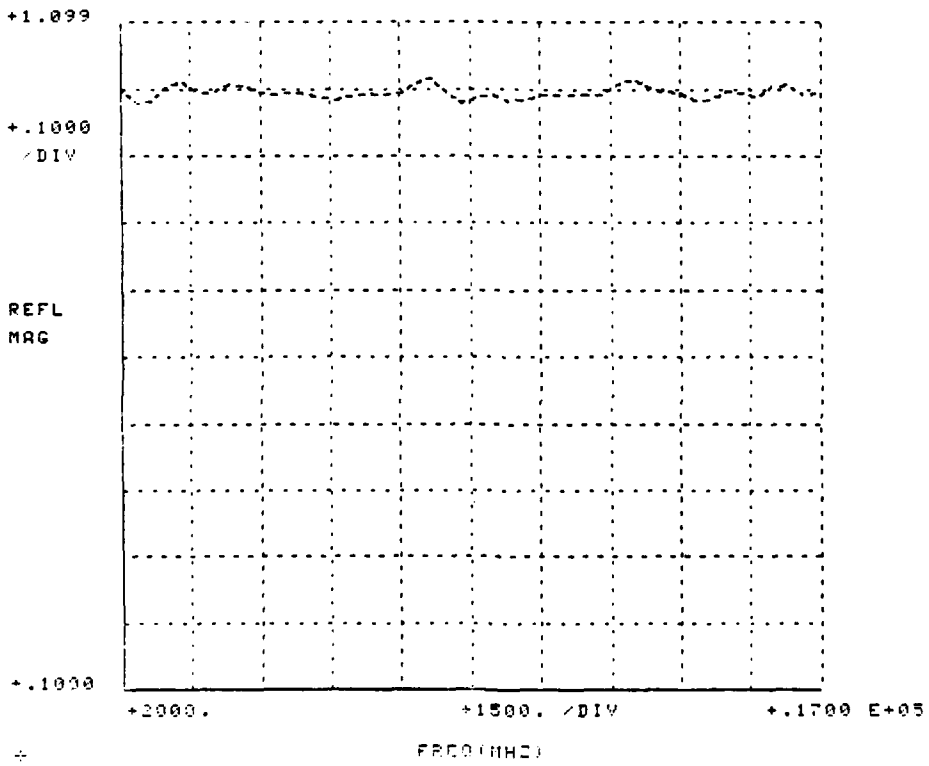

Fig. 35. Reflection of short circuit referenced to "our" line.

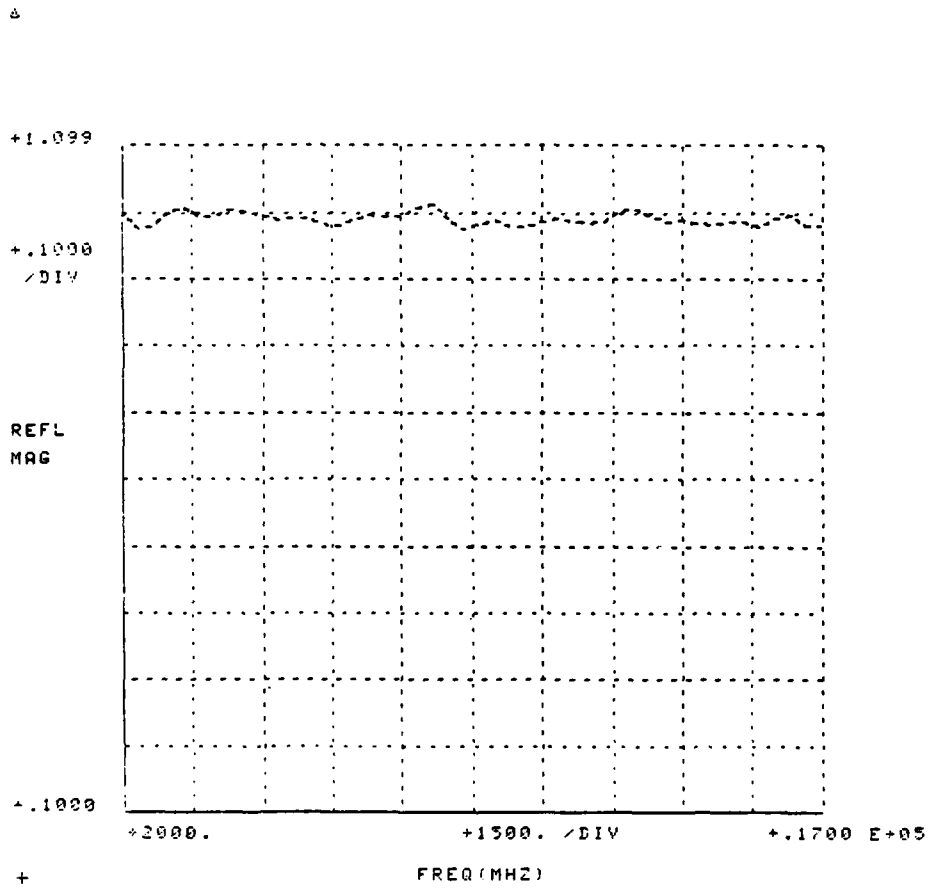

Fig. 36. Reflection of short circuit referenced to "short" line.

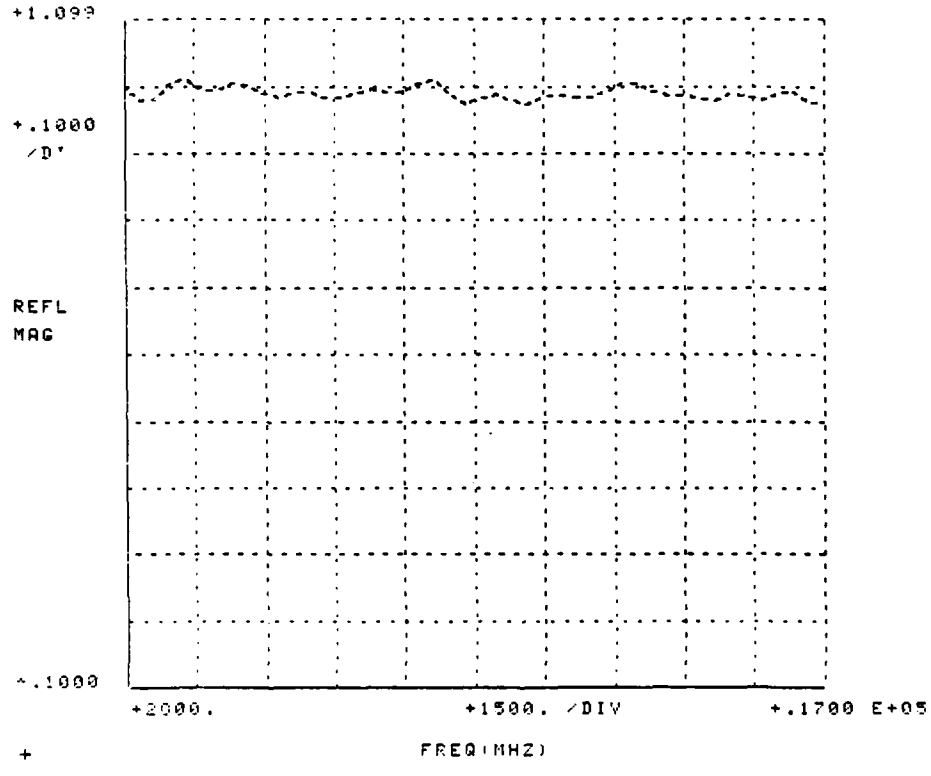

Fig. 37. Reflection of short circuit referenced to "long" line.

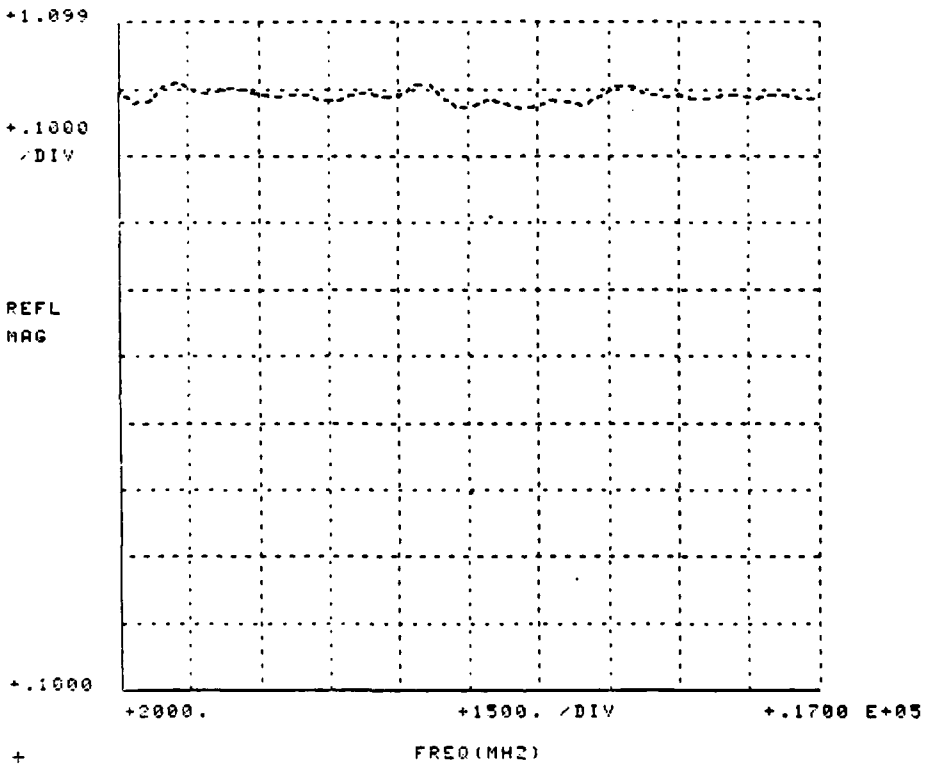

Fig. 38. Reflection of short circuit referenced to "spline" line.

Figure 39 shows a plot of the coupler directivity for the HP 8743 test set. This was measured by placing an APC-7 sliding load at the reflection measuring port, and by placing the ANA in manual mode. A time-exposed photograph of the HP 180A rectangular display was made as the sliding load was moved from stop to stop several times for each frequency band. The bisection of the envelope was taken to be a measure of the directivity. As shown, the directivity does not everywhere safely meet the assumption of being varying slowly with frequency. This deficiency could produce a small error in magnitude measurements even for a short circuit.

At this point, the system stability has been shown to be sufficient for adapter correction. Now, the averaged load and line and zero-plane short circuit will be used as standards while two conventional calibration standards (offset 4 short circuit and open circuit) will be used as DUT's in order to show the suitability of the complete calibration procedure.

The magnitude and phase plots of the offset 4 shorts for each of the lines is presented in Figs. 40-47. They are unremarkable in that they are essentially the same for each of the lines.

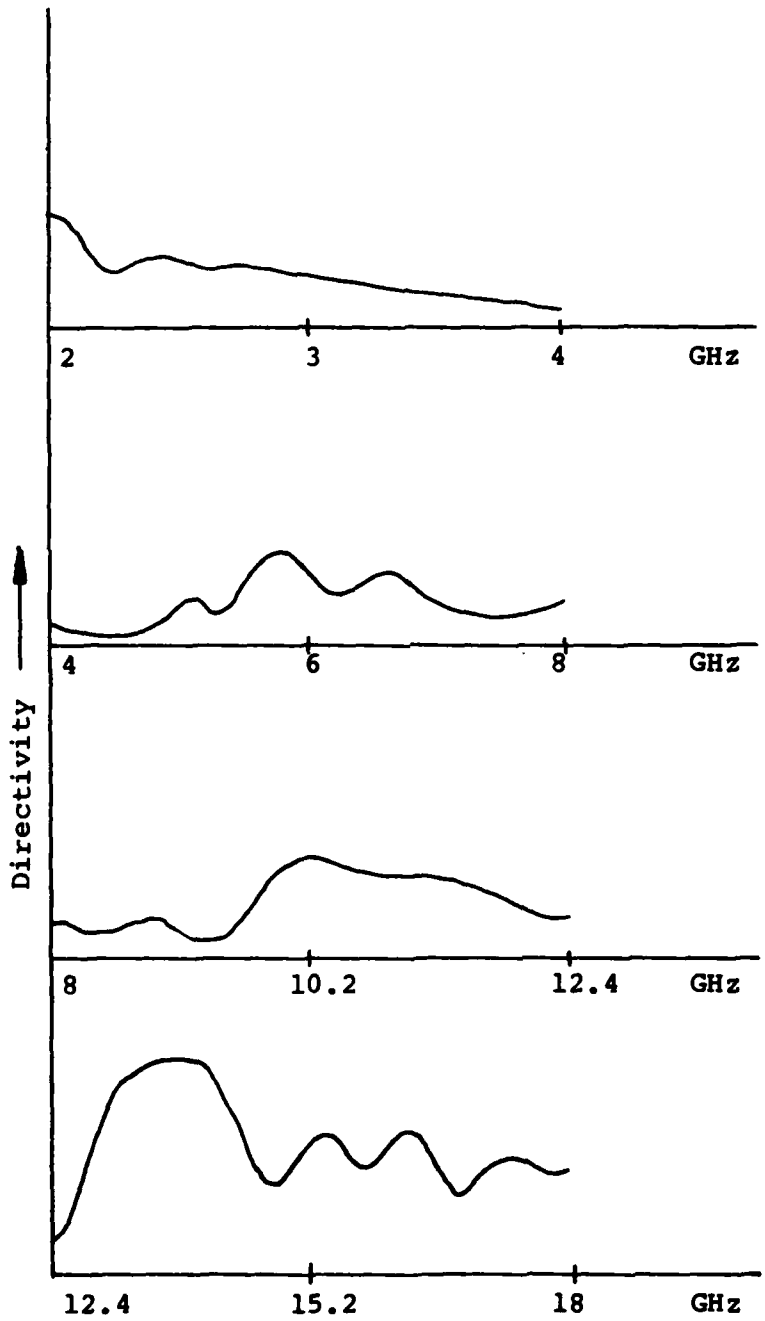

Fig. 39. Measured directivity of coupler in HP 8743A Test Set.

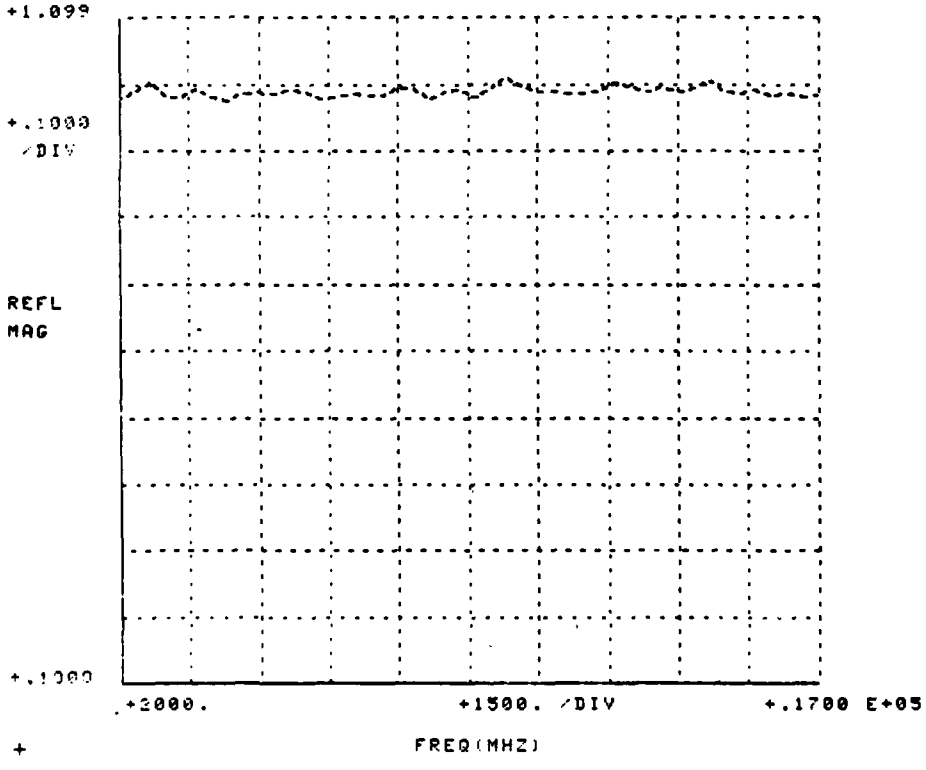

Fig. 40. Reflection of offset 4 short referenced to "our" line (Mag).

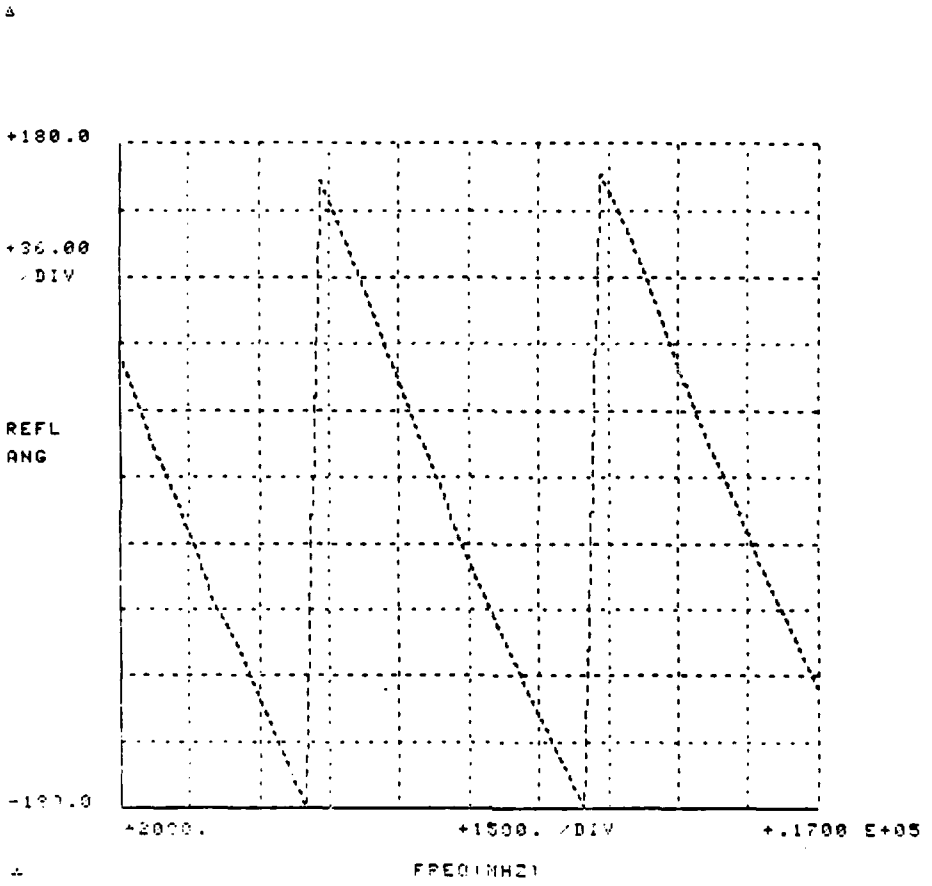

Fig. 41. Reflection of offset 4 short referenced to "our" line (Ang).

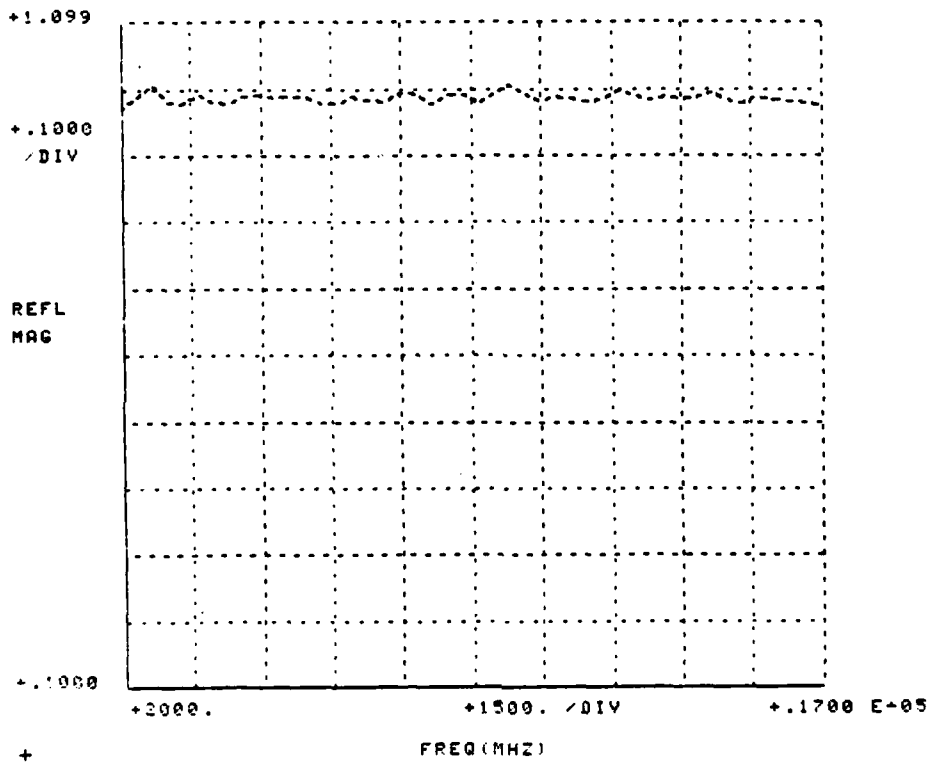

Fig. 42. Reflection of offset 4 short referenced to "short" line (Mag).

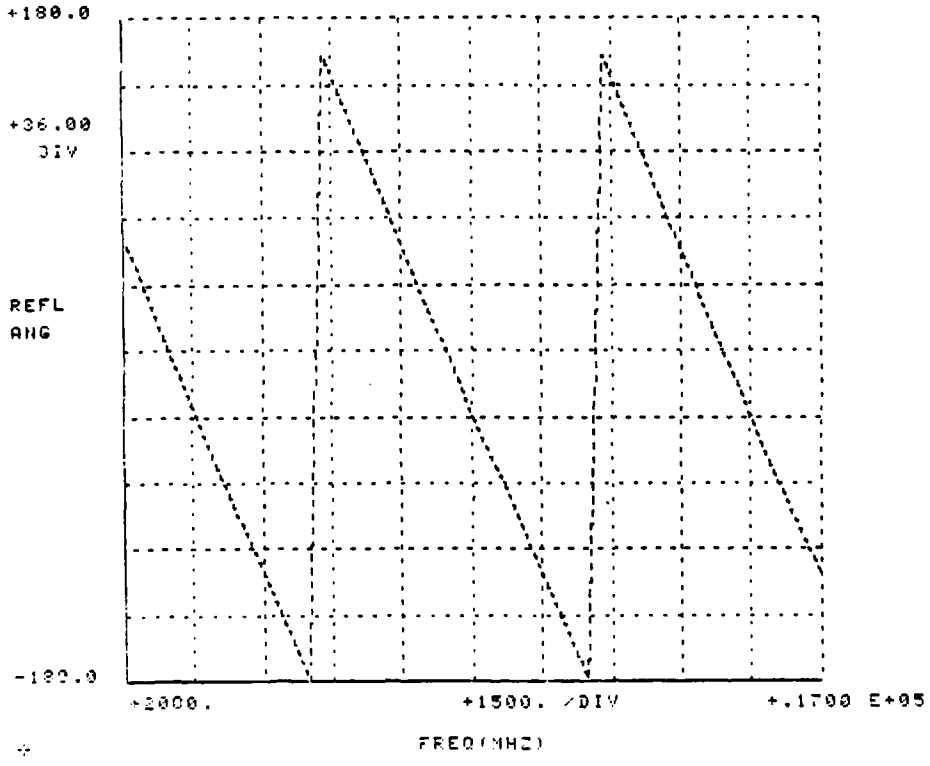

Fig. 43. Reflection of offset 4 short referenced to "short" line (Ang).

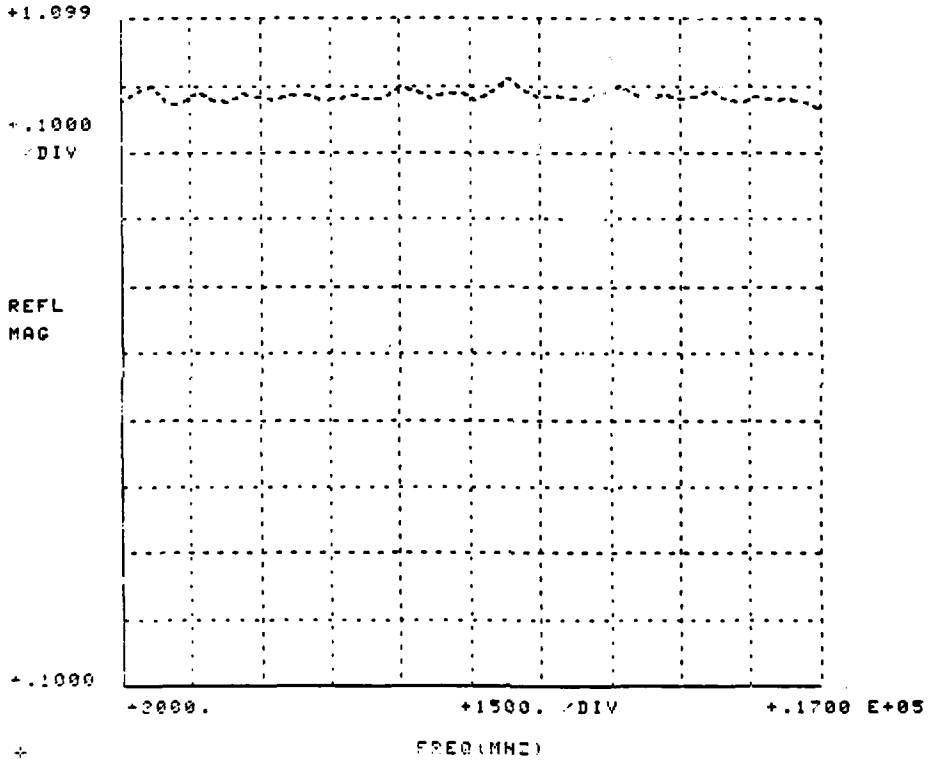

Fig. 44. Reflection of offset 4 short referenced to "long" line (Mag).

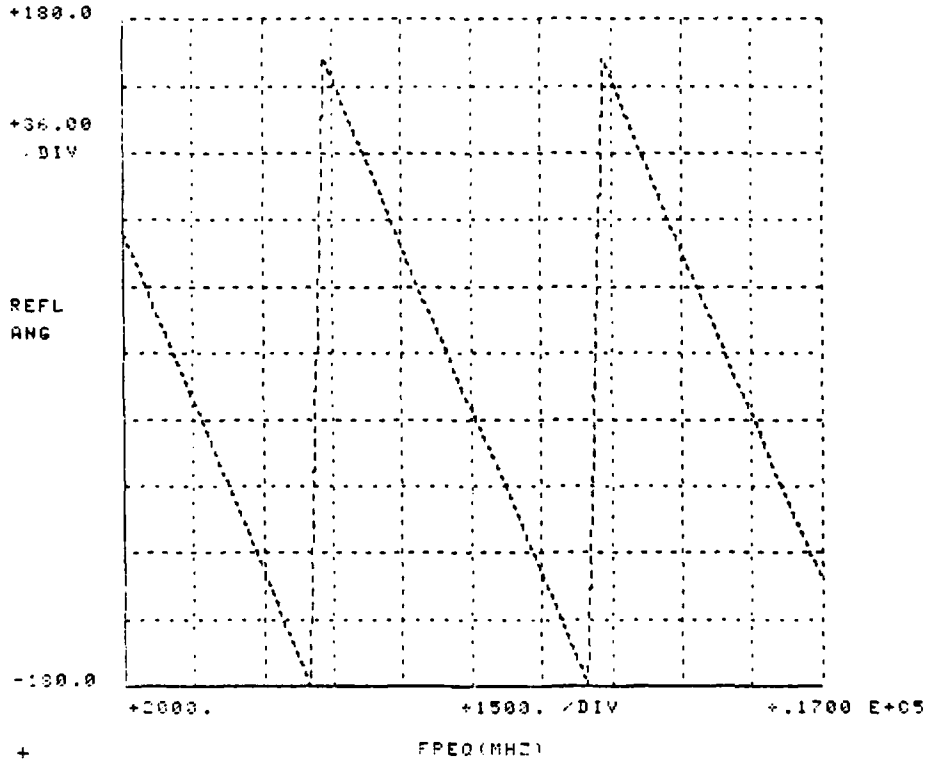

Fig. 45. Reflection of offset 4 short referenced to "long" line (Ang).

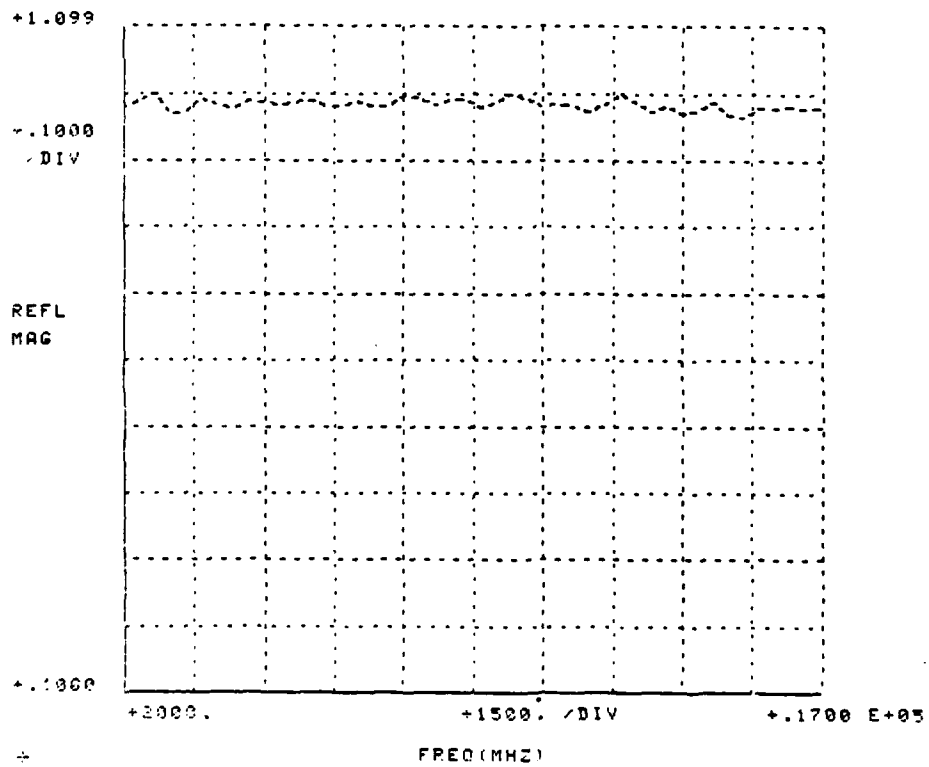

Fig. 46. Reflection of offset 4 short referenced to "spline" line (Mag).

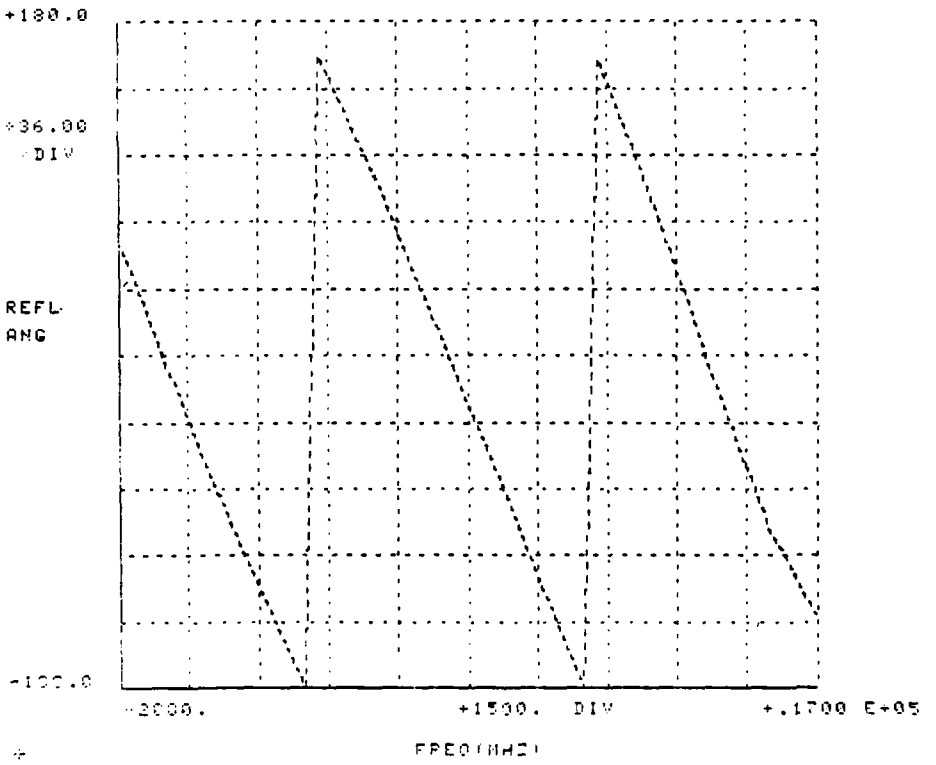

Fig. 47. Reflection of offset 4 short referenced to "spline" line (Ang).

It is important to note that the lack of difference between the lines for the zero-plane and offset 4 short circuits is due to the fact that these are high reflection standards with a well defined plane of measurement. Since zero-reflection correction provided by the calibration is so small, it becomes almost negligible in measurements of high reflection standards. Therefore, the characteristics of the different lines used for the running averaged load characterization have little affect on the measurements of these standards. However, as will be shown next, the line characteristic will have a dramatic effect on devices, such as open circuits, where, even though they are high-reflection devices, they exhibit a frequency-varying phase which is dependent upon the nature of the interconnecting transmission line.

It will also be seen that the characteristics of lines can be significantly different even among those of the same type and can be readily observed by employing the direct line comparison technique previously described.

Figures 48-55 show the corrected measurement of reflection magnitude and phase of an open circuit for each of the lines.

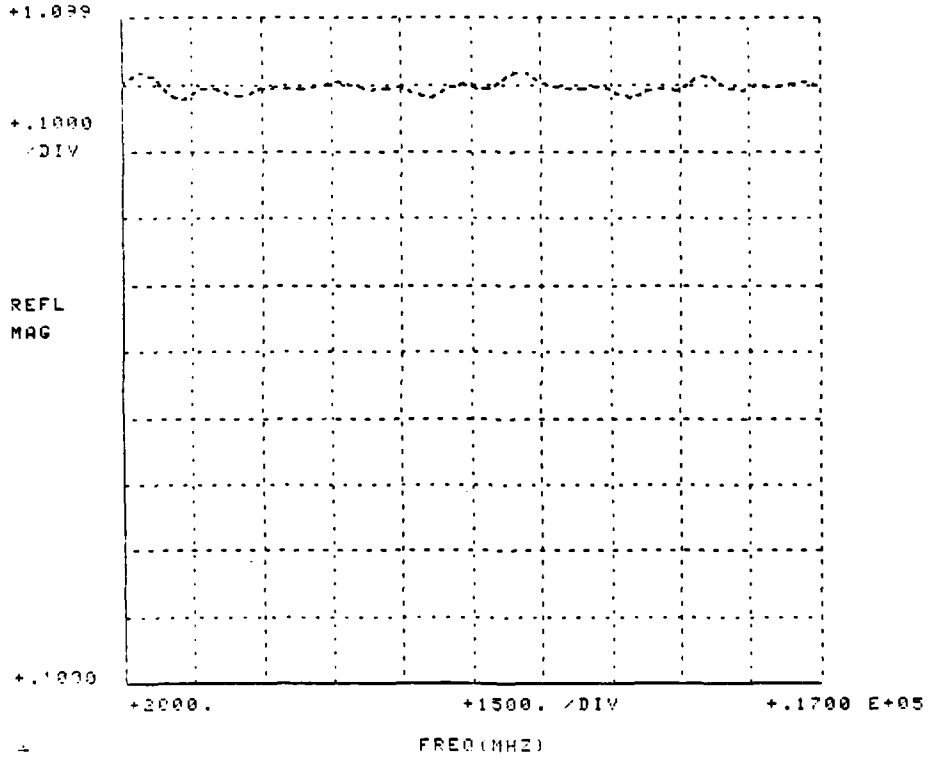

Fig. 48. Reflection of open circuit referenced to "our" line (Mag).

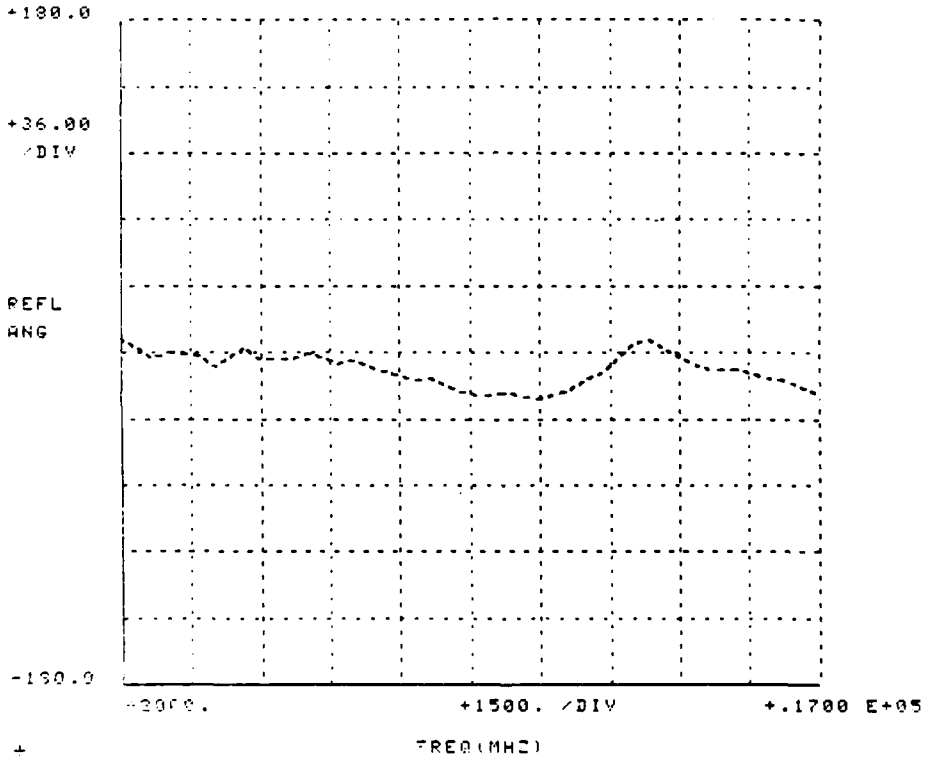

Fig. 49. Reflection of open circuit referenced to "our" line (Ang).

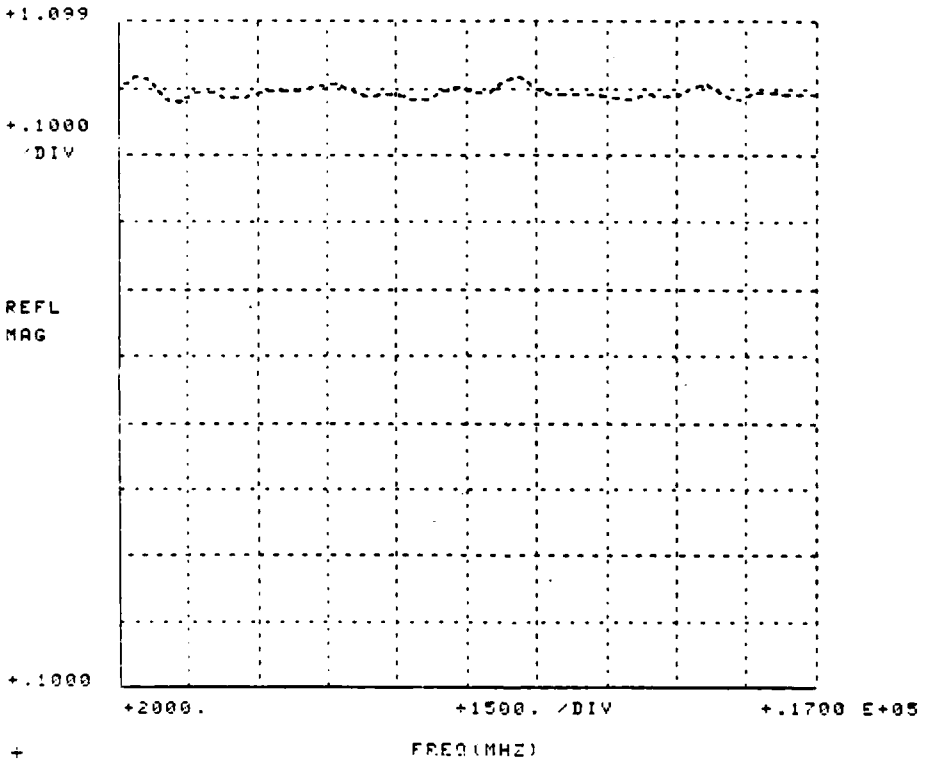

Fig. 50. Reflection of open circuit referenced to "short" line (Mag).

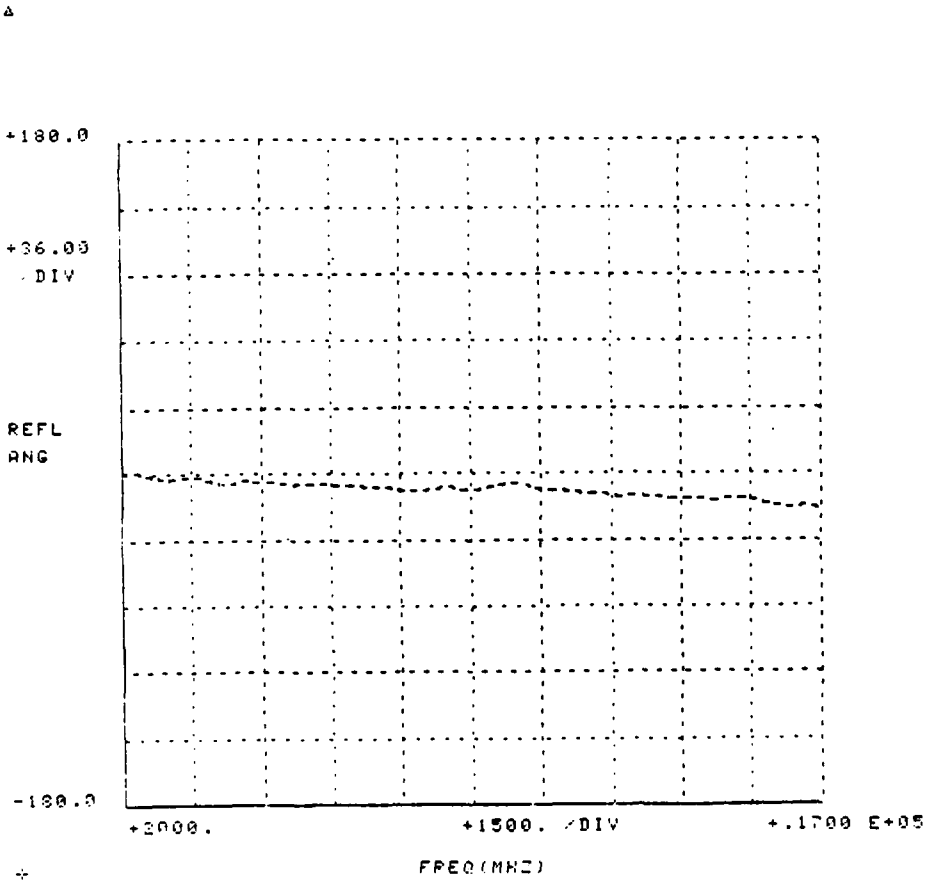

Fig. 51. Reflection of open circuit referenced to "short" line (Ang).

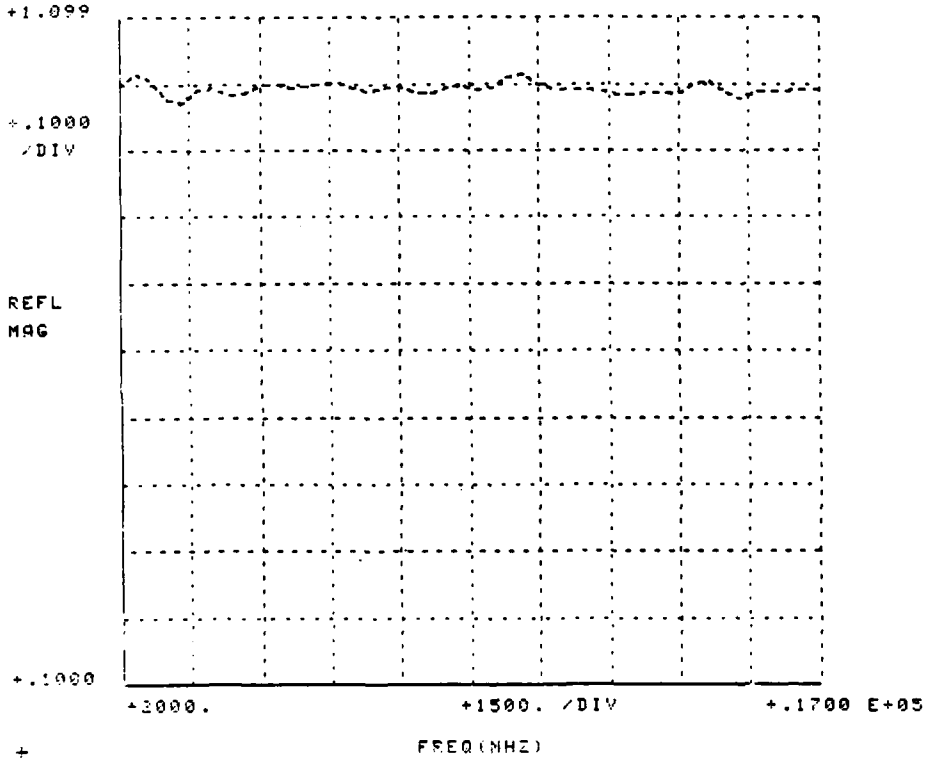

Fig. 52. Reflection of open circuit referenced to "long" line (Mag).

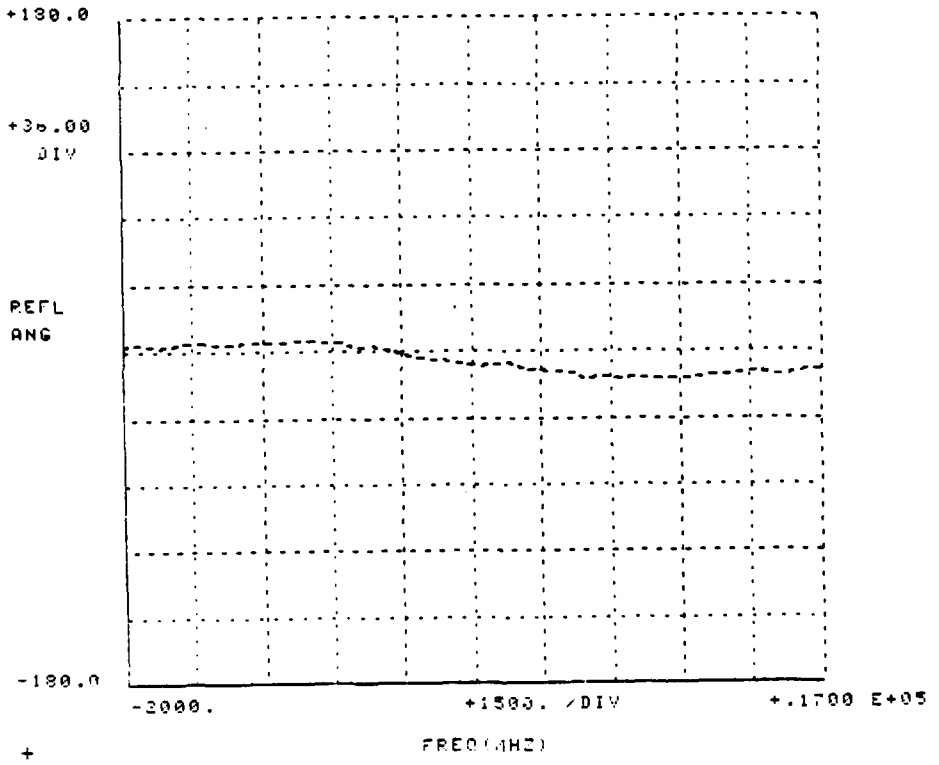

Fig. 53. Reflection of open circuit referenced to "long" line (Ang).

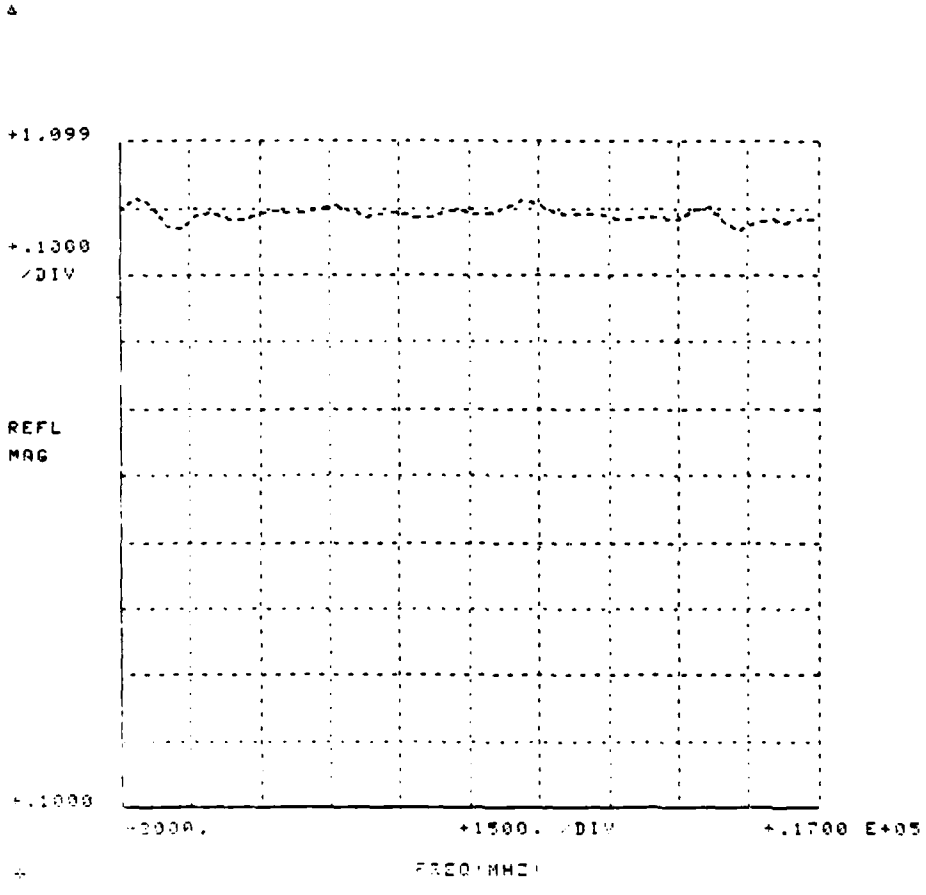

Fig. 54. Reflection of open circuit referenced to "spline" line (Mag).

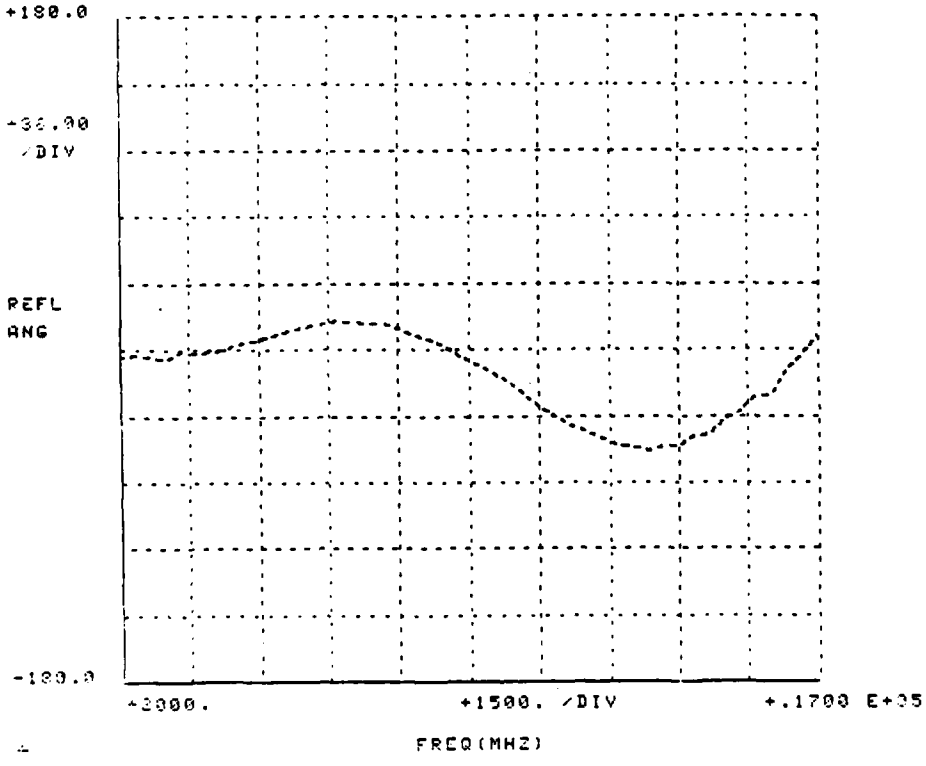

Fig. 55. Reflection of open circuit referenced to "spline" line (Ang).

The magnitude plots are virtually the same, but as would be expected, the phase plots are quite different. Even the "short" and "long" line exhibited different phase characteristics and they are of the same construction except for length. There is also no apparent correlation between the phase variations of the open circuits of the same sex either. The phase characteristics of the SMA open circuit are, therefore, more dependent upon the interconnecting line characteristics than on the general construction of the line or the connectors. This evidence supports the earlier claim that it would be practically impossible to characterize an SMA open circuit without specifying the transmission line defining zero reflection.

The final set of results contain the reflection plots for the direct comparison of each transmission line against each of the others for 14-16 GHz region. Figures 56-57 show the magnitude and phase plots of the comparison "our" line versus "our" line. Indeed, the magnitude and phase are zero as would be expected when comparing two identical lines. Figures 58-81 show the real and imaginary components of the reflection for each of the other comparisons.

Three noteworthy observations can be made. First, two lines of the same construction, but different lengths,

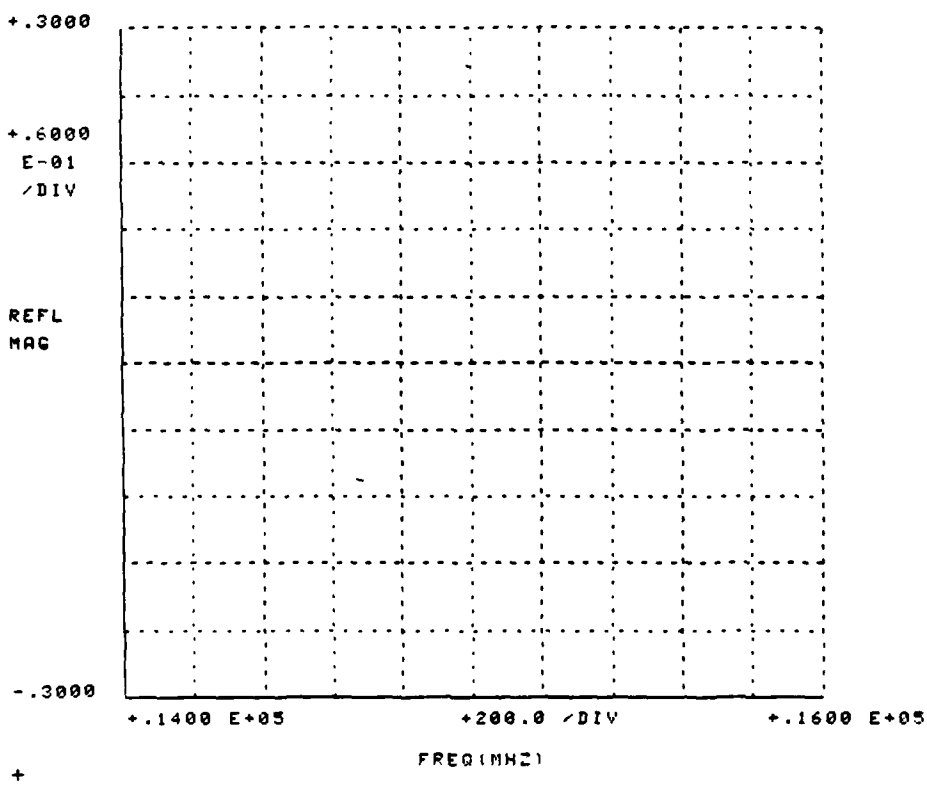

Fig. 56. Comparison of "our" line to "our" line (Mag).

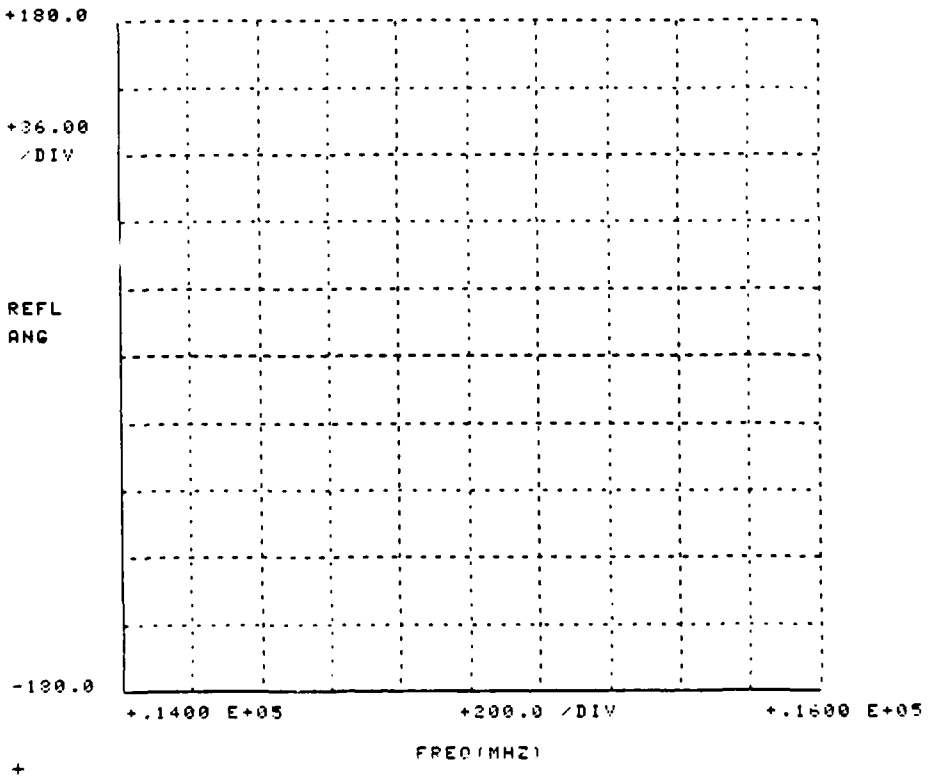

Fig. 57. Comparison of "our" line to "our" line (Ang).

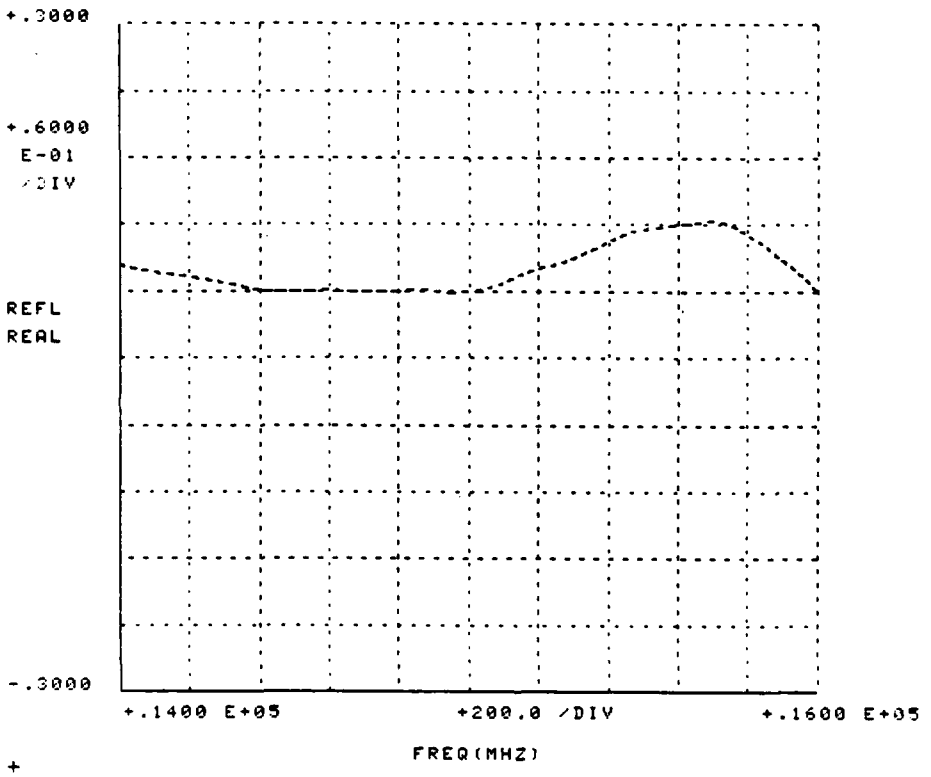

Fig. 58. Comparison of "short" line to "our" line (Real).

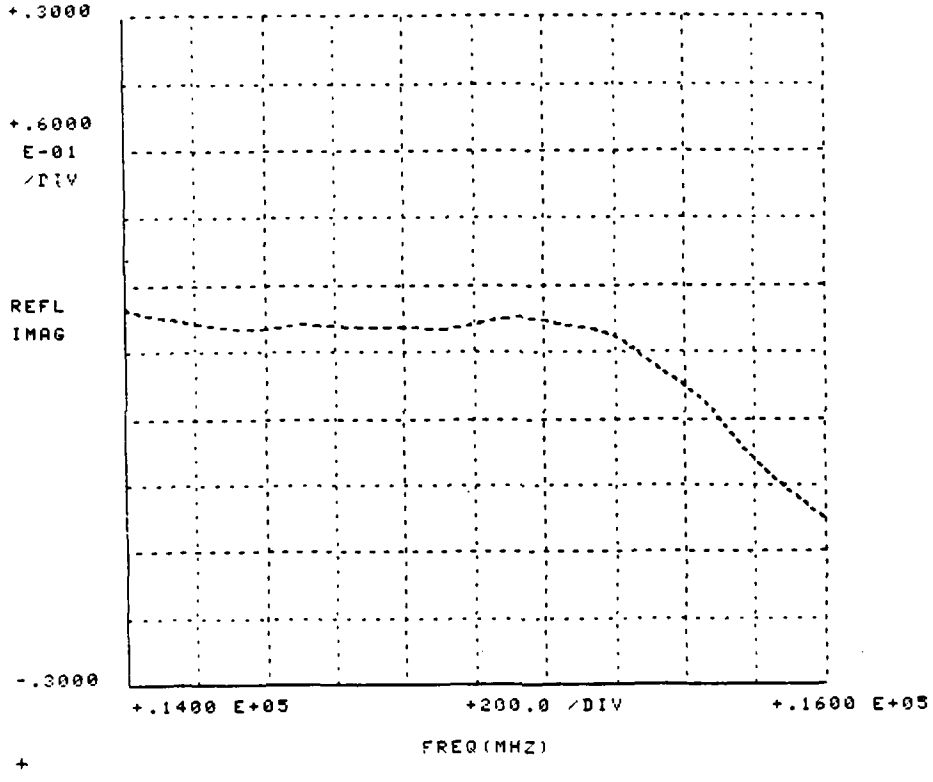

Fig. 59. Comparison of "short" line to "our" line (Imag).

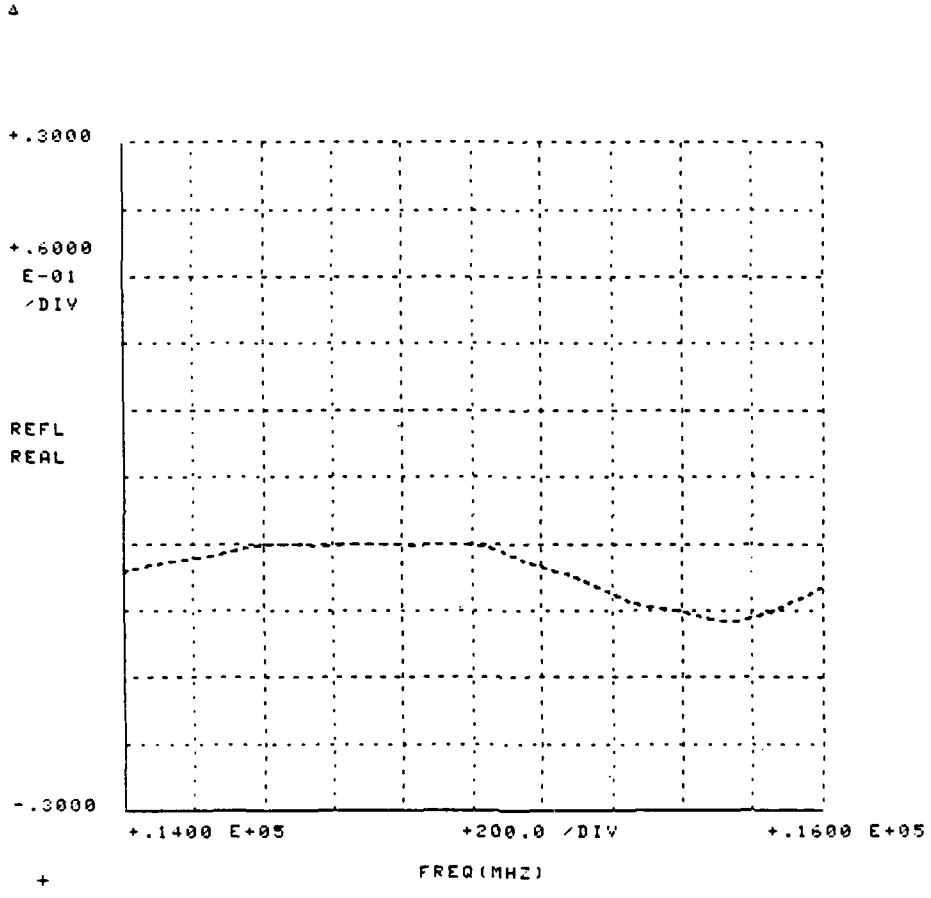

Fig. 60. Comparison of "our" line to "short" line (Real).

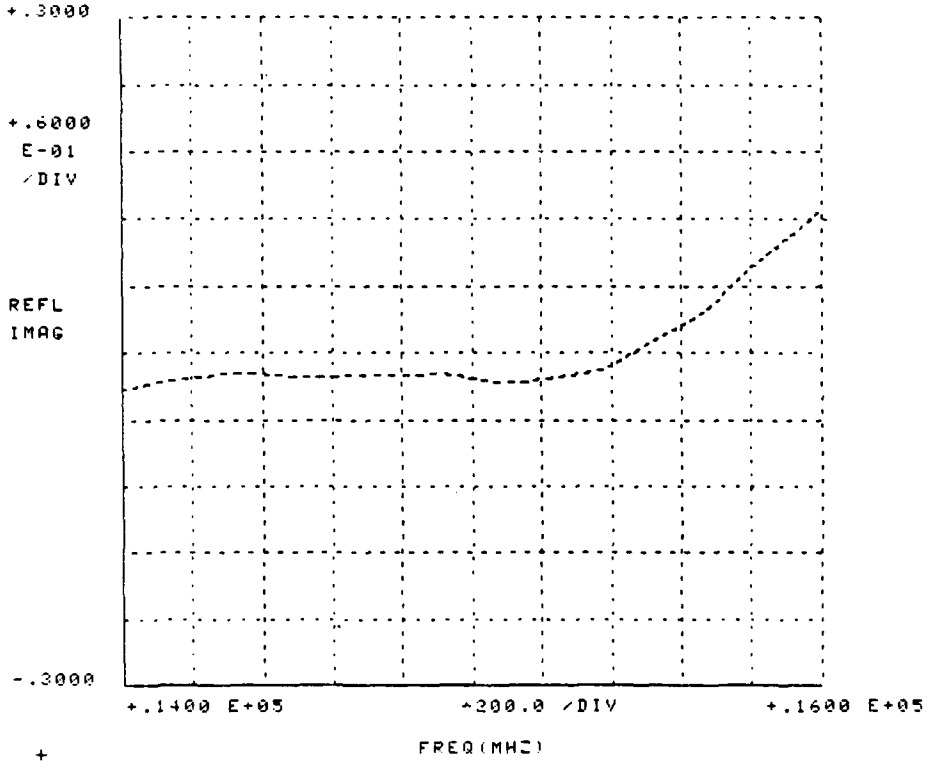

Fig. 61. Comparison of "our" line to "short" line (Imag).

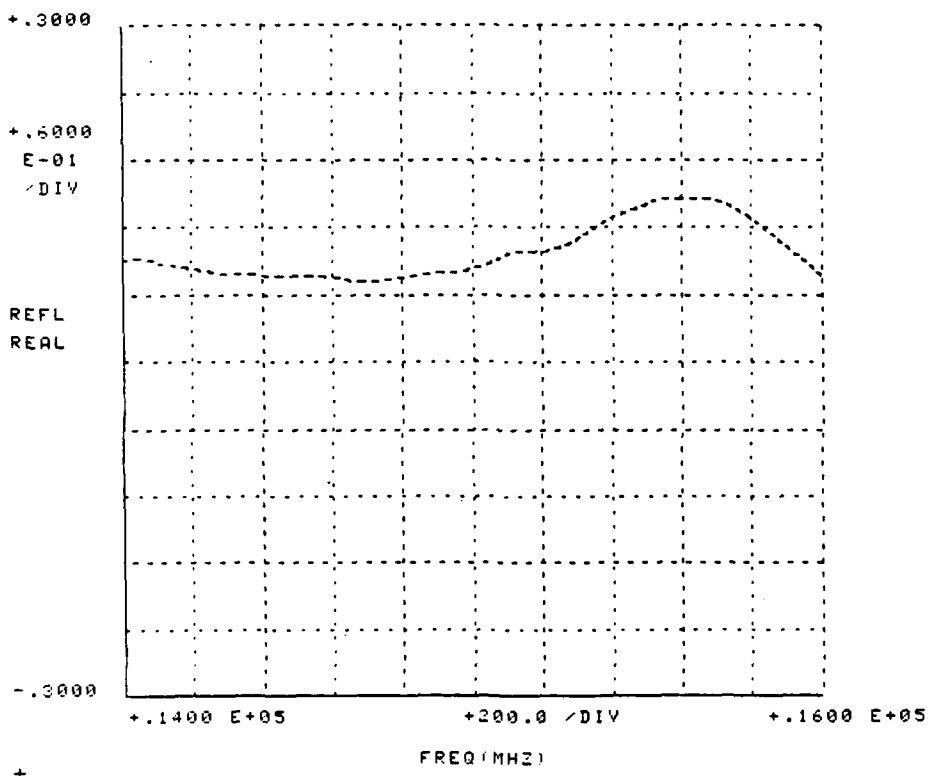

Fig. 62. Comparison of "long" line to "our" line (Real).

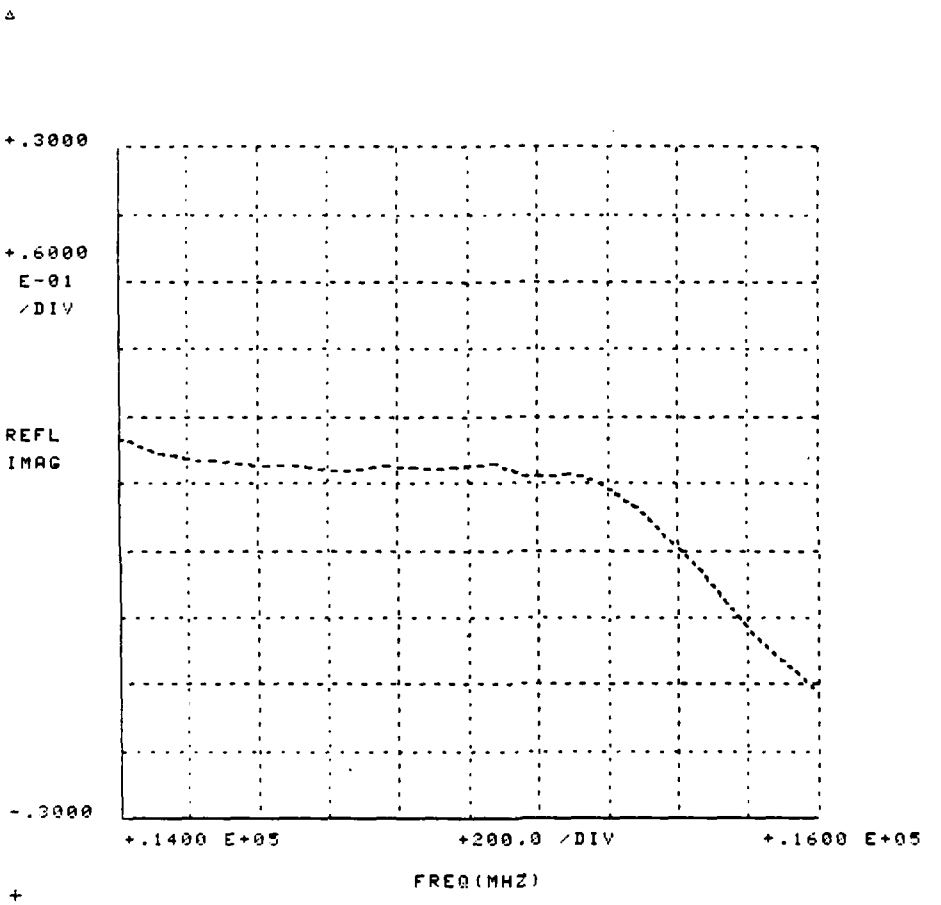

Fig. 63. Comparison of "long" line to "our" line (Imag).

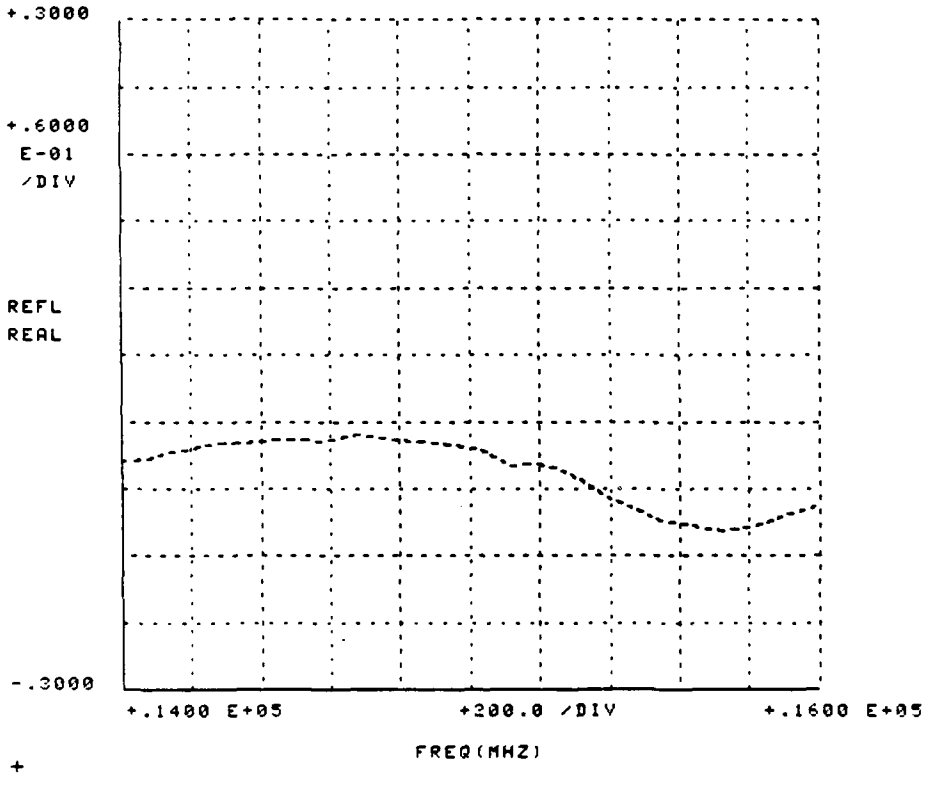

Fig. 64. Comparison of "our" line to "long" line (Real).

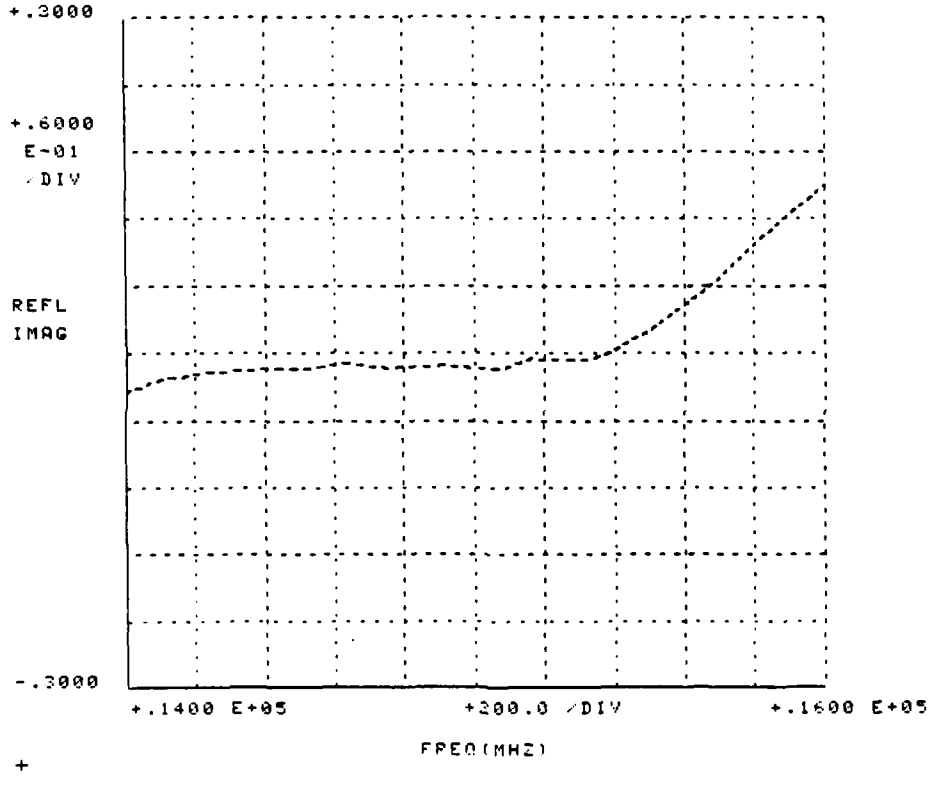

Fig. 65. Comparison of "our" line to "long" line (Imag).

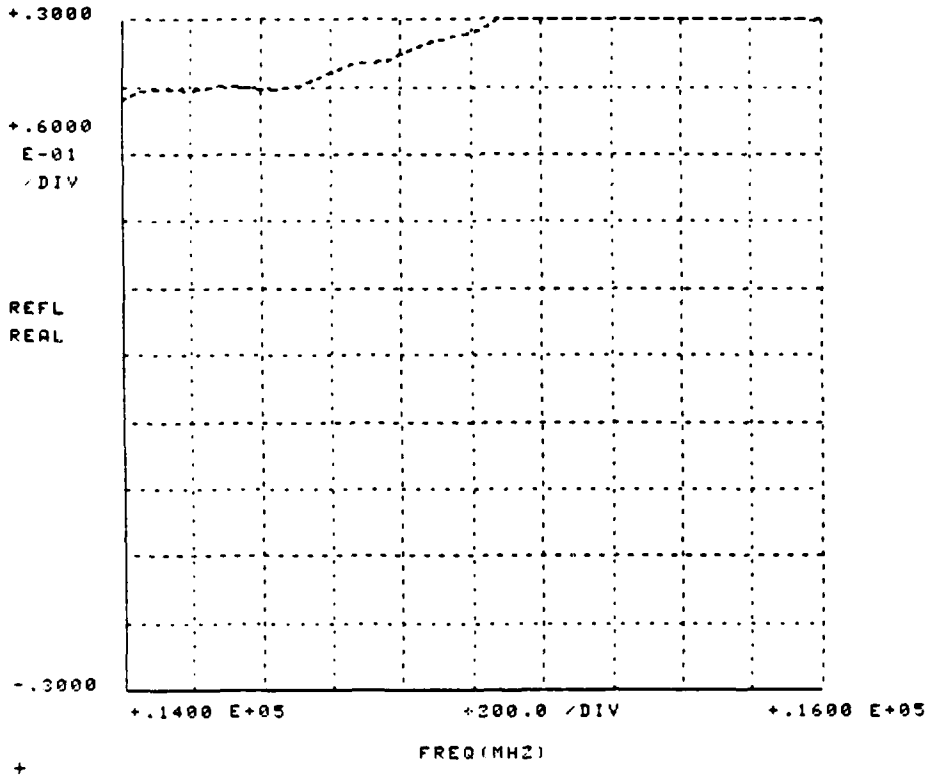

Fig. 66. Comparison of "spline" line to "our" line (Real).

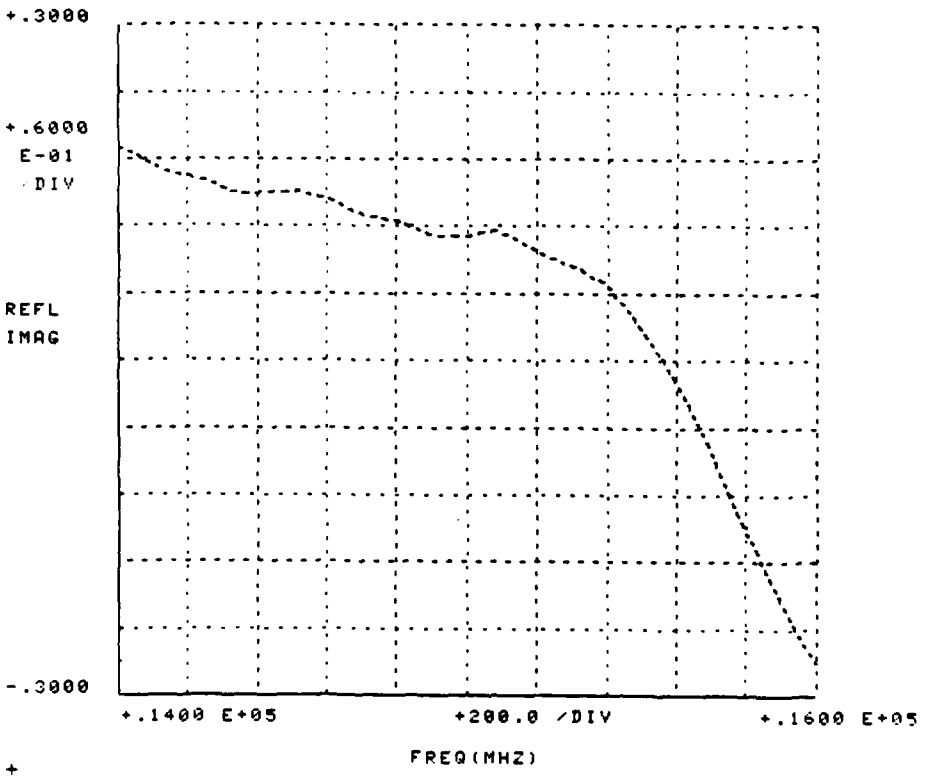

Fig. 67. Comparison of "spline" line to "our" line (Imag).

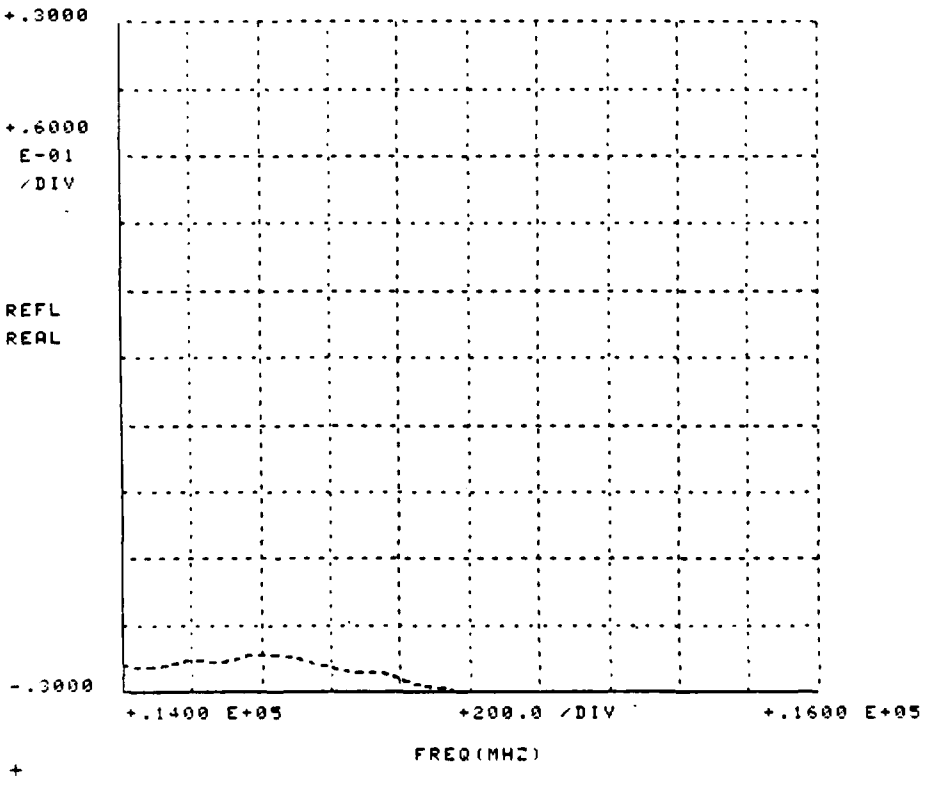

Fig. 68. Comparison of "our" line to "spline" line (Real).

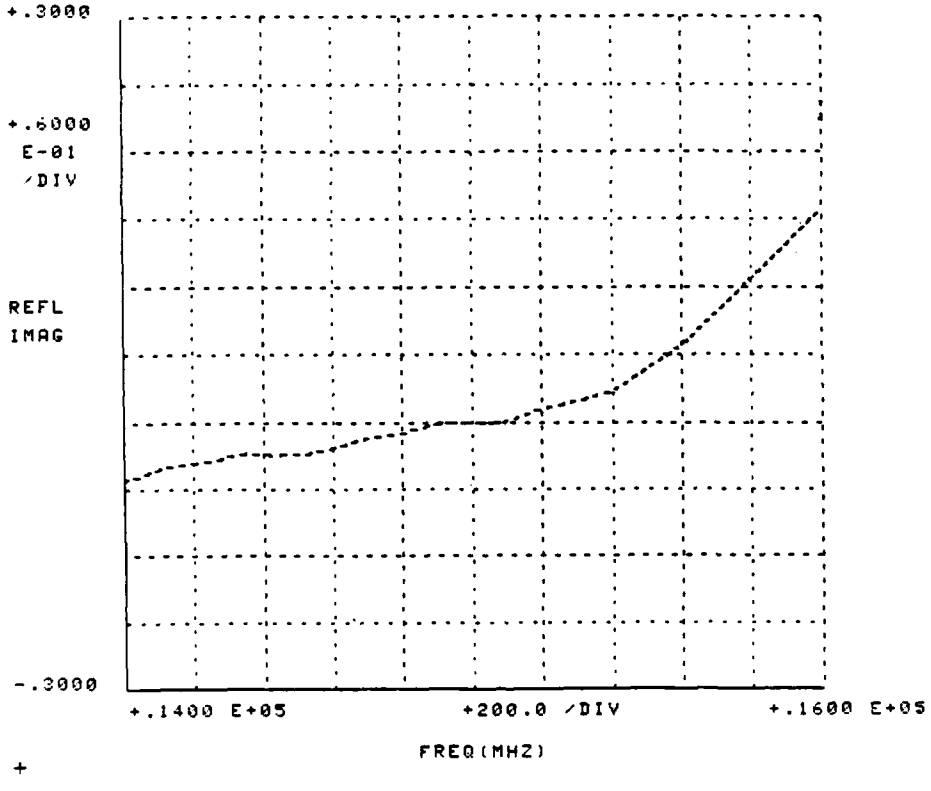

Fig. 69. Comparison of "our" line to "spline" line (Imag).

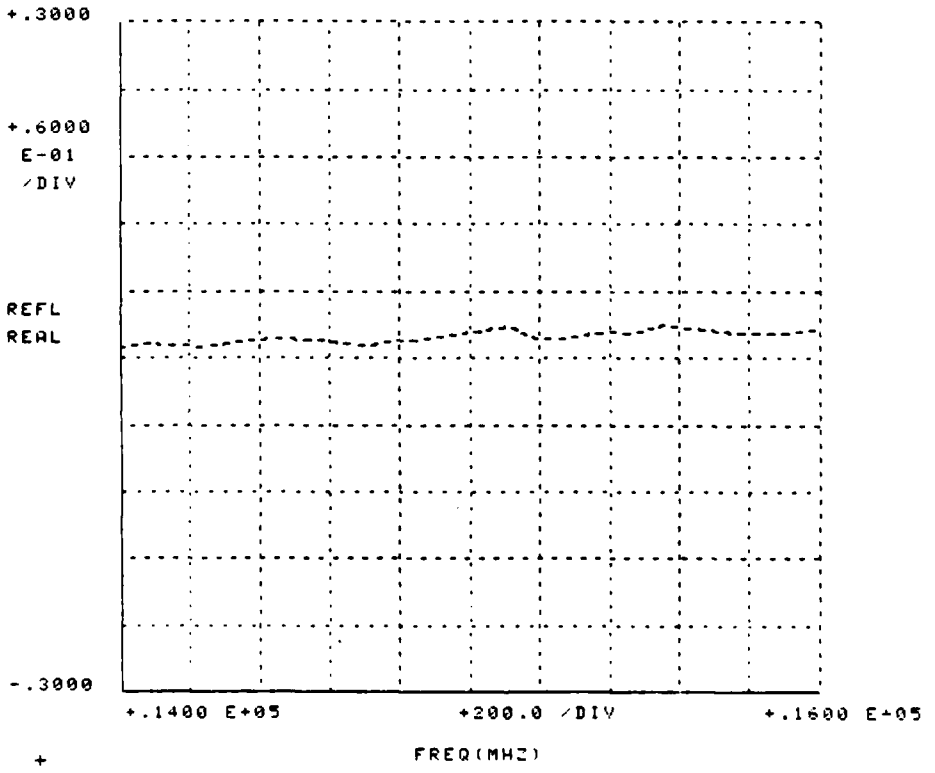

Fig. 70. Comparison of "long" line to "short" line (Real).

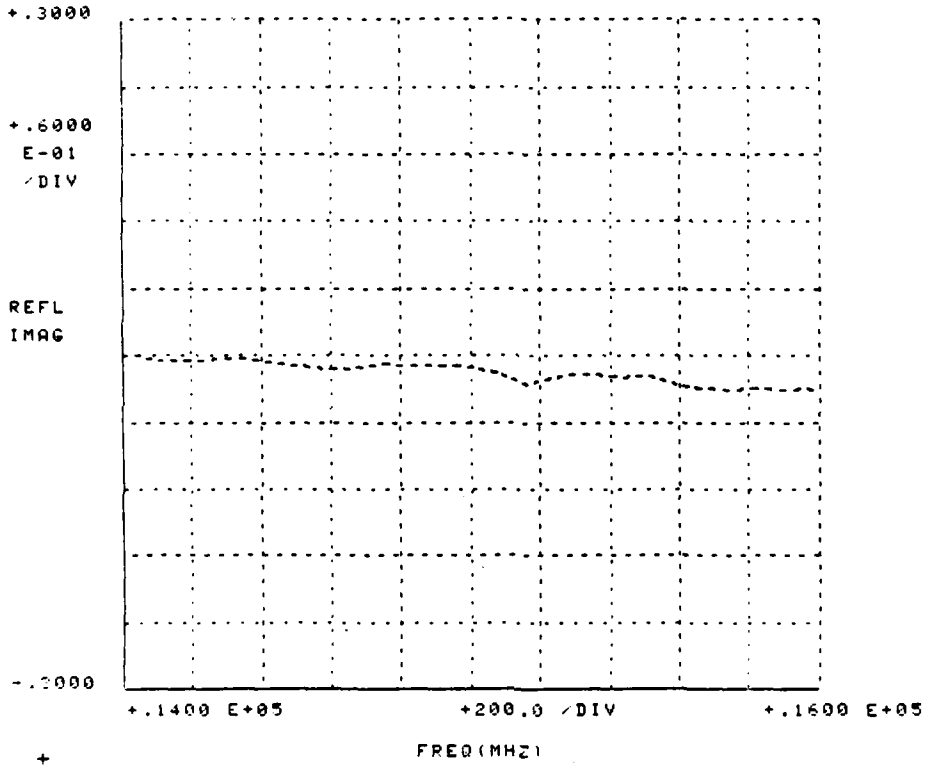

Fig. 71. Comparison of "long" line to "short" line (Imag).

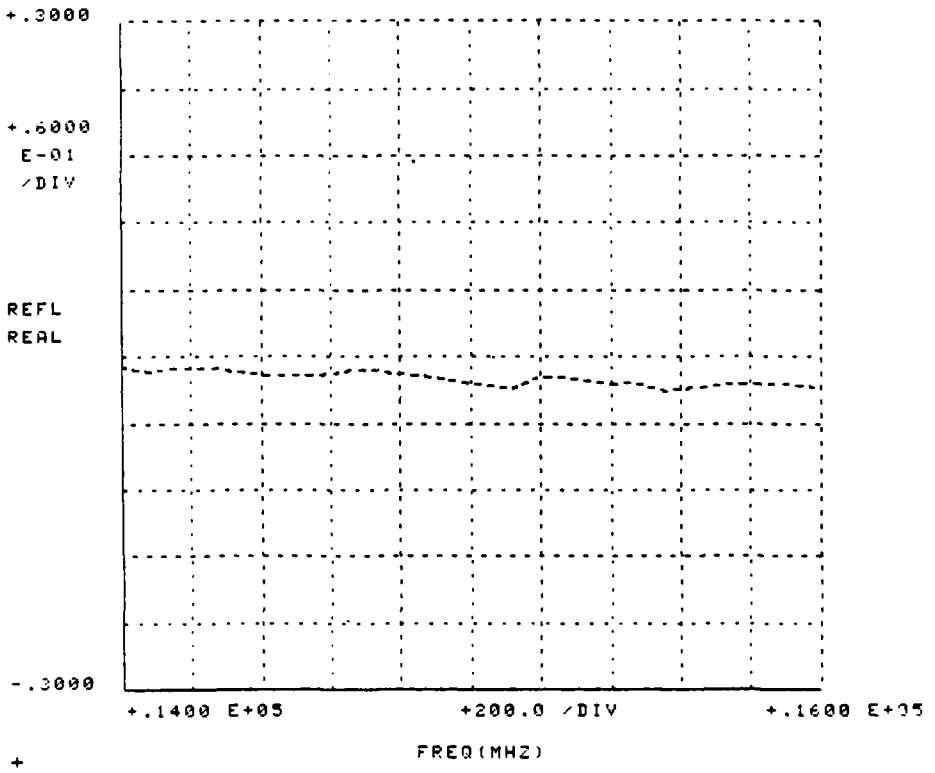

Fig. 72. Comparison of "short" line to "long" line (Real).

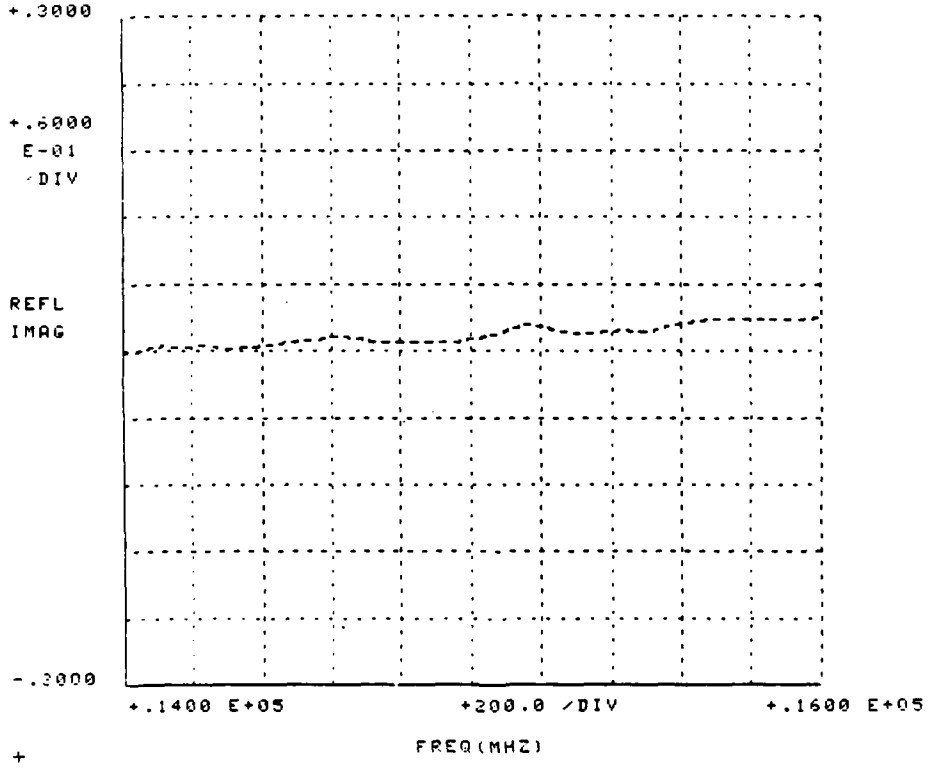

Fig. 73. Comparison of "short" line to "long" line (Imag).

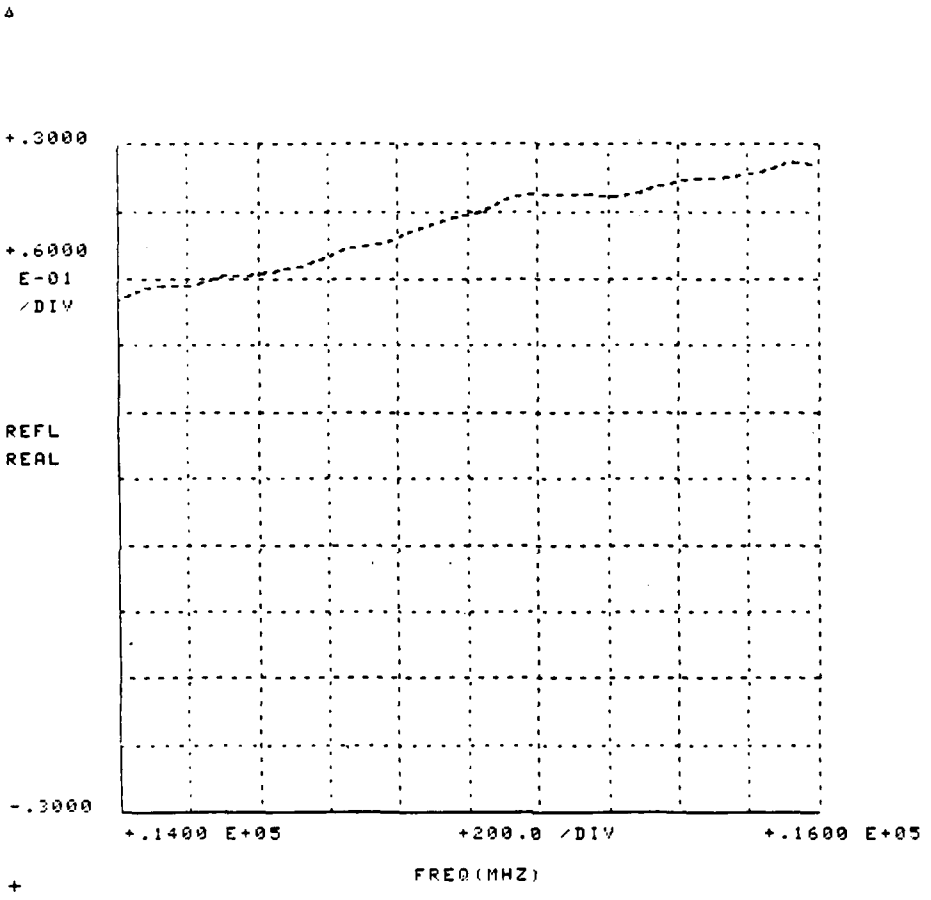

Fig. 74. Comparison of "spline" line to "short" line (Real).

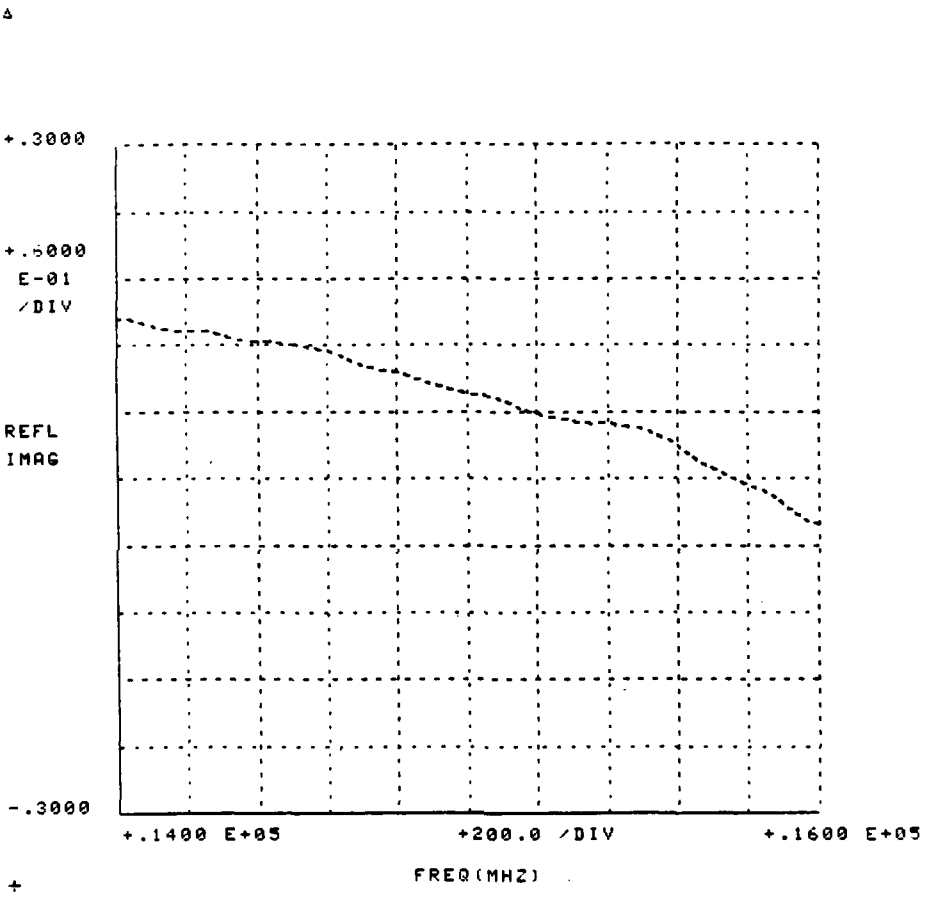

Fig. 75. Comparison of "spline" line to "short" line (Imag).

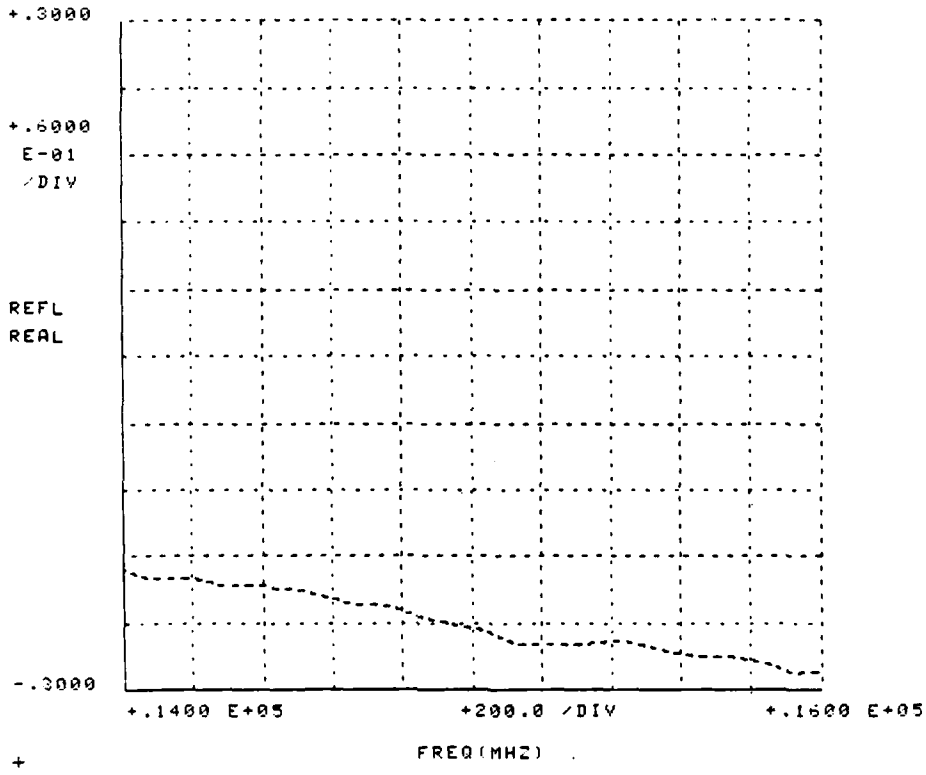

Fig. 76. Comparison of "short" line to "spline" line (Real).

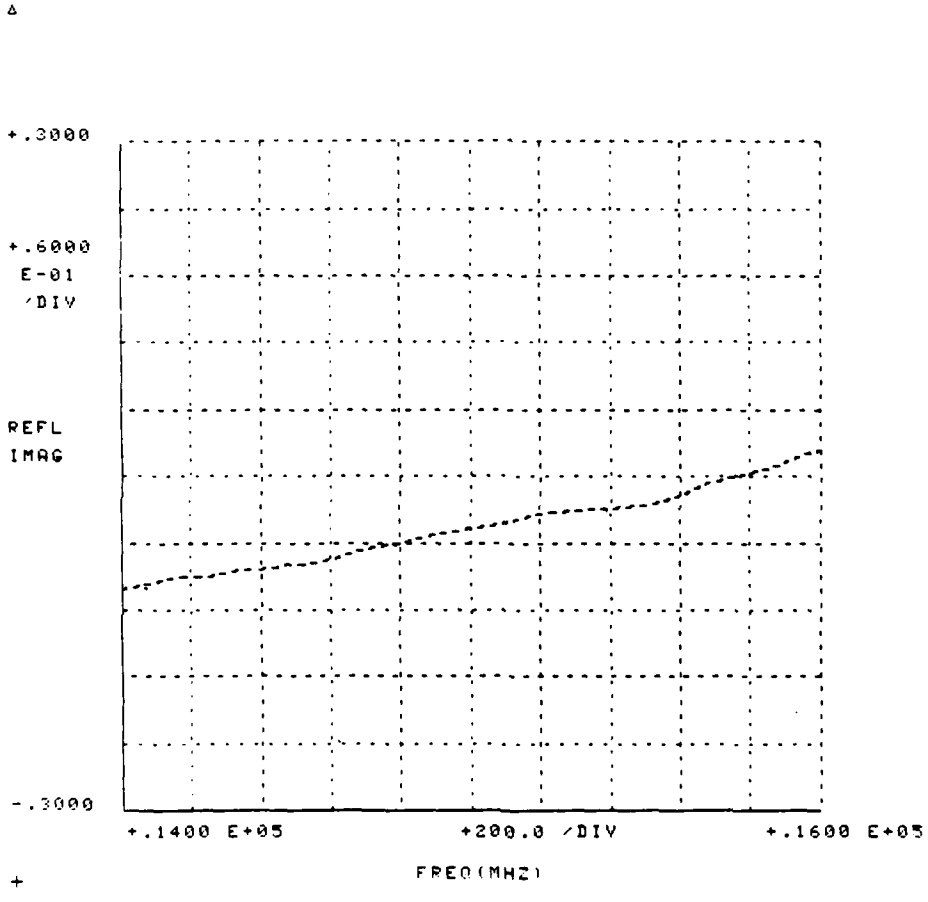

Fig. 77. Comparison of "short" line to "spline" line (Imag).

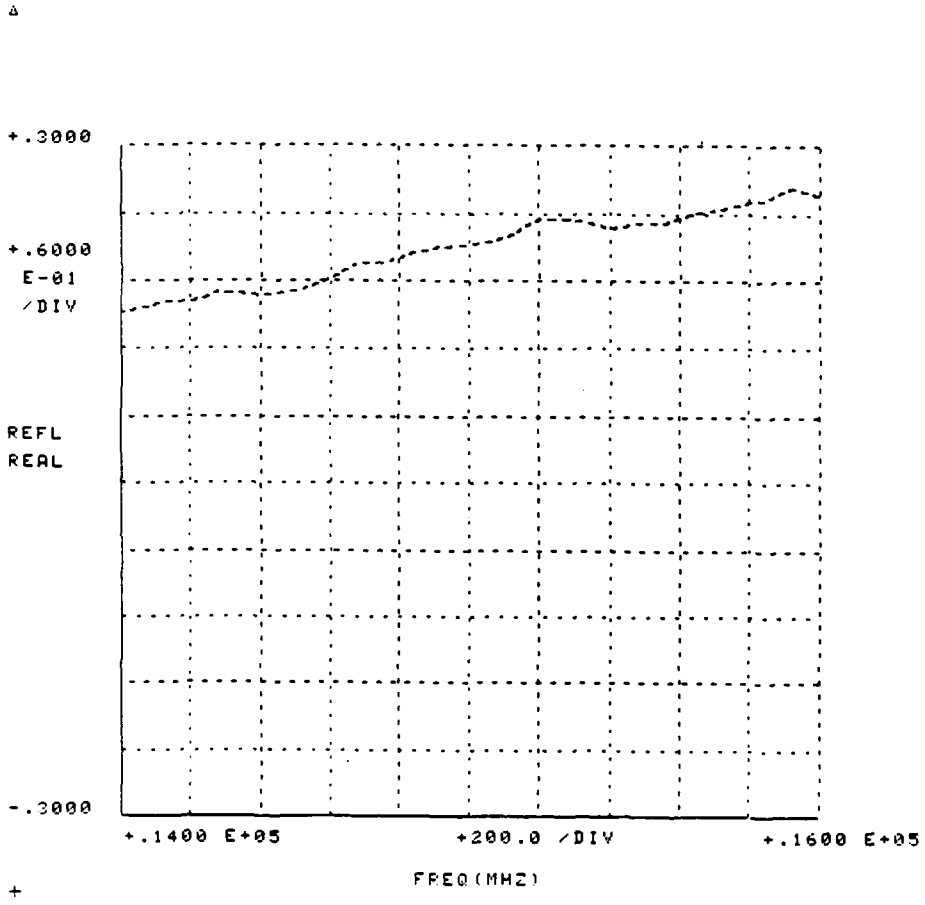

Fig. 78. Comparison of "spline" line to "long" line (Real).

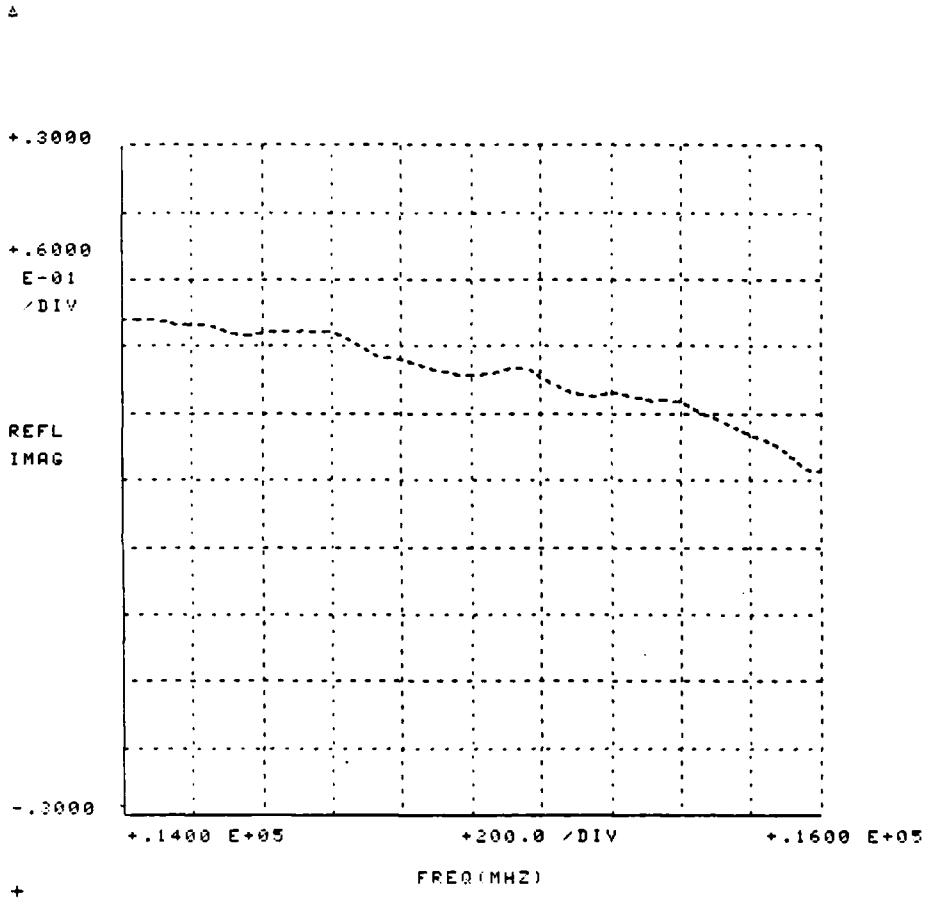

Fig. 79. Comparison of "spline" line to "long" line (Imag).

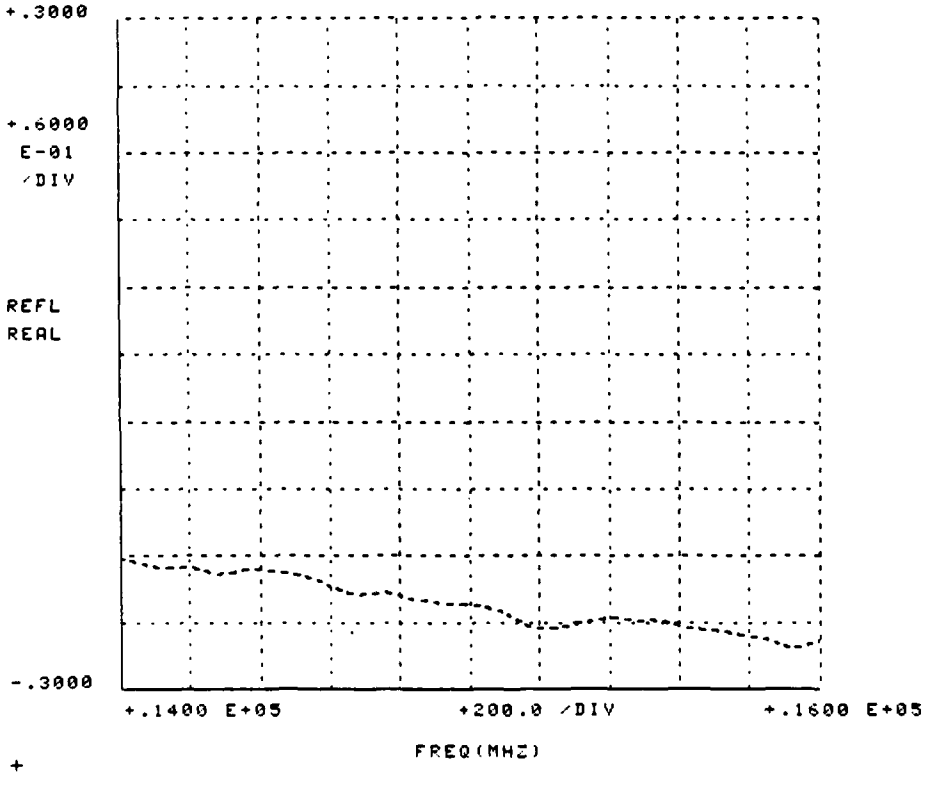

Fig. 80. Comparison of "long" line to "spline" line (Real).

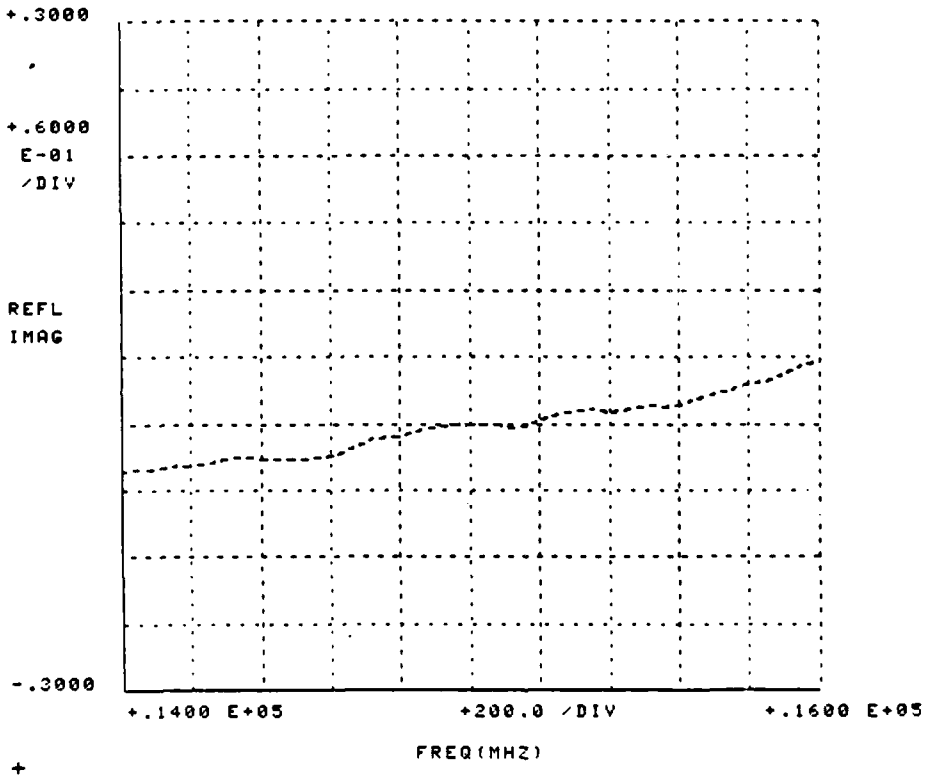

Fig. 81. Comparison of "long" line to "spline" line (Imag).

would be expected to match well. Looking at the results of the "long" vs. "short" line, one can see that they do match quite well, but they are also not identical.

Second, when comparing the "long" versus "short" and then the "short" versus "long" (or any other analagous sets of data). One can see that real and imaginary parts for one comparison are reflected from zero in the opposite comparison, as would be expected.

Third, it is clear that the characteristics of the "spline" line are very much different from those of the other three lines. On the contrary, the characteristics of the other three lines do not differ widely. Apparently the "spline" line does not have a 50 + j0 ohm characteristic impedance.

EXTENSION OF ADAPTER CORRECTION TO TWO-PORT DEVICE DE-EMBEDDING

Up to this point, discussion has been limited to 1-port reflection measurements. A large proportion of microwave devices are two-port in construction and cannot be fully characterized by reflection measurements only. Therefore, a method of extending the adapter correction to two-port measurements needed to be developed. One method will now be described.

In connection systems such as SMA there are two types of two-port devices: insertable, which have one female and one male connector, and noninsertable, which have the same sex connectors at both ports, be they male or female. As a consequence, any adapter kit used for general two-port measurements must include two adapters for each sex and the same sex adapters cannot be assumed to be identical. Therefore, a method of measuring the scattering matrices of these four adapters in order to de-embed the scattering matrix for the DUT will now be presented.

Let A and B represent the scattering matrices for the adapters of one sex and C and D of the other. It will be reasonably assumed that all adapters are passive and reciprocal, that a proper APC-7 calibration has been ac-

complished and that all measurements are corrected for system errors against this calibration. (Note that the DUT need not be reciprocal.) Also, discussion will assume that SMA adapters are being used, but the method is directly applicable to any type of adapter.

Letting the APC-7 end of one sex adapter, say female, be port 1, the SMA end be port 2, the SMA end of the male adapter be port 3, and, finally, the APC-7 end of the male adapter be port 4, one obtains the following flowgraphs:

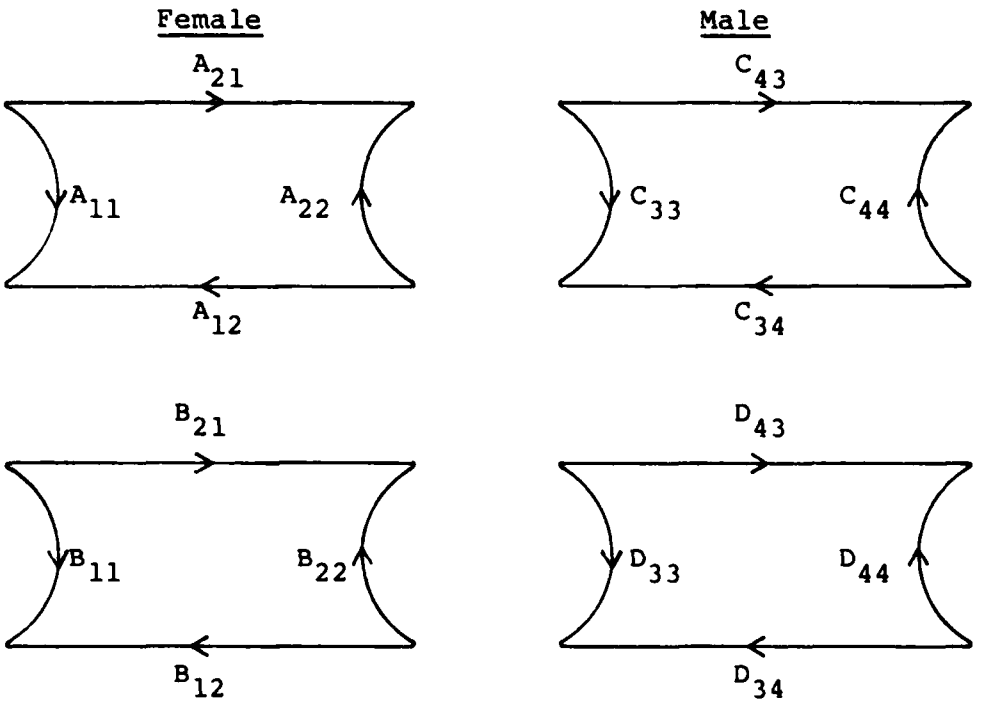

Fig. 82. Flowgraphs for one set of four adapters.

A_{11}, B_{11}, C_{44}, and D_{44} can be found directly by measuring the reflection of each adapter when terminated by a matched load (fixed, sliding, or, as previously discussed, the Running Averaged load and line) on the SMA end.

Reflection measurements are next made on each adapter with a zero-plane short circuit attached to the SMA end. The following equations result where Γ_1, Γ_2, Γ_3, and Γ_4 represent the measurements on the A, B, C, and D adapters, respectively.

$$\Gamma_1 = A_{11} + \frac{(A_{21})^2 (-1)}{1 + A_{22}} \tag{32}$$

$$\Gamma_2 = B_{11} + \frac{(B_{21})^2 (-1)}{1 + B_{22}} \tag{33}$$

$$\Gamma_3 = C_{44} + \frac{(C_{43})^2 (-1)}{1 + C_{33}} \tag{34}$$

$$\Gamma_4 = D_{44} + \frac{(D_{43})^2 (-1)}{1 + D_{33}} \tag{35}$$

By rearranging Eqs. 32-35 and solving for A_{21}^2, B_{21}^2, C_{43}^2 and D_{43}^2, one obtains

$$A_{21}^2 = (A_{11} - \Gamma_1)(1 + A_{22}) \tag{36}$$

$$B_{21}^2 = (B_{11} - \Gamma_2)(1 + B_{22}) \tag{37}$$

$$C_{43}^2 = (C_{44} - \Gamma_3)(1 + C_{33}) \tag{38}$$

$$D_{43}^2 = (D_{44} - \Gamma_4)(1 + D_{33}) \tag{39}$$

Now attaching the SMA ends of A and C and of B and D together, one makes reflection measurements on each end of each adapter pair with the other end terminated with a matched load, obtaining

$$\Gamma_5 = \frac{A_{21}^2 \, C_{33}}{1 - A_{22} \, C_{33}} \tag{40}$$

$$\Gamma_6 = \frac{C_{43}^2 \, A_{22}}{1 - A_{22} \, C_{33}} \tag{41}$$

$$\Gamma_7 = \frac{B_{21}^2 \, D_{33}}{1 - B_{22} \, D_{33}} \tag{42}$$

$$\Gamma_8 = \frac{D_{43}^2 \, B_{22}}{1 - B_{22} \, D_{33}} \tag{43}$$

where Γ_5, Γ_6, Γ_7 and Γ_8 are the measured reflection. Rearranging Eqs. 40-43 yields

$$A_{21}^2 = \frac{\Gamma_5(1 - A_{22} \, C_{33})}{C_{33}} \tag{44}$$

$$B_{21}^2 = \frac{\Gamma_7(1 - B_{22} \, D_{33})}{D_{33}} \tag{45}$$

$$C_{43}^2 = \frac{\Gamma_6(1 - A_{22} \, C_{33})}{A_{22}} \tag{46}$$

$$D_{43}^2 = \frac{\Gamma_8(1 - B_{22} \, D_{33})}{B_{22}} \tag{47}$$

Appropriately equating Eqs. 36-39 to Eqs. 44-47 and rearranging terms yields

$$X_1 = \frac{\Gamma_5}{A_{11} - \Gamma_1} = \frac{C_{33}(1 + A_{22})}{1 - A_{22}\, C_{33}} \tag{48}$$

$$X_2 = \frac{\Gamma_7}{B_{11} - \Gamma_2} = \frac{D_{33}(1 + B_{22})}{1 - B_{22}\, D_{33}} \tag{49}$$

$$X_3 = \frac{\Gamma_6}{C_{44} - \Gamma_3} = \frac{A_{22}(1 + C_{33})}{1 - A_{22}\, C_{33}} \tag{50}$$

$$X_4 = \frac{\Gamma_8}{D_{44} - \Gamma_4} = \frac{B_{22}(1 + D_{33})}{1 - B_{22}\, D_{33}} \tag{51}$$

where X_1, X_2, X_3, and X_4 are calculable as shown. Solving for C_{33} in Eq. 48, D_{33} in Eq. 49, A_{22} in Eq. 50, and B_{22} in Eq. 51, one finds

$$C_{33} = \frac{X_1}{1 + A_{22} + X_1\, A_{22}} \tag{52}$$

$$D_{33} = \frac{X_2}{1 + B_{22} + X_2 B_{22}} \tag{53}$$

$$A_{22} = \frac{X_3}{1 + C_{33} + X_3 C_{33}} \tag{54}$$

$$B_{22} = \frac{X_4}{1 + D_{33} + X_4 D_{33}} \tag{55}$$

Substituting C_{33} in Eq. 52 into Eq. 54 and D_{33} in Eq. 53 into Eq. 55, we find

$$A_{22} = \frac{X_3}{X_1 + 1} \tag{56}$$

$$B_{22} = \frac{X_4}{X_2 + 1} \tag{57}$$

Substitution of A_{22} and B_{22} into Eqs. 52 and 54 permits calculation of C_{33} and D_{33}.

Since two possible square roots exist for any complex number, each separated by 180° from the other in

the complex plane, it first appeared that a method of choosing the correct root would be necessary. However, it was observed that since the adapters are always used in pairs, and since the roots differ only in sign, it is not necessary to solve for the correct root. All that needs to be known is that the roots of A_{21}^2, B_{21}^2, C_{43}^2, and D_{43}^2 are all correct or that all are incorrect because the products $A_{21}C_{43}$, $A_{21}D_{43}$, etc. representing the transmission paths through the adapter pairs will be equal in either case. This observation greatly simplifies the task of finding the roots.

One method is to measure the transmission through adapter pairs combined in three different ways. For example, let $T_1 = A_{21}C_{43}$, $T_2 = B_{21}D_{43}$, and $T_3 = B_{21}C_{43}$. Then solve for one root of A_{21}, B_{21}, C_{43}, and D_{43} (A_r, B_r, C_r, and D_r, respectively).

If angle $(A_rC_r) \neq$ angle (T_1), then reverse the sign of either A_r or C_r. Otherwise, accept the signs as they are. Secondly, if angle $(B_rC_r) \neq$ angle (T_3), then reverse the sign of B_r; otherwise accept it. Thirdly, if angle $(B_rD_r) \neq$ angle (T_2), reverse the sign of D_r; otherwise, accept that one.

At this point, either the signs of A_r, B_r, C_r, or D_r are all correct or they are all incorrect, exactly the information needed to proceed with the de-embedding of the scattering matrix of a DUT connected between any pair of adapters. It is important to note that the numbering of the ports has been chosen for convenience here, and that they can be represented in any suitable manner. Note that the adapters are reciprocal and that the forward and reverse transmission parameters of each adapter have been freely interchanged.

Now that the scattering matrices have been found for each adapter, de-embedding of the scattering parameters for the DUT alone can be performed. By de-embedding one adapter at a time, one avoids solving a pair of complex quadratic equations and an explicit solution can be obtained with gratifying simplicity. This procedure is much easier to understand and implement than a previous technique presented by Saleh (Ref. 14).

For the sake of discussion, let's assume that a scattering matrix E is measured for a DUT in combination with adapters A and C, as above, even though any pair of adapters can be used. Treating the DUT and adapter C as a lumped device with scattering matrix $\mathcal{S}$, E can be represented by a model as illustrated below.

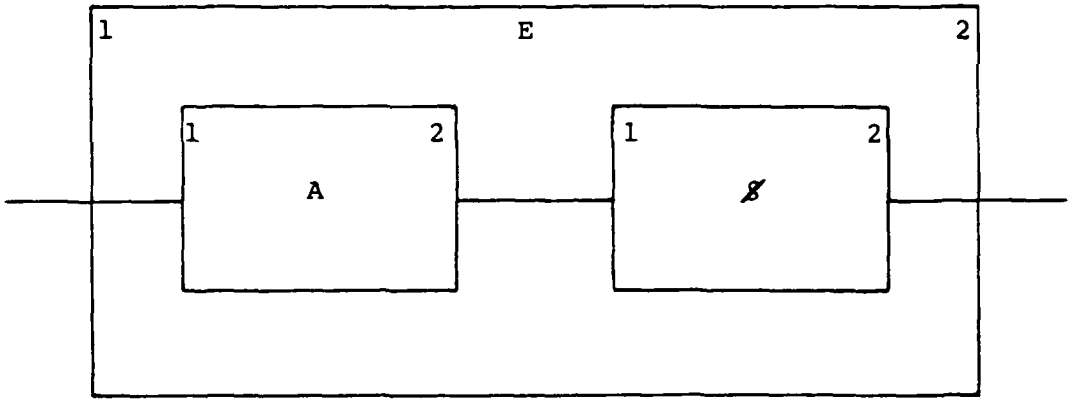

Fig. 83. Model for separating adapter A from lumped device $\mathcal{B}$.

From the flowgraph for the model above the following equations result.

$$E_{11} = A_{11} + \frac{A_{21}^2 \mathcal{B}_{11}}{1 - A_{22} \mathcal{B}_{11}} \tag{58}$$

$$E_{12} = \frac{A_{21} \mathcal{B}_{12}}{1 - A_{22} \mathcal{B}_{11}} \tag{59}$$

$$E_{21} = \frac{A_{21}\,\mathcal{S}_{21}}{1 - A_{22}\,\mathcal{S}_{11}} \tag{60}$$

$$E_{22} = \mathcal{S}_{22} + \frac{\mathcal{S}_{21}\,\mathcal{S}_{12}\,A_{22}}{1 - A_{22}\,\mathcal{S}_{11}} \tag{61}$$

Since the scattering matrix A is known, matrix $\mathcal{S}$ can be derived from the measurements of scattering matrix E.

$$\mathcal{S}_{11} = \frac{E_{11} - A_{11}}{A_{21}^2 + E_{11}\,A_{22} - A_{11}\,A_{22}} \tag{62}$$

$$\mathcal{S}_{21} = \frac{E_{21}(1 - A_{22}\,\mathcal{S}_{11})}{A_{21}} \tag{63}$$

$$\mathcal{S}_{12} = \frac{E_{12}(1 - A_{22}\,\mathcal{S}_{11})}{A_{21}} \tag{64}$$

$$\mathcal{S}_{22} = E_{22} - \frac{\mathcal{S}_{21}\,\mathcal{S}_{12}\,A_{22}}{1 - A_{22}\,\mathcal{S}_{11}} \tag{65}$$

Lastly, it is necessary to de-embed the scattering matrix S for the DUT from $\mathcal{S}$. The following model is then employed.

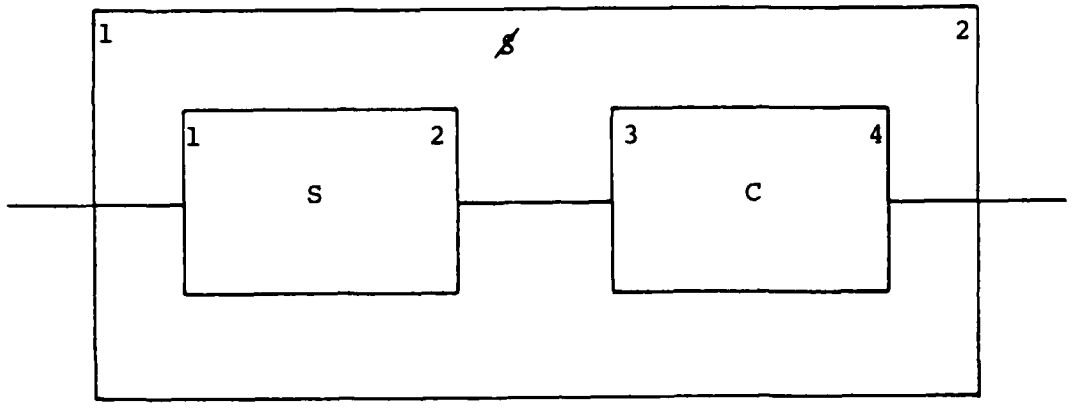

Fig. 84. Model for separating adapter C from DUT.

From this model one finds

$$\mathcal{S}_{11} = S_{11} + \frac{S_{21}\, S_{12}\, C_{33}}{1 - S_{22}\, C_{33}} \tag{66}$$

$$\mathcal{S}_{21} = \frac{S_{21}\, C_{43}}{1 - S_{22}\, C_{33}} \tag{67}$$

$$\mathcal{S}_{12} = \frac{S_{12}\, C_{43}}{1 - S_{22}\, C_{33}} \tag{68}$$

$$\mathcal{S}_{22} = C_{44} + \frac{C_{43}^2 \, S_{22}}{1 - S_{22} \, C_{33}} \tag{69}$$

As can be seen, the explicit solution for scattering matrix S can be obtained from these equations yielding

$$S_{22} = \frac{\mathcal{S}_{22} - C_{44}}{C_{43}^2 + \mathcal{S}_{22} \, C_{33} - C_{33} \, C_{44}} \tag{70}$$

$$S_{21} = \frac{\mathcal{S}_{21}(1 - S_{22} \, C_{33})}{C_{43}} \tag{71}$$

$$S_{12} = \frac{\mathcal{S}_{12}(1 - S_{22} \, C_{33})}{C_{43}} \tag{72}$$

$$S_{11} = \mathcal{S}_{11} - \frac{S_{12} \, S_{21} \, C_{33}}{1 - S_{22} \, C_{33}} \tag{73}$$

Thus, it is clear that by using this method of adapter correction and de-embedding for two-port devices, the scattering matrix for any DUT can be obtained without iteratively solving simultaneous complex quadratic equations and only with reference to zero-plane short-circuit and matched load standards.

What have been presented here are new and innovative techniques for calibrating Automatic Microwave Network Analyzers (e.g. HP 8542B) to make complex reflection measurements. These techniques offer significant advantages particularly when making measurements using miniature connector systems.

It has been shown that, by using the experimentally derived characterization of an APC-7 open circuit as a high reflection standard, band edge discontinuities can be eliminated with no loss of measurement accuracy. Use of multiple offset shorts is no longer necessary resulting in fewer connection requirements. This decrease translates into less wear of measurement port connectors or, more basically, lower maintenance costs.

The adapter correction based on low dissipative losses permits measurements in other connection and transmission formats without the need for a full calibration kit or process in the adapted format. This greatly reduces operating costs, requiring fewer standards and connections especially in the delicate and easily damaged SMA transmission system.

Finally, the use of a known length of terminated transmission line and the Double Running Average, instead of a sliding load or fixed termination, to characterize a

perfectly matched load offers a means of establishing a low-reflection standard truly relevant to the measurement medium when using dielectric filled lines for interconnection. This technique eliminates the need for air sliding loads in the adapted formats (particularly the delicate SMA), excludes the possibility of encountering defective calibration due to divergences of the circle fitting algorithm and enables direct comparisons of different transmission lines.

Thus, at the relatively insignificant cost of increased computer memory and slightly longer calibration times, important cutbacks in maintenance and equipment costs and greatly decreased operator assistance during measurements can be realized for existing types of measurements. Measurements of exotic transmission lines, such as microstrip, slotline, and dielectric image guide, and of any transmission formats developed in the future, are not only possible, but are easily accomplished without the need for perfect or sliding loads.

APPENDIX

This appendix contains the listings of the special software mentioned in the chapter entitled Frequency Characterization of APC-7 Open-Circuit Reflection. These programs used the HP error-correction algorithms, but they allowed specification of offset lengths for the zero-and $\lambda/4$-planes.

Also contained in this appendix are sectioned views of two typical SMA connectors.

```
1   REM THIS PROGRAM DEVELOPED ON 2/20/80.  IT USES COMPLEX
2   REM AVERAGED OLID SLIDING LOAD AND OFFSET REFERENCE PLANE
3   REM SHORTS AS REFERENCES TO MEASURE OPEN CIRCUIT REFLECTION
4   REM    REV 3/6/81      REM 3/6/81       1:ANU41.S
20   COM K[251],B[251],R[251],A[251],U[251],T[251],F[251],N[10]
40   DSPLAY "FREQ(MHZ) - START,STOP,STEP";
50   BELL
60   INPUT F1,F2,S
70   REM CALCULATE NUMBER OF FREQUENCIES OF INTEREST
80   LET N=1+(F2-F1)/S
85   REM INITIALIZE RF MEASUREMENT EQUIPMENT
90   FCALF(F1)
100   BCNT1(F1)
120   SSEL1(11)
140   WAIT (50)
150   REM CONNECT APC-7 REFERENCE PLANE SHORT AND MAKE
151   REM MEASUREMENTS
160   DSPLAY "CONNECT REFERENCE PLANE SHORT"
180   PAUSE
200   FOR I=1 TO N
210   REM CALCULATE AND STORE FREQUENCIES OF INTEREST
220   LET F[I]=F1+(I-1)*S
225   REM INIALIZE TO ZERO REAL AND IMAGINARY PARTS OF SLIDING
226   REM LOAD COMPLEX SUM
230   LET U[I]=0
235   LET T[I]=0
237   REM MAKE MEASUREMENTS ON REFERENCE PLANE SHORT
240   FREQ2(F[I])
260   MEAS1(150,X,Y)
280   CPAK(X,Y,A[I])
300   NEXT I
310   REM CONNECT SLIDING LOAD AND MAKE 6 MEASUREMENTS AT EACH
311   REM FREQUENCY OF INTEREST AND ACCUMULATE SUMS OF REAL AND
312   REM IMAGINARY PARTS
320   DSPLAY "CONNECT SLIDING LOAD"
330   PAUSE
340   FOR J=1 TO 6
350   IF J=1 GOTO 400
355   REM SLIDE SLIDING LOAD LAMBDA/12 FOR PRIMARY FREQUENCY
360   DSPLAY "SLIDE"
380   PAUSE
400   FOR I=1 TO N
420   FREQ2(F[I])
440   MEAS1(150,X,Y)
460   LET U[I]=U[I]+X
480   LET T[I]=T[I]+Y
500   NEXT I
520   NEXT J
530   REM PERFORM COMPLEX AVERAGE
540   FOR I=1 TO N
560   CPAK(U[I],T[I],B[I])
580   CPAK(6.0,X)
600   CDIV(B[I],X,B[I])
620   LET U[I]=REA(B[I])
640   LET T[I]=IMG(B[I])
660   NEXT I
2300   REM STORE LOCAL VARIABLES IN COMMON
2360   LET N[1]=F1
2380   LET N[2]=F2
2420   LET N[3]=S
2470   LET N[7]=N
2480   REM AUTOMATICALLY LOAD NEXT PROGRAM
2500   CHAIN("1:ANU42.S")
```

Fig. 85. Program 1 for open circuit phase measurement.

```
1   REM THIS PROGRAM DEVELOPED ON 6/3/79. IT IS A CONTINUATION
2   REM OF 1:ANU41.C FOR MEASURING THE REFLECTION OF AN OPEN
3   REM CIRCUIT
4   REM    REV 3/6/81     REM 3/6/81          1:ANU42.S
20   COM C[251,3],L[251],O[251],S[251],U[251],T[251],F[251],N[10]
30   REM LOAD LOCAL VARIABLES FROM COMMON
40   LET I=N[6]
60   LET F1=N[1]
100   LET F2=N[2]
150   LET N=N[7]
160   REM INITIALIZE RF MEASUREMENT EQUIPMENT
170   FCALF(F1)
180   BCNT1(F1)
200   SCEL1(11)
220   WAIT (50)
230   REM MAKE MEASUREMENTS ON OFFSET SHORT
240   DSPLAY "CONNECT OFFSET SHORT"
260   BELL
280   PAUSE
320   FOR I=1 TO N
340   FREQ2(F[I])
360   MEAS1(150,X,Y)
380   CPAK(X,Y,O[I])
400   NEXT I
410   REM READ IN DIFFERENCE IN LENGTHS BETWEEN REFERENCE
411   REM PLANE SHORT AND OFFSET SHORT
420   DSPLAY "WHAT IS OFFSET SHORT POSITION (CM) COMPARED TO"
421   DSPLAY "REFERENCE PLANE SHORT";
440   BELL
460   INPUT C9
470   REM CONVERT LENGTH TO RADIANS PER MHZ
480   LET C9=-C9*2*2.0965E-04
490   REM INITIALIZE (1,0) AND (-1,0) CONSTANTS
500   CPAK(1,0,D2)
520   CPAK(-1,0,D3)
580   FOR I=1 TO N
590   REM CORRECT OFFSET SHORT PHASOR TO LAMBDA/4 POSITION
591   REM COMPARED TO REFERENCE PLANE SHORT
600   PSFT(0,F[I],C9,D3,P1)
660   REM CALCULATE ERROR CORRECTION COEFFICIENTS
661   REM C(I,1)=E00, C(I,2)=E01, C(I,3)=E11
680   CPAK(U[I],T[I],C[I,1])
700   CSUB(S[I],C[I,1],N1)
720   CSUB(O[I],C[I,1],D1)
740   CDIV(N1,D1,N1)
760   CMPY(P1,N1,Q5)
800   CADD(Q5,D2,N1)
820   CSUB(P1,Q5,D1)
840   CDIV(N1,D1,C[I,3])
860   CSUB(C[I,1],3[I],N1)
880   CADD(D2,C[I,3],D1)
900   CADD(D2,C[I,3],D1)
930   CMPY(N1,D1,C[I,2])
940   CSUB(L[I],3[I],D1)
960   NEXT I
1080   CHAIN("1:ANU43.C")
```

Fig. 86. Program 2 for open circuit phase measurement.

```
1   REM THIS PROGRAM DEVELOPED ON 11/15/78. IT IS A CONTINUATION
2   REM OF 1:ANU42.S FOR MEASURING THE REFLECTION OF AN OPEN
3   REM CIRCUIT
4   REM     REV 3/6/81      REM 3/6/81          1:ANU43.S
20   COM C[251,3],K[251],R[251],S[251],U[251],T[251],F[251],N[10]
30   REM LOAD LOCAL VARIABLES FROM COMMON
40   LET S=N[6]
45   LET F1=N[1]
55   LET F2=N[2]
70   LET N=N[7]
80   REM INITIALIZE RF MEASUREMENT EQUIPMENT
90   FCALF(F1)
100   BCNT1(F1)
120   DSEL1(11)
140   WAIT (50)
150   REM CONNECT OPEN AND MAKE MEASUREMENTS
160   DSPLAY "CONNECT OPEN"
180   PAUSE
200   FOR I=1 TO N
220   FREQ2(F[I])
240   MEAS1(150,X,Y)
260   CPAK(X,Y,S[I])
280   NEXT I
290   REM READ IN LENGTH OF SHORT USED FOR REFERENCE PLANE
300   DSPLAY "WHAT IS POSITION OF REFERENCE PLANE(CM)";
320   BELL
340   INPUT M1
350   REM CONVERT LENGTH TO RADIANS PER MHZ
360   LET M1=-M1*2*2.0965E-04
2100   REM INITIALIZE (1,0) CONSTANT
2200   CPAK(1,0,D2)
2210   REM CORRECT OPEN CIRCUIT MEASUREMENTS WITH ERROR
2211   REM CORRECTION COEFFICIENTS
2220   FOR I=1 TO N
2240   CSUB(S[I],C[I,1],D1)
2260   CDIV(C[I,2],D1,D1)
2280   CADD(D1,C[I,3],D1)
2300   CDIV(D2,D1,S[I])
2310   REM ROTATE CORRECTED OPEN CIRCUIT MEASUREMENT TO 0-PLANE
2311   REM REFERENCE
2320   PSFT(0,F[I],M1,S[I],S[I])
2340   NEXT I
2500   CHAIN("1:ANU44.S")
```

Fig. 87. Program 3 for open circuit phase measurement.

```
1   REM THIS PROGRAM DEVELOPED ON 10/11/79 AND IT
2   REM OUTPUTS THE DATA GENERATED BY ANU41.S, ANU42.S, AND
3   REM ANU43.S TO THE VIDEO PLOTTER
4   REM       REV 5/1/81       REM 3/20/81       1:ANU44.S
20   COM A[251],B[251],C[251,3],K[251],R[251],M[251]
30   COM U[251],T[251],F[251],N[10]
35   REM RECALL LOCAL VARIABLES FROM COMMON
40   LET S=N[6]
120   LET F5=N[1]
140   LET F6=N[2]
150   LET N=N[7]
190   REM INITIALIZE GRAPHICS DISPLAY AND BUFFER
200   BUF(100)
220   CLEAR(0)
230   DSPLAY "WHAT IS B1 AND T1";
235   INPUT B1,T1
260   LET S1=(T1-B1)/10
270   REM CLEAR CRT, SCALE, AND PLOT REAL PART OF REFLECTION
280   CLEAR(0)
660   SCALE(F5,F6,B1,T1)
680   LET F3=(F6-F5)/10
700   SAXES(F3,S1)
710   LABEL VTAB(15),TAB(0),"REFL"
720   LABEL VTAB(16),TAB(0),"REAL"
740   LABEL VTAB(31),TAB(28),"FREQ(MHZ)"
760   BLOCK(B2)
780   FOR I=1 TO N
800   PLOT(F[I],REA(M[I]),2)
820   NEXT I
920   BELL
940   PAUSE
950   REM CLEAR REAL PLOT AND PLOT IMAGINARY PART
960   CLEAR(0)
970   SAXES(F3,S1)
975   LABEL VTAB(15),TAB(0),"REFL"
980   LABEL VTAB(16),TAB(0),"IMAG"
1000   LABEL VTAB(31),TAB(28),"FREQ(MHZ)"
1020   BLOCK(B2)
1040   FOR I=1 TO N
1060   PLOT(F[I],IMG(M[I]),2)
1080   NEXT I
1100   PAUSE
1120   CLEAR(0)
1140   DSPLAY "WHAT IS B2 AND T2";
1160   INPUT B2,T2
1170   REM CLEAR DISPLAY AND PLOT REFLECTION MAGNITUDE
1180   CLEAR(0)
1200   LET S2=(T2-B2)/10
1210   SCALE(F5,F6,B2,T2)
1220   SAXES(F3,S2)
1240   LABEL VTAB(15),TAB(0),"REFL"
1260   LABEL VTAB(16),TAB(0),"MAG"
1280   LABEL VTAB(31),TAB(28),"FREQ(MHZ)"
1300   BLOCK(B2)
1320   FOR I=1 TO N
1340   PLOT(F[I],MAG(M[I]),2)
1360   NEXT I
1380   PAUSE
```

Fig. 88. Page 1 of Program 4 for open circuit phase measurement.

```
1390  REM CLEAR MAGNITUDE PLOT AND PLOT REFLECTION ANGLE
1400  CLEAR(0)
1420  LET B3=-180
1440  LET T3=180
1460  CLEAR(0)
1480  LET S3=(T3-B3)/10
1500  SCALE(F5,F6,B3,T3)
1520  AXES(F3,S3)
1540  LABEL VTAB(15),TAB(0),"REFL"
1560  LABEL VTAB(16),TAB(0),"ANG"
1580  LABEL VTAB(31),TAB(28),"FREQ(MHZ)"
1600  BLOCK(B2)
1620  FOR I=1 TO N
1640  PLOT(F[I],ANG(M[I]),2)
1660  NEXT I
1670  REM CLEAR DISPLAY AND PRINT ALL RESULTS UPON REQUEST
1680  PAUSE
8680  CLEAR(0)
8700  DSPLAY "WANT TO PRINT RESULTS(1=YES,2=NO)";
8710  INPUT H1
8720  IF H1=1 GOTO 9000
8722  PAGE
8724  CLEAR(0)
8730  PRINT "FREQ(MHZ)   REFL(REA)   REFL(IMG)   REFL(MAG)   ";
8735  PRINT "REFL(ANG)"
8737  PRINT
8740  FOR I=1 TO N
8745  REM SET OUTPUT FORMAT IN BASIC NOTATION
8750  FDSP(F[I],7,0)
8751  DSPLAY "      ";
8753  FDSP(REA(M[I]),6,3)
8754  DSPLAY "      ";
8755  FDSP(IMG(M[I]),6,3)
8756  DSPLAY "      ";
8757  FDSP(MAG(M[I]),6,3)
8758  DSPLAY "      ";
8760  FDSP(ANG(M[I]),6,1)
8762  DSPLAY
8770  NEXT I
8810  CLEAR(0)
8820  LABEL "RESET SWITCH TO CRT"
8822  PAUSE
9000  END
```

Fig. 89. Page 2 of Program 4 for open circuit phase measurement.

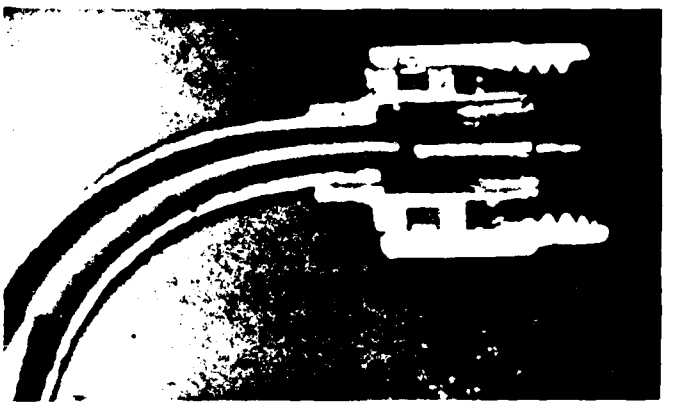

Fig. 90. Sectioned view of OSM 207-9776SF Female SMA connector.

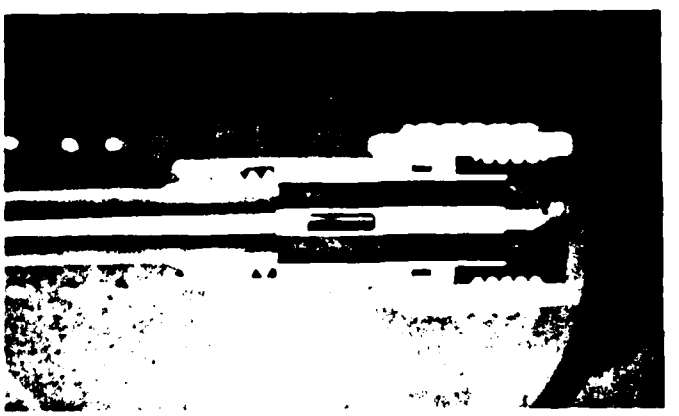

Fig. 91. Sectioned view of Narda 4401 Female SMA connector.

REFERENCES

1. B. Bianco, A. Corana, L. Gogioso, S. Ridell and M. Parodi, "Open-Circuited Coaxial Lines as Standards for Microwave Measurements", Electronics Letters, Vol. 16, No. 10, pp. 373-374, 8 May 1980.
2. A. Uhlir, Jr., "Correction for Adapters in Microwave Measurements", IEEE Trans. Microwave Theory and Tech., Vol. MTT-22, No. 3, pp. 330-332, March 1974.
3. HP 8542B Automatic Network Analyzer Programming and Operating Manual, Hewlett-Packard Co., pg. C-1, May 1975.
4. HP 8542B Automatic Network Analyzer Programming and Operating Manual, Hewlett-Packard Co., pg. 1-2, May 1975.
5. HP TODS-II Test Oriented Disc System Programming and Operating Manual, Hewlett-Packard Co., pg. 1-2, Nov. 1975.
6. HP 8542B Automatic Network Analyzer Programming and Operating Manual, Hewlett-Packard Co., pg. 10-39, May 1975.
7. C. Martini and S. Ridella, "Optimum Broad-Band Steps for a Sliding Load", IEEE Trans. Instr. and Meas., Vol. IM-26, pp. 292-295, Dec. 1977.

8. D. Hollway and P. Somlo, "A High-Resolution Swept-Frequency Reflectometer", IEEE Trans. Microwave Theory and Tech., Vol. MTT-17, No. 4, pp. 185-188, April 1969.

9. P. Lacy and W. Oldfield, "Calculable Physical Impedance References in Automated Precision Reflection Measurement", IEEE Trans. Instr. and Meas., Vol. IM-29, No. 4, pp. 390-395, Dec. 1980.

10. E. daSilva and M. McPhun, "Calibration Techniques for One-Port Measurement", Microwave Journal, pp. 97-100, June 1978.

11. M. Hines and H. Stinehelfer, Sr., "Time-Domain Oscillographic Microwave Network Analysis Using Frequency-Domain Data", IEEE Trans. Microwave Theory and Tech., Vol. MTT-22, No. 3, pp. 276-282, March 1974.

12. "Connector Relieves Nagging SMA Measurement Problems", Microwaves, Vol. 18, No. 1, pp. 97-99, Jan. 1979.

13. HP 8542B Automatic Network Analyzer Programming and Operating Manual, Hewlett-Packard Co., pg. J-5, May 1975.

14. A. Saleh, "Explicit Formulas for Error Correction in Microwave Measuring Sets with Switching-Dependent Port Mismatches", IEEE Trans. Instr. and Meas., Vol. IM-28, No. 1, pp. 67-71, March 1979.

BIBLIOGRAPHY

1. Bauer, R. F., and P. Penfield, Jr., "De-Embedding and Unterminating", IEEE Trans. Microwave Theory and Tech., Vol. MTT-22, No. 3, pp. 282-288, Mar. 1974.

2. Bianco, B., A. Corana, L. Gogioso, S. Ridella, and M. Parodi, "Open-Circuited Coaxial Lines as Standards for Microwave Measurements", Electronics Letters, Vol. 16, No. 10, pp. 373-374, May 1980.

3. Bianco, B., A. Corana, S. Ridella, and C. Simicich, "Evaluation of Errors in Calibration Procedures for Measurements of Reflection Coefficient", IEEE Trans. Instr. and Meas., Vol. IM-27, No. 4, pp. 354-358, Dec. 1978.

4. Churchill, R. V., J. W. Brown, and R. F. Verhey, Complex Variables and Applications, McGraw-Hill Book Co., New York, 1976.

5. Collin, R. E., Foundations for Microwave Engineering, McGraw-Hill Book Co., New York, 1966.

6. Cronson, H. M., and L. Susman, "A Dual Six-Port Automatic Network Analyzer", IEEE International Symposium Digest, Vol. MTT-S, 1980.

7. da Silva, E. F., and M. K. McPhun, "Calibration Techniques for One Port Measurement", Microwave Journal, pp. 97-100, Jun. 1978.

8. de Ronde, F. C., "A Precise and Sensitive X-Band Reflecto 'meter' Providing Automatic Full-Band Display of Reflection Coefficient", IEEE Trans. Microwave Theory and Tech., Vol. MTT-13, No. 7, pp. 435-440, Jul. 1965.

9. Edmondson, A. S., "The Matching of High-Frequency Transmission Lines Using a Frequency-Variation Method", Proc. Phys. Soc., Vol. 59, Pt. 6, pp. 982-989, Nov. 1947.

10. Engen, G. F., "Calibration Technique for Automated Network Analyzers with Application to Adapter Evaluation", IEEE Trans. Microwave Theory and Tech., Vol. MTT-22, No. 12, pp. 1255-1260, Dec. 1974.

11. Engen, G. F., and C. A. Hoer, "'Thru-Reflect-Line' An Improved Technique for Calibrating the Dual Six-Port Automatic Network Analyzer", IEEE Trans. Microwave Theory and Tech., Vol. MTT-27, No. 12, pp. 987-993, Dec. 1979.

12. Franzen, N. R., and R. A. Speciale, "A New Procedure for System Calibration and Error Removal in Automated S-Parameter Measurements", 5th European Microwave Conference Proc., pp. 69-73, Sep. 1975.

13. Glasser, L. A., "An Analysis of Microwave De-Embedding Errors", IEEE Trans. Microwave Theory and Tech., Vol. MTT-26, No. 5, pp. 379-380, May 1978.

14. Hackborn, R. A., "An Automatic Network Analyzer System", Microwave Journal, pp. 47-50, Apr. 1964.

15. Hewlett-Packard Co., ATS BASIC for Use with Cassette Operating Systems, California, 1972.

16. Hewlett-Packard Co., HP 8500A System Console User's Manual, California, 1973.

17. Hewlett-Packard Co., HP 8542B Automatic Network Analyzer Programming and Operating Manual, California, 1975.

18. Hewlett-Packard Co., TODS-II Test Oriented Disc System Programming and Operating Manual, California, 1975.

19. Hillbun, H., "Compensate Analyzer Errors and De-Embed S-Parameters", Microwaves, pp. 87-92, Jan. 1980.

20. Hines, M. E., and H. E. Stinehelfer, Sr., "Time-Domain Oscillographic Microwave Network Analysis Using Frequency-Domain Data", IEEE Trans. Microwave Theory and Tech., Vol. MTT-22, No. 3, pp. 276-282, Mar. 1974.

21. Hoer, C. A., "A Network Analyzer Incorporating Two Six-Port Reflectometers", IEEE Trans. Microwave Theory and Tech., Vol. MTT-25, No. 12, pp. 1070-1074, Dec. 1977.

22. Hoer, C. A., "Performance of a Dual Six-Port Automatic Network Analyzer", IEEE Trans. Microwave Theory and Tech., Vol. MTT-27, No. 12, pp. 993-998, Dec. 1979.

23. Hollway, D. L., "The Comparison Reflectometer", IEEE Trans. Microwave Theory and Tech., Vol. MTT-15, No. 4, pp. 250-259, Apr. 1967.

24. Hollway, D. L., and P. I. Somlo, "A High-Resolution Swept-Frequency Reflectometer", IEEE Trans. Microwave Theory and Tech., Vol. MTT-17, No. 4, pp. 185-188, Apr. 1969.

25. Kasa, I., "A Circle Fitting Procedure and Its Error Analysis", IEEE Trans. Instr. and Meas., Vol. IM-25, No. 1, pp. 8-14, Mar. 1976.

26. Kreider, D. L., R. G. Kuller, D. R. Ostberg, and F. W. Perkins, An Introduction to Linear Analysis, Addison-Wesley Publishing Co., Massachusetts, 1966.

27. Lacy, P. D., and W. Oldfield, "A Precision Swept Reflectometer", Microwave Journal, Vol. 21, No. 6, pp. 31-50, Apr. 1973.

28. Lacy, P. D., and W. Oldfield, "Calculable Physical Impedance References in Automated Precision Reflection Measurement", IEEE Trans. Instr. and Meas., Vol. IM-29, No. 4, pp. 390-395, Dec. 1980.

29. Martini, C., and S. Ridella, "Optimum Broad-Band Steps for a Sliding Load", IEEE Trans. Microwave Theory and Tech., Vol. MTT-26, No. 4, pp. 292-295, Dec. 1977.

30. Rehnmark, S., "On the Calibration Process of Automatic Network Analyzer Systems", IEEE Trans. Microwave Theory and Tech., Vol. MTT-22, No. 4, pp. 457-458, Apr. 1974.

31. Saleh, A. A. M., "Explicit Formulas for Error Correction in Microwave Measuring Sets with Switching-Dependent Port Mismatches", IEEE Trans. Instr. and Meas., Vol. IM-28, No. 1, pp. 67-71, Mar. 1979.

32. Somlo, P. I., "The Locating Reflectometer", IEEE Trans. Microwave Theory and Tech., Vol. MTT-20, No. 2, pp. 105-112, Feb. 1972.

33. Speciale, R. A., "Results of TSD Calibrated Scattering Parameter Measurements Performed on a Commercial ANA", 9th European Microwave Conference Proc., pp. 350-354, Sep. 1979.

34. Speciale, R. A., R. E. Grabowski, and N. R. Franzen, "Accurate Scattering Parameter Measurements on Non-Connectable Microwave Networks", 6th European Microwave Conference Proc., pp. 210-214, Sep. 1976.

35. Swanson, D., "Ferret Out Fixture Errors With Careful Calibration", Microwaves, pp. 79-85, Jan. 1980.

36. Uhlir, A., Jr., "Correction for Adapters in Microwave Measurements", IEEE Trans. Microwave Theory and Tech., Vol. MTT-22, No. 3, pp. 330-332, Mar. 1974.

37. Weinschel, B. O., "Air-Filled Coaxial Lines as Absolute Impedance Standards", Microwave Journal, pp. 47-50, Apr. 1964.

38. Whinnery, J. R., H. W. Jamieson, and T. E. Robbins, "Coaxial-Line Discontinuities", Proc. IRE, Vol. 32, pp. 695-710, Nov. 1944.

39. Wiltron Co., "Connector Relieves Nagging SMA Measurement Problems", Microwaves, Vol. 18, No. 1, pp. 97-99, Jan. 1979.

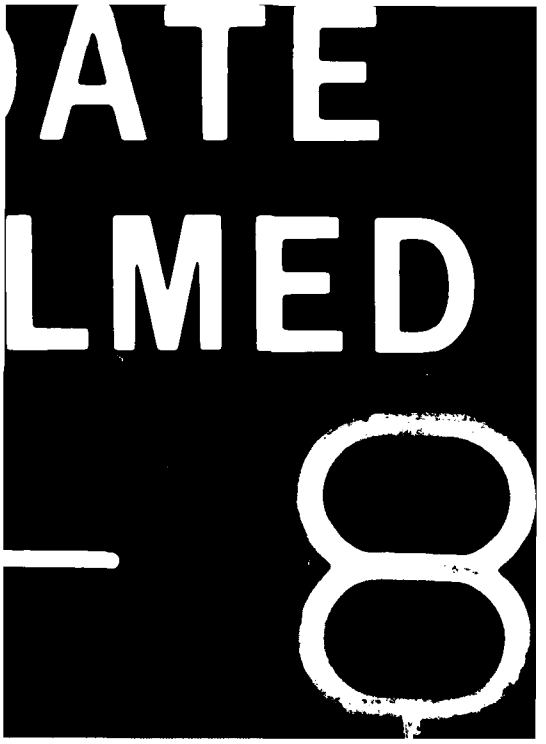
ATE
LMED
8